USGS
science for a changing world

Questa Baseline and Pre-Mining Ground-Water Quality Investigation. 14. Interpretation of ground-water geochemistry in catchments other than the Straight Creek catchment, Red River Valley, Taos County, New Mexico, 2002-2003

Scientific Investigations Report 2005-5050

Prepared in cooperation with the New Mexico Environment Department

U.S. Department of the Interior
U.S. Geological Survey

Front cover: Photograph of the town of Questa from near Capulin Canyon.

Questa Baseline and Pre-Mining Ground-Water Quality Investigation. 14. Interpretation of ground-water geochemistry in catchments other than the Straight Creek catchment, Red River Valley, Taos County, New Mexico, 2002-2003

By D. Kirk Nordstrom, R. Blaine McCleskey, Andrew G. Hunt, and Cheryl A. Naus

Scientific Investigations Report 2005-5050

U.S. Department of the Interior
U.S. Geological Survey

U.S. Department of the Interior
Gale A. Norton, Secretary

U.S. Geological Survey
Charles G. Groat, Director

U.S. Geological Survey, Boulder, Colorado 2004
Revised and reprinted: 2005

For product and ordering information:
World Wide Web: http://www.usgs.gov/pubprod
Telephone: 1-888-ASK-USGS

For more information on the USGS—the Federal source for science about the Earth,
its natural and living resources, natural hazards, and the environment:
World Wide Web: http://www.usgs.gov
Telephone: 1-888-ASK-USGS

Contents

FIGURES

Maps showing:

TABLES

Explanation of Abbreviations

---	not analyzed, measured, or calculated
<	less than
°C	degrees Celsius
cc	cubic centimeter
cc/kg	cubic centimeters per kilogram
CFC	chlorofluorocarbon
C.I.	charge imbalance
CVAFS	cold-vapor atomic fluorescence spectrometry
DDW	double-distilled water
DIW	deionized water
DOC	dissolved organic carbon
FA	filtered-acidified
FU	filtered-unacidified
FIAS	flow injection analysis system
GC	gas chromatography
GFAAS	graphite furnace atomic absorption spectrometry
GMWL	global meteoric water line
GW	ground water
HDPE	high-density polyethylene
HGAAS	hydride generation atomic absorption spectrometry
IC	ion chromatography
ICP-MS	inductively coupled plasma-mass spectrometry
ICP-OES	inductively coupled plasma-optical emission spectrometry
ID	identification
ISE	ion-selective electrode
km	kilometers
m	meters
mm	millimeter
meq/L	milliequivalents per liter
mM	millimoles per liter
mg/L	milligrams per liter
MS	mass spectrometry
µg/L	micrograms per liter
µm	micrometer
µS/cm	microsiemens per centimeter
µcc/kg	micro cubic centimeters per kilogram
N	normal
ng/L	nanograms per liter
nm	nanometer
NMED	New Mexico Environment Department
n	number of analyses
pg/kg	picograms per kilogram
PE	polyethylene
QSP	quartz-sericite-pyrite
RA	raw-acidified
REE	rare-earth element
RU	raw-unacidified
RMMWL	Rocky Mountain meteoric water line
	standard deviation
SC	specific conductance
SRWS	standard reference water sample
SW	surface water
THGA	transversely heated graphite atomizer
TOC	total organic carbon
TU	tritium units
UV	ultra-violet
v/v	volume per volume

CONVERSION FACTORS, WATER-QUALITY ABBREVIATIONS, AND DATUMS

SI to Inch/Pound

Multiply	By	To obtain
	Length	
micrometer (μm)	0.00003937	inch (in.)
millimeter (mm)	0.03937	inch (in.)
meter (m)	3.281	foot (ft)
kilometer (km)	0.6214	mile (mi)
	Area	
square meter (m^2)	0.0002471	acre
	Volume	
liter (L)	33.82	ounce, fluid (fl. oz)
liter (L)	2.113	pint (pt)
cubic meter (m^3)	264.2	gallon (gal)
liter (L)	61.02	cubic inch (in^3)
	Mass	
gram (g)	0.03527	ounce, avoirdupois (oz)
Kilogram (kg)	2.205	pound avoirdupois (lb)

Temperature in degrees Celsius (°C) may be converted to degrees Fahrenheit (°F) as follows:
°F=(1.8×°C)+32

Specific conductance is given in microsiemens per centimeter at 25 degrees Celsius (μS/cm at 25°C).

Concentrations of chemical constituents in water are given either in milligrams per liter (mg/L), micrograms per liter (μg/L), nanograms per liter (ng/L), or mM (millimoles per liter).

Coordinate information is referenced to the North American Datum 27 – Continental United States (NAD27-CONUS)

QUESTA BASELINE AND PRE-MINING GROUND-WATER QUALITY INVESTIGATION. 14. INTERPRETATION OF GROUND-WATER GEOCHEMISTRY IN CATCHMENTS OTHER THAN THE STRAIGHT CREEK CATCHMENT, RED RIVER VALLEY, TAOS COUNTY, NEW MEXICO, 2002-2003

By D. Kirk Nordstrom, R. Blaine McCleskey, Andrew G. Hunt, and Cheryl A. Naus

ABSTRACT

The U.S. Geological Survey, in cooperation with the New Mexico Environment Department, is investigating the pre-mining ground-water chemistry at the Molycorp molybdenum mine in the Red River Valley, New Mexico. The primary approach is to determine the processes controlling ground-water chemistry at an unmined, off-site but proximal analog. The Straight Creek catchment, chosen for this purpose, consists of the same Tertiary-age quartz-sericite-pyrite altered andesite and rhyolitic volcanics as the mine site. Straight Creek is about 5 kilometers east of the eastern boundary of the mine site. Both Straight Creek and the mine site are at approximately the same altitude, face south, and have the same climatic conditions.

Thirteen wells in the proximal analog drainage catchment were sampled for ground-water chemistry. Eleven wells were installed for this study and two existing wells at the Advanced Waste-Water Treatment (AWWT) facility were included in this study. Eight wells were sampled outside the Straight Creek catchment: one each in the Hansen, Hottentot, and La Bobita debris fans, four in a well cluster in upper Capulin Canyon (three in alluvial deposits and one in bedrock), and an existing well at the U.S. Forest Service Questa Ranger Station in Red River alluvial deposits. Two surface waters from the Hansen Creek catchment and two from the Hottentot drainage catchment also were sampled for comparison to ground-water compositions. In this report, these samples are evaluated to determine if the geochemical interpretations from the Straight Creek ground-water geochemistry could be extended to other ground waters in the Red River Valley, including the mine site.

Total-recoverable major cations and trace metals and dissolved major cations, selected trace metals, anions, alkalinity; and iron-redox species were determined for all surface- and ground-water samples. Rare-earth elements and low-level As, Bi, Mo, Rb, Re, Sb, Se, Te, Th, U, Tl, V, W, Y, and Zr were determined on selected samples. Dissolved organic carbon (DOC), mercury, sulfate stable isotope composition ($\delta^{34}S$ and $\delta^{18}O$ of sulfate), stable isotope composition of water ($\delta^{2}H$ and $\delta^{18}O$ of water) were measured for selected samples. Chlorofluorocarbons (CFC) and ^{3}He and ^{3}H were measured for age dating on selected samples.

Linear regressions from the Straight Creek ground-water data were used to compare ground-water chemistry trends in non-Straight Creek ground waters with Straight Creek alluvial ground-water chemistry dilution trends. Most of the solute trends for the ground waters are similar to those for Straight Creek but there are some notable exceptions. In lithologies that contain substantial pyrite mineralization, acid waters form with similar chemistries to those in Straight Creek and all the waters tend to be calcium-sulfate type. Hottentot ground waters contain substantially lower calcium concentrations relative to those in Straight Creek. This anomaly results from the exposure of rhyolite porphyry in the Hottentot scar and weathering zone. The rhyolite contains less calcium than the altered andesites and tuffs in the Straight Creek catchment and probably does not have the abundant gypsum and calcite. The Hansen ground waters have reached gypsum saturation and have similar calcium, magnesium, and beryllium concentrations as Straight Creek ground waters but have lower concentrations of fluoride, manganese, zinc, cobalt, nickel, copper, and lithium. Lower concentrations of elements related to mineralization at

Hansen likely reflect the more distal location of Hansen with respect to intrusive centers that provided the heat source for hydrothermal alteration.

The other ground water with water chemistry trends that are outside the Straight Creek trends was from an alluvial well from Capulin Canyon (CC2A). Although it had pH values near 6.0 and most major ions similar to the other Capulin Canyon ground waters, it contained high concentrations of fluoride, manganese, aluminum, iron, beryllium, and zinc similar to a mineralized zone and had low alkalinity.

Saturation indices indicate that solubility constraints continue to provide upper limits on some solute concentrations. Siderite, ferrihydrite, calcite, gypsum, rhodochrosite, and barite provide limits for concentrations of Fe(II), Fe(III), Ca, Mn, and Ba, respectively. Beryllium concentrations may be subject to an upper concentration limit by the solubility of $Be(OH)_2$ but these concentrations probably are not reached in the ground waters.

Ground-water isotopic data were consistent with the meteoric water line estimated for precipitation in the Red River Valley, indicating that all the ground waters examined in this study were meteoric, recent in origin, and showed no substantial indication of evaporation. Tritium-helium-3 and chlorofluorocarbon (CFC) age dating were partially successful. Generally, dates were consistent with location and depth of wells. Two samples had good agreement between CFC dates and tritium-helium dates, whereas a third reflected either substantial mixing with younger or older waters or complications arising from excess helium-4. The well at La Bobita appeared to contain a large component of modern water, most likely as a result of mixing with water from Red River alluvial deposits.

INTRODUCTION

In April 2001, the U.S. Geological Survey (USGS) and the New Mexico Environment Department began a cooperative study to infer the pre-mining ground-water chemistry at the Molycorp molybdenum mine site in the Red River Valley (fig. 1). This study was prompted by the Water Quality Act, under the jurisdiction of the New Mexico Water Quality Control Commission, which requires a mine operator to develop and complete an approved closure plan. The plan must prevent the exceedence of (1) ground-water quality standards set forth in New Mexico Water Quality Control Commission Regulations (§20.6.2.3103 NMAC) or (2) natural background concentrations.

The Molycorp molybdenum mine has been in operation since the 1920s, and no ground-water measurements or chemical analyses were obtained prior to mining. To infer the pre-mining ground-water chemistry, analogous off-site areas were studied. These analog sites are often disturbed by other non-mining, anthropogenic activities including exploration drilling, road construction, power and telephone line construction, construction and maintenance by the forest service, and residential, commercial, and municipal development. The existing conditions of these analog sites are referred to as “baseline conditions” which, when combined with relevant data and interpretation for mined areas, pre-mining conditions of the mine site can be inferred.

The Straight Creek catchment (fig. 1) was selected as the primary analog site for this study because of its similar terrain and geology to the mine site, accessibility, permission for well construction, and minimal anthropogenic activity. Other sites are Hottentot Creek and Hansen Creek catchments, an un-named catchment east of the mine property (La Bobita), and Capulin Canyon (fig. 1). These four catchments were chosen to represent the range of natural conditions applicable to the mine site. Like Straight Creek, the other catchments are analogous to parts of the mine site but have had little or no impact from mining activities.

As part of this study, 29 observation wells and piezometers were installed in the Red River Valley. The wells and piezometers were drilled, constructed, and developed in three phases. Eight observation wells were installed in the Straight Creek catchment during Phase I of the drilling program (November 2001 through February 2002). Eleven wells were installed in analog areas during Phase II (October 2002 to January 2003). Observation well installation and development, lithologic and geophysical logging, and water-level data collection were described by Naus and others (2005) and P.J. Blanchard and others (USGS, written commun., 2004).

This interpretation of major- and trace-element concentrations for ground waters outside the Straight Creek catchment has helped to determine to what extent the Straight Creek results serve as a useful analog for estimating the pre-mining ground-water quality at the Questa molybdenum mine site.

Purpose and Scope

The purpose of this report is to provide water-quality data for samples from the phase II wells and to interpret the ground-water geochemistry in sites other than Straight Creek. Methods and results of ground- and surface-water sample collection conducted from February 2002 to October 2003 and interpretation of Straight Creek water chemistry were discussed by Naus and others (2005). This report utilizes the same approach as that by Naus and others (2005) for the interpretations of the Straight Creek data, and trends from Straight Creek are used as a framework for interpreting ground-water geochemistry in other catchments.

Physical Description of Study Area

The Red River, a tributary to the Rio Grande within the Carson National Forest, is located in Taos County in north-central New Mexico (fig. 1). The terrain is rugged with steep slopes and V-shaped valleys. The main area of study within the Red River Valley extends from the town of Red River to the USGS streamflow-gaging station near Questa (08265000, Red River near Questa) and includes approximately 101 square kilometers of the drainage basin and approximately 19 kilometers of river reach. The Molycorp, Inc. Questa molybdenum mine, referred to as the mine site, is located east of the Ranger Station on the north side of State Highway No. 38 and the Red River. The mine site is approximately 10 square kilometers in area (U.S. Department of Agriculture Forest Service, 2001) and it encompasses three tributary valleys to the Red River: Capulin Canyon, Goat Hill Gulch, and Sulphur Gulch, from west to east respectively (fig. 1).

Mining activities produced extensive underground workings and an open pit approximately 900 meters in diameter (covering approximately 0.7 square kilometers) near or in Sulphur Gulch (URS, 2001). Waste-rock piles cover steep slopes on the north side of the Red River between Capulin Canyon and Spring Gulch (a tributary valley of Sulphur Gulch). Hydrothermally altered bedrock (alteration scars) is found in Capulin, Goat Hill, Sulphur, Hansen, Straight, and Hottentot drainages (fig. 1). Weathering of extensively altered rock has resulted in steep, highly erosive, sparsely vegetated “scars” that are clearly visible from the ground and in aerial photographs.

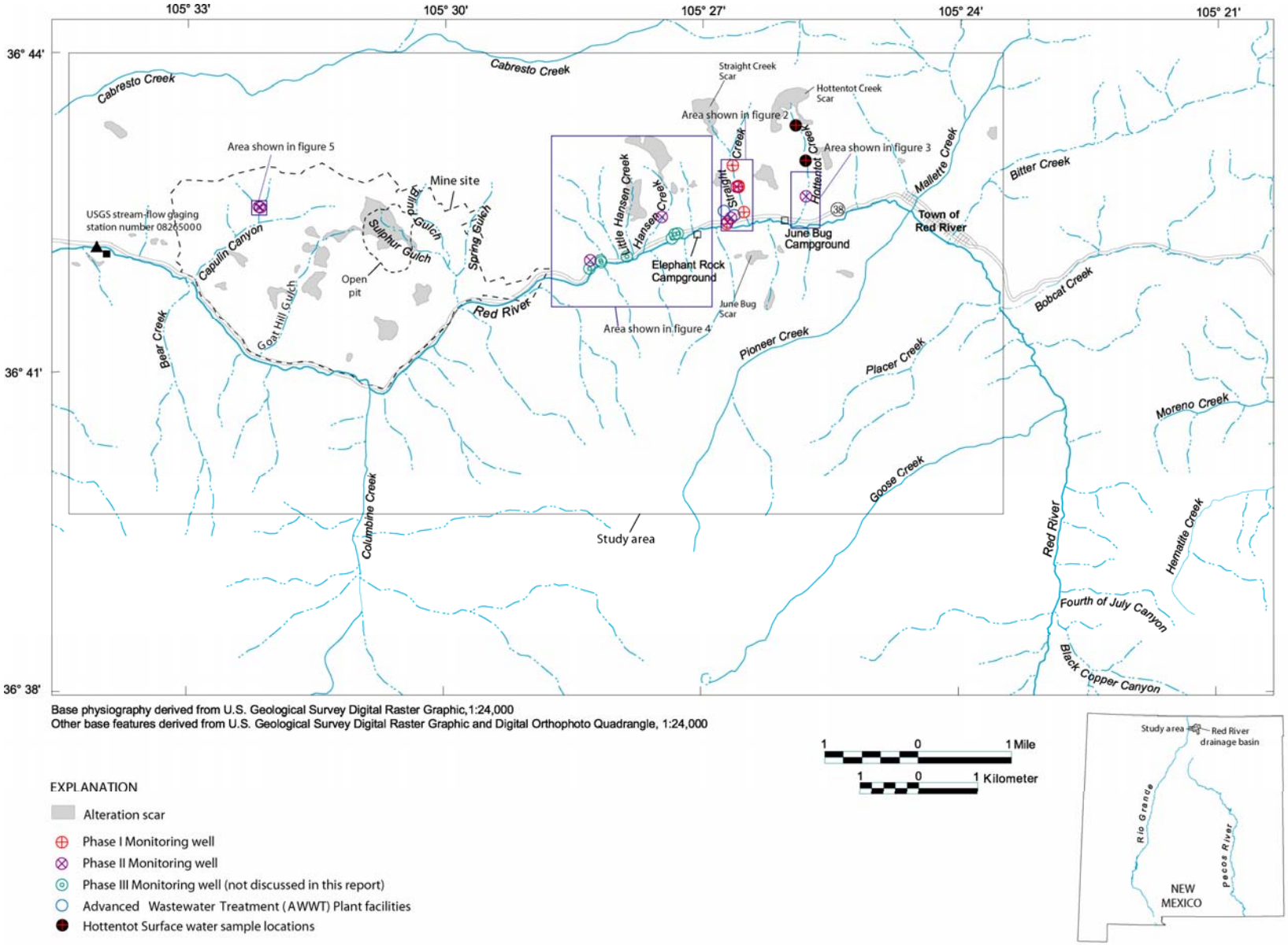

Figure 1. Map showing the location of the mine site, wells sampled, and Hottentot surface water samples and the study area within the Red River valley.

Climate and Vegetation

The Red River Valley is located within a semi-arid desert that receives precipitation throughout the year and sustains moderate biodiversity. Between 1915 and 2002, the annual average temperature was 4 °C and the annual average precipitation and snowfall were approximately 50 and 371 centimeters, respectively. Daily temperatures generally fluctuated by 18 °C throughout the year (Western Regional Climate Center, 2003).

Climate and vegetation vary greatly within short distances, primarily because of differences in topography. Topography in the study area is steep, rising rapidly from the basin floor altitude of approximately 2,270 meters at the streamflow-gaging station near Questa to ridge crests at altitudes exceeding 3,200 meters. Orographic effects of mountainous topography lead to precipitation on the windward slopes and localized storms within tributary valleys. Runoff from thunderstorms is responsible for mass wasting in hydrothermally altered areas, producing debris flows that form debris fans at the mouths of most tributaries to the Red River (K. Vincent, USGS, written commun., 2003). Winter snowpack contributes to ground-water recharge through snowmelt infiltration.

Prevalent vegetation in the Red River Valley is representative of the following altitude zones: piñon-juniper woodland (1,800-2,300 meters in altitude), mixed conifer woodland (2,300-2,700 meters in altitude), and spruce-fir woodland (2,700-3,700 meters in altitude) (Knight, 1990). Willows, cottonwoods, shrubs, perennial grasses, and flowering vegetation are common near the banks of the Red River. Widely spaced piñon pines and junipers extend from the river. Gains in altitude give rise to an abundance of ponderosa and limber pines, while Douglas- and white-fir are found at higher altitudes. This typical mountain community, while diverse, is dominated by ponderosa pines (L. Gough, USGS, oral commun., 2003).

Hydrogeology

Ground water passes through, and geochemically interacts with, various earth materials in the Red River Valley. Major rock types, minerals, water-bearing units, and generalized aquifer and ground-water-chemistry information are described in this section. The geology and mineralogy of the Red River Valley have been described by Schilling (1956), Rehrig (1969), Lipman (1981), and Meyer and Leonardson (1990, 1997). Information in this section draws largely upon these sources, with additional information from Ludington and others (2004) and other USGS scientists participating in this study.

The Red River Valley is located along the southern edge of the Questa caldera and contains complex structural features (Caine, 2003) and extensive hydrothermal alteration. Volcanic and intrusive rocks of Tertiary age are underlain by metamorphic rocks of Precambrian age that were intruded by granitic stocks. The volcanic rocks are primarily intermediate to felsic composition (andesite to rhyolite); granites and porphyries have intruded the volcanics and are the apparent source of hydrothermal fluids and molybdenite mineralization.

The mineral deposits in the Red River Valley are considered Climax-type deposits that are associated with silica- and fluorine-rich rhyolite porphyry and granitic intrusives. Climax-type hydrothermal alteration produces zones of alteration assemblages with a central zone of fluorine-rich potassic alteration, a quartz-sericite-pyrite (QSP) zone (often with a carbonate-fluorite veinlet overprint), and a propylitic zone. In the potassic zone, rocks are altered to a mixture of biotite, potassium feldspar, quartz, fluorite, and molybdenite; these rocks usually contain less than 3 percent sulfide (including molybdenite). Quartz-sericite-pyrite (QSP) alteration, as the name implies, produces a mixture of quartz, pyrite (as much as 10 percent), and fine-grained mica (sericite) or illite. Chlorite, epidote, albite, and calcite typically are found in the propylitic zones.

Ore deposits in the Red River Valley contain quartz, molybdenite, pyrite, fluorite, calcite, manganiferous calcite, dolomite, ankerite, and rhodochrosite. Lesser amounts of galena, sphalerite, chalcopyrite, magnetite, and hematite also are present. The hydrothermal alteration related to mineralization overprints an older, regional propylitic alteration. In these areas, rocks can contain a

mixture of quartz, pyrite, and illite clays replacing feldspars, chlorite, carbonates, and epidote. Abundant minerals in waste rock produced by mining activities include chlorite, gypsum, illite, illite-smectite, jarosite, kaolinite, and muscovite (Gale and Thompson, 2001).

Andesite volcanic and volcaniclastic rocks are present in most scar-area bedrock outcrops and are the dominant bedrock units in the Straight Creek, South and Southeast Straight Creek, South Goat Hill, Sulphur Gulch, and Southwest Hansen scars. Amalia Tuff, a mildly alkaline, rhyolitic tuff, is the dominant rock type in the Goat Hill and Hansen scars, and quartz latite porphyry is the main rock type in the June Bug and Southeast Hottentot scars. Rhyolite porphyry is the main rock type in the Hottentot scar, and quartz latite and rhyolite porphyries form the hill slopes of many scars. Advanced argillic alteration was identified in the Hansen and Hottentot scars and in areas southwest of the Molycorp open pit. Propylitized andesite bedrock is present in the La Bobita drainage, an area that does not contain alteration scars.

Samples collected from a weathering profile in the Straight Creek scar were studied in detail to characterize the mineralogic variations in a weathered profile. Unweathered bedrock exposed in the creek bottom is propylitized andesite with a QSP overprint. Depending on location within the weathering profile, altered rocks contain variable amounts of quartz, illite, chlorite, and plagioclase feldspar, with smaller amounts of pyrite, gypsum, rutile, jarosite, and goethite (Livo and Clark, 2002; Ludington and others, 2004).

Scar-area bedrock outcrops are composed of andesite volcanic and volcaniclastic rocks, rhyolitic tuff, quartz latite, and rhyolite porphyry. The dominant alteration type in all scars is QSP; carbonates also are found in all scar areas. Most of the andesite and quartz latite has been propylitically altered and contains plagioclase feldspar and chlorite, with fewer QSP alteration minerals. Rhyolite porphyry and tuff do not seem to have been substantially affected by propylitization. In Straight Creek, unweathered bedrock exposed in the creek bottom is propylitized andesite with a QSP overprint. Other dominant rock types include rhyolite porphyry and rhyolitic tuff. Depending on location within the weathering profile, altered rocks contain variable amounts of quartz, illite, chlorite, and plagioclase feldspar, with smaller amounts of pyrite, gypsum, rutile, jarosite, and goethite (Livo and Clark, 2002; Ludington and others, 2004).

The three major water-bearing units in the Red River Valley are fractured and weathered bedrock, debris fan deposits, and Red River alluvial deposits. Bedrock constitutes the largest aquifer in the study area in terms of rock mass, but probably contains only small amounts of ground water because of low porosity and hydraulic conductivity that are controlled by fractures. Although debris fan deposits and Red River alluvial deposits are restricted in areal extent and thickness compared to bedrock aquifers, they contain most of the ground water in the valley. Debris fans and the Red River alluvial deposits are less than 300 meters wide and less than 60 meters thick (K. Vincent, USGS, written commun., 2003).

Debris fans are composed of sediments transported from their watersheds, which are tributary to the Red River. Where the tributary watersheds contain scars, the debris fans are large and active and contain both coarse- and fine-grained debris fan sediments. The chemistry of these sediments reflects the chemistry of their rapidly eroding and altered erosion scars. In contrast, Red River alluvial deposits often consist of well-washed sandy gravel and are composed of several lithologies found in the entire Red River basin. The Red River aggraded behind the largest debris fans during the Quaternary Period. Thus water flowing in the shallow aquifers likely passes alternately through Red River alluvial deposits and debris fan deposits (K. Vincent, USGS, written commun., 2003).

Although chemical analyses of ground water were not obtained prior to mining in the Red River Valley, a substantial amount of post-mining ground-water data are available (LoVetere and others, 2004). Most wells in the Red River Valley were installed to monitor water quality downgradient from mining operations (waste rock and tailings piles) and (or) scar areas. Bedrock, debris fan, and alluvial ground water are dominantly of the calcium-sulfate type.

Surface Water

The Red River originates at an altitude of approximately 3,700 meters near Wheeler Peak and flows roughly 56 kilometers to its confluence with the Rio Grande River at an altitude of 2,000 meters. Total basin drainage area is 300 square kilometers; the drainage area upstream from the Questa Ranger Station gaging station is 180 square kilometers. Peak streamflow usually occurs from late May to mid-June, with snowmelt-related flows beginning in late March and increasing through mid-April. Summer thunderstorms are prevalent in July and August. Between 1930 and 2001, the mean annual discharge of the Red River at the Questa Ranger Station gage ranged from 0.4 to 3.0 cubic meters per second (m^3/s), while the average daily discharge ranged from 0.1 to 21 m^3/s with an average of 1.3 m^3/s (U.S. Geological Survey, 2004a).

Springs and shallow alluvial ground water discharge to the Red River, rendering it a gaining stream over much of its length (Smolka and Tague, 1989). Between the town of Red River and the gaging station near Questa, there are roughly 25 ephemeral seeps and springs along the banks of the Red River and approximately 20 intermittent seeps and springs in tributary drainages on the north side of the river (South Pass Resources, Inc., 1995; Steffen Robertson & Kirsten, 1995; Robertson GeoConsultants, Inc., 2001). Most seeps and springs along the north side of the Red River are acidic (pH 2-4) with high specific conductance, dissolved solids, and metal concentrations. Aluminum hydroxide often precipitates from springs downgradient from scar and mined areas on the north side of the Red River, affecting the color and turbidity of the river (Vail Engineering, Inc. 1989).

Mining History

A pair of prospectors first discovered molybdenite in Sulphur Gulch in 1914 although it was not identified as such until 1916. Underground mining operations occurred between 1919 and 1958; by 1954, there were over 56 kilometers of underground mine workings (Robertson Geoconsultants, 2000; U.S. Environmental Protection Agency, 2000). Molycorp began removing the rock overburden at Sulphur Gulch in 1964, and the first molybdenite ore was extracted from the open pit in 1965. Overburden and waste rock from open-pit mining was deposited at several locations on the south-facing slopes north of the Red River between Capulin Canyon and Spring Gulch (Robertson Geoconsultants, 2000; URS, 2001). Tailings were transported by pipeline from the mine to the tailings facility in the Rio Grande Valley near Questa. Water used in the mill operation was produced from the Red River, the Red River alluvial aquifer, and water collected from dewatering the mine (URS, 2002).

In 1983, Molycorp ceased open-pit mining and initiated a new phase of underground mining in Goat Hill Gulch. Roughly 3×10^{11} kilograms of waste rock were deposited between 1964 and 1983 (Steffen Robertson & Kirsten, 1995; Slifer, 1996; Robertson GeoConsultants, Inc., 2000). Low market values for molybdenum caused the mine to shut down between 1986 and 1989 and again in 1992. From 1992 to 1995, while the underground mine was shut down, pumping of ground water from the underground mine stopped and the workings were allowed to flood. After mine dewatering and repair, production resumed in late 1996 and development of a new ore body began in 1998 (Molycorp, Inc., n.d.).

Acknowledgments

The authors are grateful to the project advisory committee (New Mexico Environment Department, Molycorp, Inc., and Amigos Bravos) for their contributions to the design and implementation of the study. Advice and cooperation from the U.S. Environmental Protection Agency Region 6 and the U.S. Forest Service are gratefully acknowledged. The authors also acknowledge Jim Ball and Ann Maest (USGS) for providing extensive technical assistance in development of the ground-water sampling plan.

METHODS

Water-chemistry data were collected to determine geochemical signatures of solute sources in the aquifer materials and identify processes contributing to the chemistry of ground water. Surface- and ground-water samples were collected for determination of concentrations of total recoverable major cations and selected trace metals; dissolved major cations, selected trace metals, and rare-earth elements; anions and alkalinity; dissolved-iron and arsenic redox species; dissolved organic carbon; dissolved mercury; dissolved sulfide, water and sulfur isotopes, and dissolved helium, tritium, and chlorofluorocarbons. This section describes sampling locations and methods used to collect and analyze samples.

Sampling Sites

Well Locations

The locations of wells installed for this study (figs. 1-5) were chosen to provide information about ground-water geochemistry in settings that are analogous to the mined area. Observation wells in the Straight Creek catchment (fig. 2) were located along the hypothesized path of ground-water flow in debris fan from the upper part of the catchment to near its mouth where it flows into the Red River. Wells SC2B, SC3A, SC3B, SC4A and SC6A were grouped to facilitate conducting an aquifer test in the Straight Creek catchment. Six of the observation wells (SC1A / SC1B, SC3A / SC3B, and SC5A / SC5B) are debris fan/bedrock well pairs. Well SC2B was intended to be completed within debris fan deposits, but this well was screened within bedrock because the debris fan material was not saturated. Wells SC4A, SC6A, SC7A, and SC8A were completed within debris fan deposits. Red River alluvial deposits probably mix with debris fan deposits in the vicinity of wells SC5A and SC5B, SC7A and SC8A.

The relatively higher rate of ground-water flow within the Red River alluvial deposits compared with the rate of flow within the Straight Creek debris fan was expected to cause acidic water to flow southwestward as it merged with near-neutral pH water in the Red River alluvial deposits. Wells SC7A and SC8A were installed in the Red River alluvial deposits during Phase II to intercept this ground-water mixing zone, and well SC7A was screened across an interval of approximately 27 meters to facilitate water-sample collection at selected depths within the mixing zone.

Wells in the Hottentot Creek (fig. 3) and Hansen Creek (fig. 4) catchments were screened in the debris fan from scar-affected drainages. Water-chemistry data from these wells, combined with data from Straight Creek, permitted monitoring and evaluation of a range of conditions in debris fans associated with scars. The observation well in the La Bobita campground area (fig. 4) was screened in unconsolidated deposits not associated with a scar.

To evaluate the comparability of analog sites upstream from the mine to conditions on the mine site, additional data from an onsite analog area were required. Capulin Canyon is located on Molycorp property but appears to be the least perturbed by mining-related activities. Paired wells (bedrock/unconsolidated deposits) in Capulin Canyon (fig. 5) provided information about ground-water chemistry in areas outside the influence of mining in close proximity to the mine site.

Surface Water

Surface-water samples were collected from the Hansen Creek (fig. 4) and Hottentot Creek (fig. 1). The surface-water data are reported here so that their influence on the ground-water chemistry can be demonstrated. Flow of surface water in Hottentot Creek and Hansen Creek is intermittent and generally disappears underground before it reaches the Red River. In each of the catchments, surface samples were collected as low in altitude in the catchment as possible, or just before the water disappears underground, and fairly high in altitude in the drainages.

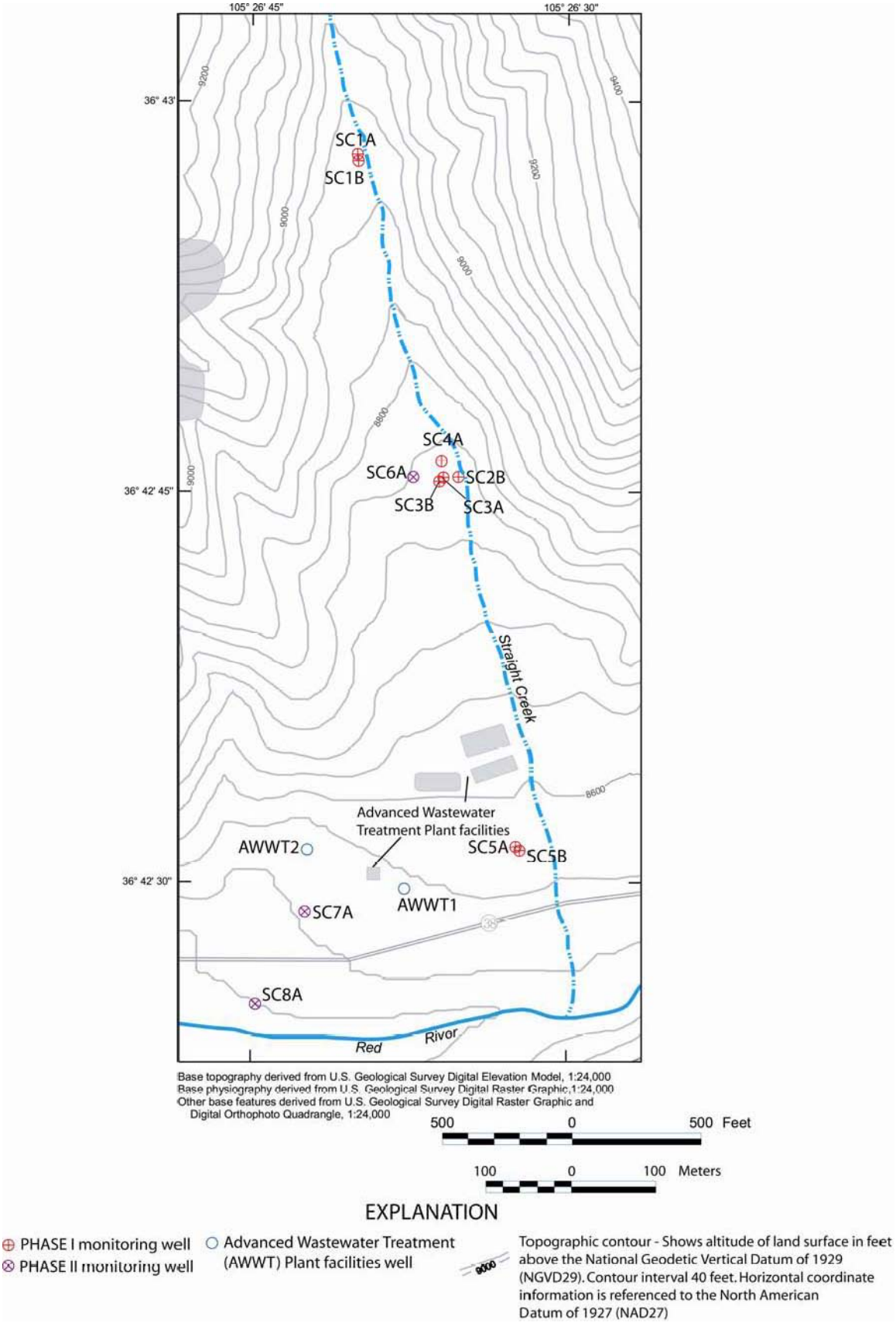

Figure 2. Map showing locations of monitoring wells in the Straight Creek catchment.

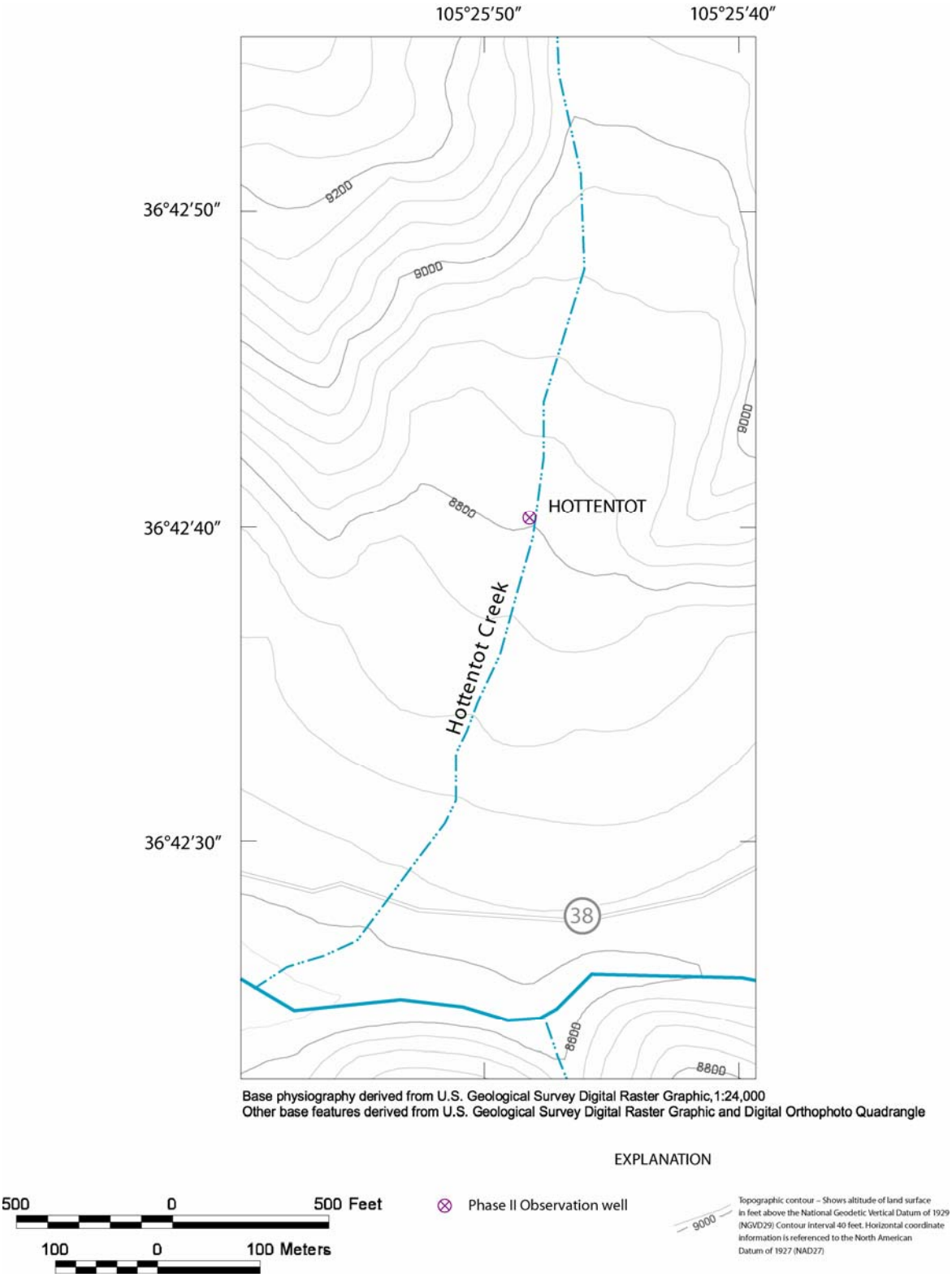

Figure 3. Map showing location of Hottentot Creek well. Surface water samples collected upstream of map area.

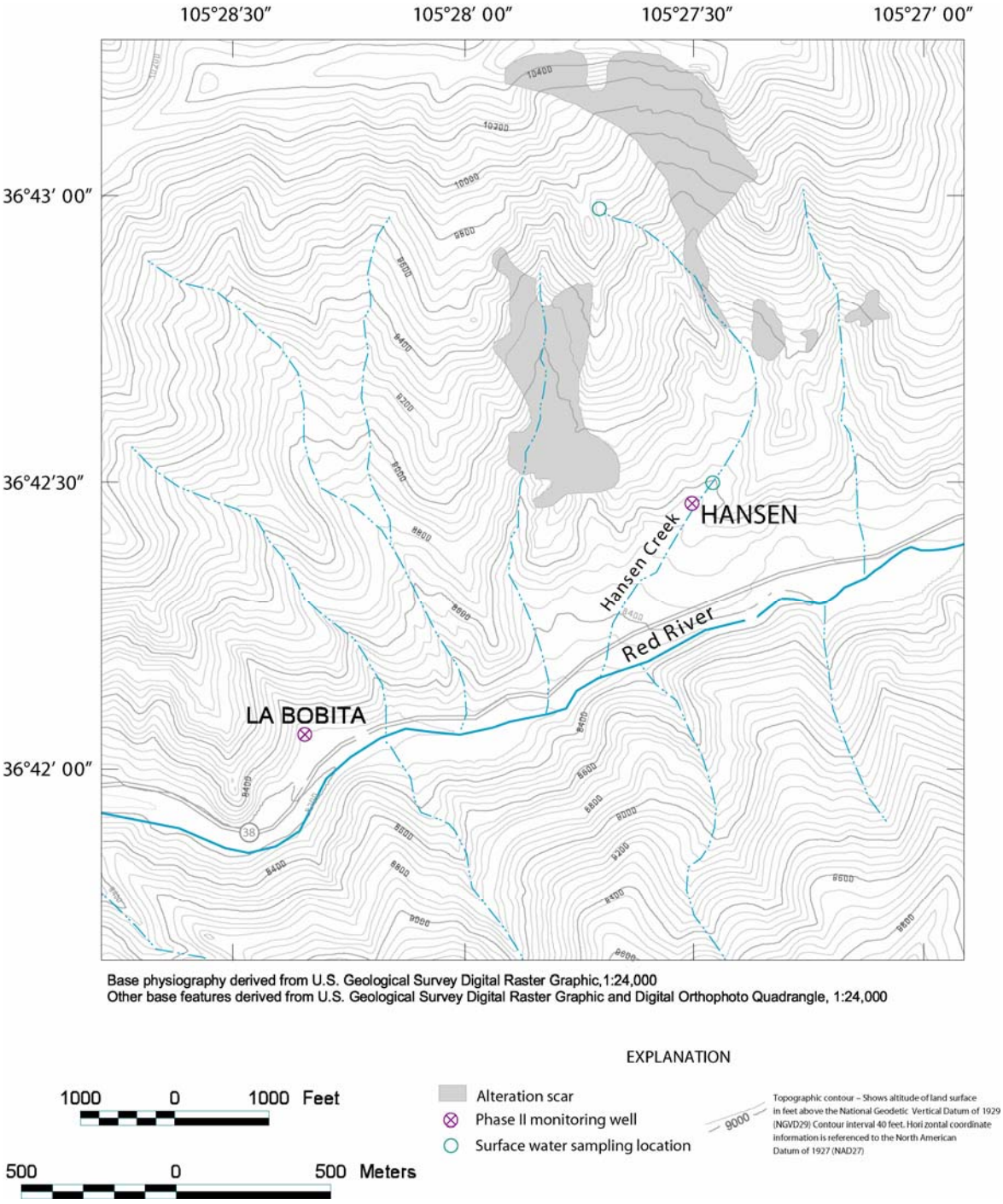

Figure 4. Map showing locations of the Hansen Creek, La Bobita, and Phase III wells and surface water sampling sites.

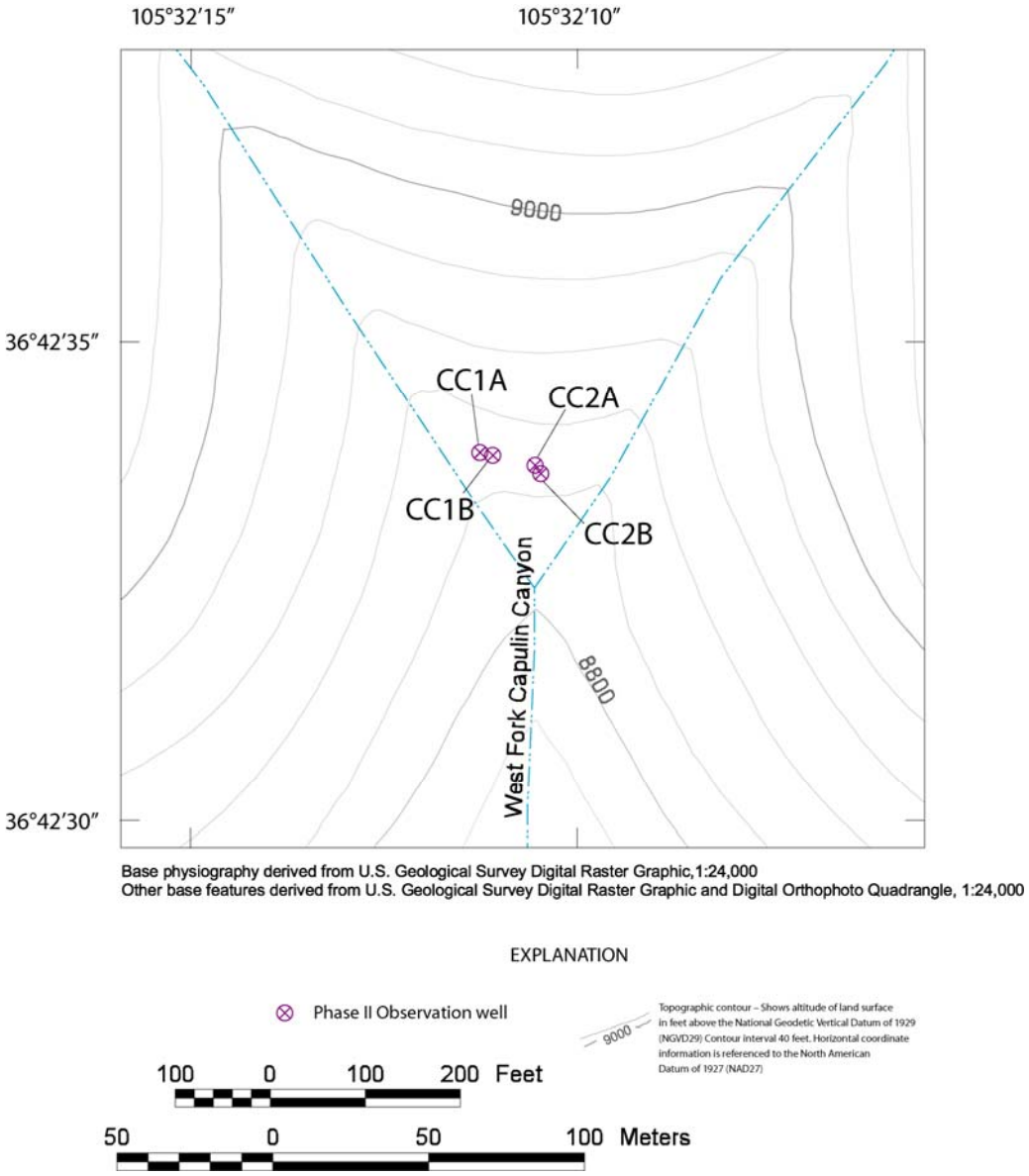

Figure 5. Map showing locations of wells in Capulin Canyon.

Water Sample Collection

Ground- and surface-water samples were routinely collected for determination of concentrations of total recoverable major cations and selected trace metals and dissolved major cations, selected trace metals, anions, alkalinity, and iron-redox species. A total recoverable sample is unfiltered and acidified (RA) with nitric acid and is comprised of dissolved constituents and suspended material. Dissolved concentrations are operationally defined as the concentration of constituents that pass through a filter (either 0.45, 0.2, or 0.1 μm in this study). Concentrations of rare-earth elements were determined on selected filtered samples only. Samples were collected for determination of dissolved organic carbon (DOC), sulfide (H_2S), and mercury concentrations and sulfur isotopic ($\delta^{34}S$ and $\delta^{18}O$ of sulfate) and stable water isotopic ($\delta^{2}H$ and $\delta^{18}O$) compositions during selected samplings. The types and sizes of bottles used and cleaning, filtration, and preservation methods for each sample type are presented in table 1. One set of ground-water samples was collected for helium-3/tritium and chlorofluorocarbon age dating.

Procedures for collecting samples from observation wells and surface water were modified slightly from the USGS National Field Manual for the Collection of Water-Quality Data (U.S. Geological Survey, 1997-99). Sampling procedures are described in detail in the project field sampling plans (C.A. Naus, written commun., 2001). This section summarizes procedures used to collect water samples and describes on-site measurements for monitoring water-quality.

Table 1. Sample types, container preparation and stabilization methods for filtered samples

[HCl, hydrochloric acid; HDPE, high-density polyethylene HNO_3, nitric acid; H_2SO_4, sulfuric acid; $K_2Cr_2O_7$, potassium dichromate; mL, milliliters; N, normal; v/v, volume per volume; %, percent]

Sample type(s)	Storage container and preparation	Stabilization treatment in addition to refrigeration
Cations and trace metals (Al, As, B, Ba, Be, Bi, Ca, Cd, Ce, Co, Cr, Cs, Cu, Dy, Er, Eu, Fe, Gd, Hf, Ho, K, La, Li, Lu, Mg, Mn, Mo, Na, Nd, Ni, Pb, Pr, Rb, Re, Sb, Se, SiO_2, Sm, Sr, Ta, Tb, Te, Th, Tl, Tm, U, V, W, Y, Yb, Zn, and Zr)	Polyethylene bottles, soaked in 5% HCl and rinsed 3 times with distilled water	1% (v/v) concentrated HNO_3 added (redistilled or trace metal grade)
Mercury (Hg)	Borosilicate glass bottles, soaked with 5% HNO_3 and rinsed 3 times with deionized water	5 mL of concentrated redistilled HNO_3 (added in the field) + 0.04% w/v $K_2Cr_2O_7$ per 125 mL of sample (added in the laboratory)
Iron and arsenic redox species (Fe(T), Fe(II), As(T), and As(III))	Opaque polyethylene bottles, soaked in 5% HCl and rinsed 3 times with distilled water	1% (v/v) HCl added (redistilled or trace metal grade)
Major anions, alkalinity, and density (Br, Cl, F, HCO_3, NO_3, and SO_4)	Polyethylene bottles filled with distilled water and allowed to stand for 24 hours, then rinsed 3 times with distilled water	None
Dissolved organic carbon (DOC)	Baked glass bottle	None

Ground Water Collection

For ground waters, both unfiltered (RA) and filtered samples were routinely collected. Disposable capsule filters with a nominal pore size of 0.45 micrometer (μm) were used for routine ground-water filtration. Because fine colloidal material may pass through a 0.45-μm filter membrane (Kennedy and others, 1974; 1976; Laxen and Chandler, 1982), duplicate samples were collected from selected Phase I wells (Naus and others, 2005) and filtered through a plate filter with a 0.1-μm membrane. Filters were connected inline with the sample tubing to collect samples directly from the well.

Dedicated bladder pumps designed specifically for purging and sampling at low flow rates were installed in observation wells located in the Straight Creek, Capulin Canyon, and Hottentot Creek drainages. The pumps were constructed of PVC with Teflon® bladders and equipped with dedicated discharge tubing for collection of samples. Because observation wells in Hansen and La Bobita drainages did not have a large enough saturated screened interval to accommodate dedicated pumps, a portable, low-flow bladder pump was used to collect samples from these wells. For Hansen and La Bobita wells, tubing was dedicated sample collection, and samples were collected approximately 24 hours after pump and tubing installation. Both dedicated and portable pumps were operated using compressed gas and an electronic bladder-pump control unit.

The USGS standard procedure for purging (Gibs and Wilde, 1999) requires monitoring water-quality parameters to determine when water withdrawn from the well is representative of water flowing through the aquifer and thus when sampling should begin. A sufficient volume has been purged from the well when the variability in sequential field measurements is stable within prescribed criteria. Water-quality parameters measured for this study were pH, specific conductance, redox potential (Eh), dissolved oxygen, temperature, and turbidity. Sensors for all measurements except turbidity were housed in a 250-mL in-line flow-through cell. Water-quality-parameter measurement equipment (Naus and others, 2005), stabilization criteria, and guidelines for instrument calibration are listed in table 2. In general, manufacturers' recommendations and USGS guidelines (Wilde and Radtke, 1998) for testing, calibration, and calibration stability checks were followed.

Using a target rate of less than 0.5 liter per minute, pump flow rates were optimized during the first several months of sampling and were kept as constant as possible thereafter. The water level (drawdown) was continuously monitored (using and water-level tape) during purging to avoid dewatering the well screen, if applicable. The following information was recorded to document well purging activities: pumping rate, drawdown, and volume purged; water-quality parameter values (table 2); visual evaluation of purge-water turbidity, particulates, and floc; any deviations from standard well-purging procedures and anomalies; and difficulties and adjustments.

Dissolved-oxygen and temperature measurements made in the flow-through cell may not be representative of in situ ground-water properties. The sensitivity of these water-quality parameters to the measurement methods used and a technique used to test the degree of this sensitivity are discussed in the following paragraphs.

During each cycle of the bladder pump, water pumped through the well discharge tubing enters the base of the flow-through cell, flows past the sensors, and exits from the top of the flow-through cell. Each pump cycle consists of refill and discharge periods during which water enters and is expelled from the pump bladder. The lengths of refill and discharge time periods were specified for each well on the basis of pump flow-rate optimization (Naus and others, 2005). For all wells, there is a time lag between discharge cycles, and although the flow-through cell is always full, water does not continuously flow past the sensors. Therefore, measured dissolved-oxygen concentrations fluctuate with the pump cycles, and the recorded value depends on when the value was recorded during the cycle. Therefore, each time water-quality parameters were recorded, the dissolved-oxygen concentrations were observed for a complete pump cycle, and the highest and lowest concentrations were recorded. The lowest concentrations correspond to the flow of water past the dissolved-oxygen sensor and are most representative of actual dissolved-oxygen concentrations.

Table 2. Water-quality parameters, measuring equipment, stabilization criteria, and calibration guidelines

[±, plus or minus; >, greater than; <, less than; ≤, less than or equal to; µS/cm, microsiemens per centimeter at 25 degrees Celsius; Eh, redox potential; emf, electromotive force, mV, millivolts; NTU, nephelometric turbidity unit]

Parameter	Equipment used[1]	Stabilization criteria (variability should be within the value shown)	Calibration guidelines
pH	Beckman 265 pH meter or Orion model 1230 multi-parameter meter with Orion Ross 815600, Orion 9107 Triode, or WTW SenTix 41-3 electrode	±0.1 pH unit[1]	Calibrate each morning. Check calibration at each sample site; recalibrate if not within 0.05 standard pH unit.
Specific conductance	Orion model 1230 multi-parameter meter with Orion 013010 DuraProbe or WTW TetraCon 325 conductivity cell	≤ 100 µS/cm: ±5 percent[1] > 100 µS/cm: ±3 percent[1]	Calibrate each morning.
Eh[2]	Orion model 1230 multi-parameter meter with Orion 96-78-00 or WTW SenTix ORP electrode	±10 mv or <10 mV drift in 10 minutes	Check using ZoBell's solution at the start and end of each trip (more often if necessary). (ZoBell, 1946; Nordstrom, 1977).
Dissolved oxygen	Orion model 1230 multi-parameter meter with Orion 083010 or WTW CellOx 325 galvanic dissolved-oxygen probe	±0.3 milligram per liter[1]	Calibrate each morning. Inspect electrode for bubbles under membrane at each sample site; replace if necessary.
Temperature	Thermistors included in pH electrodes or dissolved-oxygen probes	±0.2 degrees Celsius[1]	Calibrate annually; check calibration quarterly.
Turbidity[3]	Hach 2100P turbidimeter	±10 percent[1] if turbidity is below 10 NTU; cease monitoring turbidity when turbidity is below 10 NTU	Calibrate with a primary standard on a quarterly basis. Check calibration against secondary standards at the beginning of each trip.

[1] U. S. Geological Survey (Wilde and Radtke, 1998).

[2] Electromotive force (emf) was measure and Eh was then calculated. Eh should not be a limiting factor in determining stability prior to monitoring.

[3] Turbidity criteria should not be too stringent to avoid excessive purge times and should not be a limiting factor in determining stability prior to monitoring.

The dissolved-oxygen sensor is placed immediately adjacent to the well discharge tubing inlet at the base of the cell, which minimizes the possibility of measuring dissolved-oxygen concentration in water that has contacted air. However, head space can exist at the top of the flow-through cell and could affect these dissolved-oxygen concentrations. To test the effect of head space, dissolved-oxygen concentrations were remeasured after sample collection by placing the sensor and well discharge tubing in a graduated cylinder and allowing the cylinder to overflow, thereby eliminating headspace. The lowest recorded flow-through cell dissolved-oxygen concentrations were compared with the dissolved-oxygen concentrations measured in the graduated cylinder.

The temperature of water in the flow-through cell could be affected by air temperature, especially during summer and winter months. Water temperature also was measured in the flow-through cell during purging and in the graduated cylinder during dissolved-oxygen tests (or in a beaker when no dissolved-oxygen tests were conducted), and the temperatures were compared. Dissolved-oxygen concentrations and temperatures measured in the graduated cylinder are considered more accurate because the graduated cylinder method eliminates the possibility of ground water contacting oxygen in the head space in the flow-through cell and of air temperature warming or cooling water in the flow-through cell.

Equipment in contact with water from more than one well during a sampling trip (non-dedicated equipment) was decontaminated in the laboratory prior to each sampling trip and in the field between well visits. The portable bladder pump was decontaminated using one of two methods. Prior to May 2003, the pump was cleaned by disassembling the pump, soaking the pump housing and fittings in (and scrubbing with, if necessary) non-phosphate laboratory detergent, and rinsing with deionized water (DIW). Beginning in May 2003, the portable pump was decontaminated by disassembling the pump and rinsing with sulfuric acid and DIW. Bladders were dedicated to each well and did not require decontamination. The electric water-level tape was decontaminated in the field by spraying it with DIW and in the laboratory by soaking it in (and scrubbing with, if necessary) non-phosphate laboratory detergent and rinsing with DIW. Equipment that did not contact sample water did not require decontamination between well visits unless its exterior became visibly dirty. Dedicated pumps and tubing required no decontamination.

Surface Water Collection

Surface waters were collected by pumping water from as close to the center of flow as possible using a peristaltic pump. Dissolved sample splits were filtered through either a 142-mm diameter plastic filter holder (Kennedy and others, 1976) containing a 0.1-µm pore size mixed cellulose-ester filter membrane or a disposable capsule filters having a nominal pore size of 0.45 µm. A few samples were collected by filtering samples through syringe filters having a pore size of either 0.2 or 0.45 µm. For those samples that were syringed filtered, a 4-L grab sample was collected from the source from which the syringe was filled. Total recoverable samples were unfiltered and the bottles were filled using a peristaltic pump or from the 4-L grab sample.

Laboratory Methods

For routine sampling, stable water isotope samples were analyzed by the USGS Stable Isotope Laboratory in Reston, Virginia. Sulfur isotope samples were analyzed by the USGS Crustal Imaging and Characterization Team Laboratory in Denver, Colorado. Analyses of all other samples were performed by the USGS Branch of Regional Research Laboratory in Boulder, Colorado. Dissolved inorganic carbon concentrations were calculated using the program WATEQ4F (Ball and Nordstrom, 1991). For samples collected for age dating of water, the USGS Noble Gas Laboratory in Denver, Colorado, analyzed dissolved-gas (CFC) and tritium samples. Chlorofluorocarbon determinations were performed by the USGS Chlorofluorocarbon Laboratory in Reston, Virginia.

Analytical techniques, detection limits, typical precision, equipment used, and analytical method references are summarized in table 3. Estimates of detection limits are assumed equal to 3 times the standard deviation of several dozen measurements of the constituent in a blank solution treated as a

sample. The accuracy and precision typically result in a maximum of 2 significant figures; however, 3 significant figures are reported for concentrations of constituents greater than 100 times the detection limit to avoid the loss of information used for calculations and plots (Silva and other, 1995).

All reagents were of purity at least equal to the reagent-grade standards of the American Chemical Society. Double-distilled or de-ionized water and re-distilled or trace-metal-grade acids were used in all preparations. Samples were diluted as necessary to bring the analyte concentration within the optimal range of the method. Each sample was analyzed in at least duplicate for each dilution for all constituents. Reagent blanks were analyzed as a means to detect contamination from reagents used to prepare standards and dilutions.

Quality Assurance and Quality Control

Several techniques were used to assure the quality of the analytical data (McCleskey and others, 2004). These techniques include analysis of field blanks, standard reference water samples (SRWSs), calculation of charge imbalance (C.I.), spike recoveries, determinations using alternative methods, and determinations by multiple laboratories. Quality assurance and quality control checks for dissolved organic carbon included analyses of laboratory reagent blanks and of synthetic samples made from potassium biphthalate, sodium bicarbonate, and sodium benzoate. Quality assurance and quality control results for samples reported in this study are found in McCleskey and others (2004).

Table 3. Analytical techniques, detection limits, typical precision, equipment used, and analytical method references

[N, normal; ICP-OES, inductively coupled plasma-optical emission spectrometry; mg/L, milligrams per liter; nm, nanometer; IC, ion chromatography; mM, millimolar; ISE, ion-selective electrode; GC, gas chromatography; GFAAS, graphite furnace atomic absorption spectrometry; µg, microgram; ICP-MS, inductively coupled plasma-mass spectrometry; ºC, degrees Celsius; HGAAS, hydride generation atomic absorption spectrometry; TOC, total organic carbon; MS, mass spectrometry; CVAFS, cold-vapor atomic fluorescence spectrometry; µg/L, micrograms per liter; cc/kg, cubic centimeters per kilogram; µcc/kg, microcubic centimeters per kilogram; pcc/kg, picocubic centimeters per kilogram]

Constituent	Analytical technique	Detection limit[1]	Equipment used	Reference(s) and comments
pH	Potentiometry	0.02 pH unit[2]	Beckman 265 pH meter with an Orion Ross combination electrode	Two -or three-buffer calibration at sample temperature using two or three buffers with pH of 10.00, 7.00, 4.01, 2.00, or 1.68
Specific conductance	Conductometry	~0.5 percent[3]	Orion Research model 1230 multiparameter meter with conductivity electrode	automatic temperature correction, calibration with 0.0100 N KCl
Calcium (Ca)	ICP-OES	0.4 mg/L	Leeman Labs Direct Reading Echelle	analytical wavelength: 315.887 nm, view: radial
Magnesium (Mg)	ICP-OES	0.04 mg/L	Leeman Labs Direct Reading Echelle	analytical wavelength: 280.270 nm, view: axial
Sodium (Na)	ICP-OES	0.05 mg/L	Leeman Labs Direct Reading Echelle	analytical wavelength: 589.592 nm, view: radial
Potassium (K)	ICP-OES	0.02 mg/L	Leeman Labs Direct Reading Echelle	analytical wavelength: 766.490 nm, view: axial
Sulfate (SO_4)	IC	0.3 mg/L	Dionex model 2010i ion chromatograph with AG4A guard and AS4A separator columns and Anion Self-Regenerating Suppressor-II	1.8 mM $NaHCO_3$ + 1.7 mM Na_2CO_3 eluent (Brinton and others, 1995)
Alkalinity (as HCO_3)	Titration	1.0 mg/L	Orion Research model 960/940 autotitrator; potentiometric detection; end-point determined by the first derivative technique	Barringer and Johnsson (1989); Fishman and Friedman (1989)
Fluoride (F)	ISE	0.05 mg/L	Orion Research model 96-09 combination F-electrode	Sample mixed 1:1 with total ionic strength adjustment buffer (Barnard and Nordstrom, 1980)
Chloride (Cl)	IC	0.09 mg/L	Dionex model 2010i ion chromatograph with AG4A guard and AS4A separator columns and	1.8 mM $NaHCO_3$ + 1.7 mM Na_2CO_3 eluent (Brinton and others, 1995)
Bromide (Br)	IC	0.1 mg/L	Dionex model 2010i ion chromatograph with AG4A guard and AS4A separator columns and	1.8 mM $NaHCO_3$ + 1.7 mM Na_2CO_3 eluent (Brinton and others, 1995)
Silica (SiO_2)	ICP-OES	0.06 mg/L	Leeman Labs Direct Reading Echelle	Sample diluted 1:10 in field, analytical wavelength: 251.611 nm, view: axial
Aluminum (Al)	ICP-OES GFAAS[4]	0.07 mg/L 0.001 mg/L	Leeman Labs Direct Reading Echelle or Perkin-Elmer model 4110ZL	analytical wavelength: 308.215 nm, view: axial analytical wavelength: 309.3 nm, modifier: 15 µg $Mg(NO_3)_2$, atomization temperature: 2,300°C
Total iron (Fe(T))	ICP-OES Colorimetry	0.07 mg/L 0.001 mg/L	Leeman Labs Direct Reading Echelle or Hewlett-Packard model 8452A diode array spectrometer with 1- and 5- cm cells	analytical wavelength: 238.204. nm, view: axial Colorimetry: FerroZine method (Stookey, 1970; To and others, 1999)
Ferrous iron (Fe(II))	Colorimetry	0.002 mg/L	Hewlett-Packard model 8452A diode array spectrometer with 1- and 5- cm cells	FerroZine method (Stookey, 1970; To and others, 1999)
Boron (B)	ICP-OES	0.010 mg/L	Leeman Labs Direct Reading Echelle	analytical wavelength: 249.678 nm, view: axial
Lithium (Li)	ICP-OES	0.001 mg/L	Leeman Labs Direct Reading Echelle	analytical wavelength: 670.784 nm, view: axial

Table 3. Analytical techniques, detection limits, typical precision, equipment used, and analytical method references - Continued

[N, normal; ICP-OES, inductively coupled plasma-optical emission spectrometry; mg/L, milligrams per liter; nm, nanometer; IC, ion chromatography; mM, millimolar; ISE, ion-selective electrode; GC, gas chromatography; GFAAS, graphite furnace atomic absorption spectrometry; µg, microgram; ICP-MS, inductively coupled plasma-mass spectrometry; ºC, degrees Celsius; HGAAS, hydride generation atomic absorption spectrometry; TOC, total organic carbon; MS, mass spectrometry; CVAFS, cold-vapor atomic fluorescence spectrometry; µg/L, micrograms per liter; cc/kg, cubic centimeters per kilogram; µcc/kg, microcubic centimeters per kilogram; pcc/kg, picocubic centimeters per kilogram]

Constituent	Analytical technique	Detection limit[1]	Equipment used	Reference(s) and comments
Strontium (Sr)	ICP-OES	0.0003 mg/L	Leeman Labs Direct Reading Echelle	analytical wavelength: 421.552 nm, view: axial
Barium (Ba)	ICP-OES	0.0008 mg/L	Leeman Labs Direct Reading Echelle	analytical wavelength: 455.403 nm, view: axial
Manganese (Mn)	ICP-OES	0.002 mg/L	Leeman Labs Direct Reading Echelle	analytical wavelength: 257.610 nm, view: axial
Zinc (Zn)	ICP-OES	0.005 mg/L	Leeman Labs Direct Reading Echelle	analytical wavelength: 206.200 nm, view: radial
Lead (Pb)	ICP-OES	0.008 mg/L	Leeman Labs Direct Reading Echelle or	analytical wavelength: 220.353 nm, view: axial
	GFAAS[4]	0.0003 mg/L	Perkin-Elmer model 4110ZL	analytical wavelength: 283.3 nm, view: axial; modifier: 50 µg PO_4 + 3 µg $Mg(NO_3)_2$, atomization temperature: 1,600°C
Nickel (Ni)	ICP-OES	0.002 mg/L	Leeman Labs Direct Reading Echelle or	analytical wavelength: 231.604. nm, view: axial
	GFAAS[4]	0.0005 mg/L	Perkin-Elmer model 4110ZL	analytical wavelength: 231.604 nm, view: axial, atomization temperature: 2300°C
Copper (Cu)	ICP-OES	0.002 mg/L	Leeman Labs Direct Reading Echelle or	analytical wavelength: 324.754. nm, view: axial
	GFAAS[4]	0.0005 mg/L	Perkin-Elmer model 4110ZL	analytical wavelength: 324.8 nm, modifier: 5 µg Pd + 3 µg $Mg(NO_3)_2$, atomization temperature: 2,000 °C
Cadmium (Cd)	ICP-OES	0.002 mg/L	Leeman Labs Direct Reading Echelle or	analytical wavelength: 214.428. nm, view: axial
	GFAAS[4]	0.0002 mg/L	Perkin-Elmer model 4110ZL	analytical wavelength: 228.8 nm, modifier: 50 µg PO_4 + 3 µg $Mg(NO_3)_2$, atomization temperature: 1,500 °C
Chromium (Cr)	ICP-OES	0.002 mg/L	Leeman Labs Direct Reading Echelle or	analytical wavelength: 206.149. nm, view: axial
	GFAAS[4]	0.0005 mg/L	Perkin-Elmer model 4110ZL	analytical wavelength: 357.9 nm, modifier: 15 µg $Mg(NO_3)_2$, atomization temperature: 2,300 °C
Cobalt (Co)	ICP-OES	0.007 mg/L	Leeman Labs Direct Reading Echelle or	analytical wavelength: 228.616. nm, view: axial
	GFAAS[4]	0.0008 mg/L	Perkin-Elmer model 4110ZL	analytical wavelength: 242.5 nm, modifier: 15 µg $Mg(NO_3)_2$, atomization temperature: 2,400 °C
Beryllium (Be)	ICP-OES	0.001 mg/L	Leeman Labs Direct Reading Echelle	analytical wavelength: 313.042 nm, view: axial
Molybdenum (Mo)	ICP-OES	0.007 mg/L	Leeman Labs Direct Reading Echelle	analytical wavelength: 277.540 nm, view: axial
	ICP-MS[5]	0.0005 mg/L	Perkin-Elmer SCIEX ELAN 6000	Isotope: 95 (Garbarino and Taylor, 1995)
Vanadium (V)	ICP-OES	0.002 mg/L	Leeman Labs Direct Reading Echelle	analytical wavelength: 292.401 nm, view: axial
	ICP-MS[5]	0.0003 mg/L	Perkin-Elmer SCIEX ELAN 6000	Isotope: 51 (Garbarino and Taylor, 1995)
Arsenic (As)	ICP-OES	0.04 mg/L	Leeman Labs Direct Reading Echelle or	analytical wavelength: 188.977. nm, view: axial
	HGAAS	0.0001 mg/L	Perkin-Elmer AAnalyst 300 atomic absorption spectrometer with an FIAS-100 flow-injection analysis system, quartz cell, and furnace	pre-reduction of As(V) using KI + ascorbic acid + HCl (McCleskey and others, 2003)

Table 3. Analytical techniques, detection limits, typical precision, equipment used, and analytical method references - Continued

[N, normal; ICP-OES, inductively coupled plasma-optical emission spectrometry; mg/L, milligrams per liter; nm, nanometer; IC, ion chromatography; mM, millimolar; ISE, ion-selective electrode; GC, gas chromatography; GFAAS, graphite furnace atomic absorption spectrometry; µg, microgram; ICP-MS, inductively coupled plasma-mass spectrometry; ºC, degrees Celsius; HGAAS, hydride generation atomic absorption spectrometry; TOC, total organic carbon; MS, mass spectrometry; CVAFS, cold-vapor atomic fluorescence spectrometry; µg/L, micrograms per liter; cc/kg, cubic centimeters per kilogram; µcc/kg, microcubic centimeters per kilogram; pcc/kg, picocubic centimeters per kilogram]

Constituent	Analytical technique	Detection limit[1]	Equipment used	Reference(s) and comments
Selenium (Se)	ICP-OES	0.04 mg/L	Leeman Labs Direct Reading Echelle	analytical wavelength: 196.026. nm, view: axial
	GFAAS[4]	0.001 mg/L	Perkin-Elmer model 4110ZL	analytical wavelength: 196.0 nm, modifier: 5 µg Pd + 3 µg $Mg(NO_3)_2$, atomization temperature: 1,300 °C
	ICP-MS[5]	0.0002 mg/L	Perkin-Elmer SCIEX ELAN 6000	Isotope: 77 (Garbarino and Taylor, 1995)
Mercury (Hg)	CVAFS	0.4 mg/L	PS Analytical, model Galahad, direct cold-vapor atomic fluorescence spectrometry	Taylor and others (1997); Roth and others (2001)
Bismuth (Bi)	ICP-MS[5]	0.001 µg/L	Perkin-Elmer SCIEX ELAN 6000	Isotope: 209
Cerium (Ce)	ICP-MS[5]	0.0004 µg/L	Perkin-Elmer SCIEX ELAN 6000	Isotope: 140 (Verplanck and others, 2001)
Cesium (Cs)	ICP-MS[5]	0.002 µg/L	Perkin-Elmer SCIEX ELAN 6000	Isotope: 133
Dysprosium (Dy)	ICP-MS[5]	0.0004 µg/L	Perkin-Elmer SCIEX ELAN 6000	Isotope: 163 (Verplanck and others, 2001)
Erbium (Er)	ICP-MS[5]	0.0004 µg/L	Perkin-Elmer SCIEX ELAN 6000	Isotope: 167 (Verplanck and others, 2001)
Europium (Eu)	ICP-MS[5]	0.001 µg/L	Perkin-Elmer SCIEX ELAN 6000	Isotope: 151, problems with Ba interference (Verplanck and others, 2001)
Gadolinium (Gd)	ICP-MS[5]	0.0006 µg/L	Perkin-Elmer SCIEX ELAN 6000	Isotope: 158 (Verplanck and others, 2001)
Holmium (Ho)	ICP-MS[5]	0.0002 µg/L	Perkin-Elmer SCIEX ELAN 6000	Isotope: 165 (Verplanck and others, 2001)
Lanthanum (La)	ICP-MS[5]	0.0004 µg/L	Perkin-Elmer SCIEX ELAN 6000	Isotope: 139 (Verplanck and others, 2001)
Lutetium (Lu)	ICP-MS[5]	0.0002 µg/L	Perkin-Elmer SCIEX ELAN 6000	Isotope: 175 (Verplanck and others, 2001)
Neodymium (Nd)	ICP-MS[5]	0.0008 µg/L	Perkin-Elmer SCIEX ELAN 6000	Isotope: 146 (Verplanck and others, 2001)
Lead (Pb)	ICP-MS[5]	0.01 µg/L	Perkin-Elmer SCIEX ELAN 6000	A weighted average of the 206, 207, and 208 isotopes is used (Garbarino and Taylor, 1995; Taylor and Garbarino, 1991)
Praseodymium (Pr)	ICP-MS[5]	0.0002 µg/L	Perkin-Elmer SCIEX ELAN 6000	Isotope: 141 (Verplanck and others, 2001)
Rubidium (Rb)	ICP-MS[5]	0.001 µg/L	Perkin-Elmer SCIEX ELAN 6000	Isotope: 85
Rhenium (Re)	ICP-MS[5]	0.0007 µg/L	Perkin-Elmer SCIEX ELAN 6000	Isotope: 187
Antimony (Sb)	ICP-MS[5]	0.004 µg/L	Perkin-Elmer SCIEX ELAN 6000	Isotope: 121 (Garbarino and Taylor, 1995; Taylor and Garbarino, 1991)
Samarium (Sm)	ICP-MS[5]	0.0008 µg/L	Perkin-Elmer SCIEX ELAN 6000	Isotope: 147 (Verplanck and others, 2001)
Terbium (Tb)	ICP-MS[5]	0.0002 µg/L	Perkin-Elmer SCIEX ELAN 6000	Isotope: 159 (Verplanck and others, 2001)
Tellurium (Te)	ICP-MS[5]	0.008 µg/L	Perkin-Elmer SCIEX ELAN 6000	Isotope: 126
Thorium (Th)	ICP-MS[5]	0.001 µg/L	Perkin-Elmer SCIEX ELAN 6000	Isotope: 232
Thallium (Tl)	ICP-MS[5]	0.004 µg/L	Perkin-Elmer SCIEX ELAN 6000	Isotope: 205 (Garbarino and Taylor, 1995; Taylor and Garbarino, 1991)
Thulium (Tm)	ICP-MS[5]	0.0002 µg/L	Perkin-Elmer SCIEX ELAN 6000	Isotope: 169 (Verplanck and others, 2001)
Uranium (U)	ICP-MS[5]	0.0005 µg/L	Perkin-Elmer SCIEX ELAN 6000	Isotope: 238 (Garbarino and Taylor, 1995; Taylor and Garbarino, 1991)
Tungsten (W)	ICP-MS[5]	0.006 µg/L	Perkin-Elmer SCIEX ELAN 6000	Isotope: 182
Yttrium (Y)	ICP-MS[5]	0.0003 µg/L	Perkin-Elmer SCIEX ELAN 6000	Isotope: 89
Ytterbium (Yb)	ICP-MS[5]	0.0005 µg/L	Perkin-Elmer SCIEX ELAN 6000	Isotope: 174 (Verplanck and others, 2001)

Table 3. Analytical techniques, detection limits, typical precision, equipment used, and analytical method references - Continued

[N, normal; ICP-OES, inductively coupled plasma-optical emission spectrometry; mg/L, milligrams per liter; nm, nanometer; IC, ion chromatography; mM, millimolar; ISE, ion-selective electrode; GC, gas chromatography; GFAAS, graphite furnace atomic absorption spectrometry; µg, microgram; ICP-MS, inductively coupled plasma-mass spectrometry; ºC, degrees Celsius; HGAAS, hydride generation atomic absorption spectrometry; TOC, total organic carbon; MS, mass spectrometry; CVAFS, cold-vapor atomic fluorescence spectrometry; µg/L, micrograms per liter; cc/kg, cubic centimeters per kilogram; µcc/kg, microcubic centimeters per kilogram; pcc/kg, picocubic centimeters per kilogram]

Constituent	Analytical technique	Detection limit[1]	Equipment used	Reference(s) and comments
Zirconium (Zr)	ICP-MS[5]	0.001 µg/L	Perkin-Elmer SCIEX ELAN 6000	Isotope: 90
Dissolved organic carbon (DOC)	TOC	0.1 mg/L	Oceanography International Model 700 TOC Analyzer	Wet oxidation method (Aiken, 1992)
Hydrogen sulfide (H_2S)	Colorimetry	0.002 mg/L	Hach model DR-2000 UV-Vis absorption spectrometer and Hach method # 8131 reagents	Method based on APHA (1985)
$^{18}O/^{16}O$ ($\delta^{18}O$)	MS	0.1 per mil[2]	DuPont model 21-491 mass spectrometer	Standardization against Vienna Standard Mean Ocean Water (VSMOW) ($\delta^{18}O$ = 0 per mil) and Standard Light Antartic Precipitation (SLAP) ($\delta^{18}O$ = ‑55.5 per mil) (Epstein and Mayeda, 1953)
$^{2}H/^{1}H$ ($\delta^{2}H$)	MS	0.1 per mil[2]	V.G. Micromass model 602 mass spectrometer	Standardization against VSMOW (δ2H = 0 per mil) and SLAP (δ2H = ‑428 per mil) (Coplen and others, 1991)
$^{34}S/^{32}S$ ($\delta^{34}S$) of sulfate	MS	0.1 per mil[2]	Carlo Erba NC2500 elemental analyzer coupled to either a Micromass Optima or a Finnigan Delta Plus XL mass spectrometer	Analyses were done by combustion using continuous flow methods described by Giesemann and others (1994). Sulfate ion removed from the samples using barium sulfate precipitation method
$^{18}O/^{16}O$ ($\delta^{18}O$) of sulfate	MS	0.1 per mil[2]	Micromass Optima mass spectrometer	Sulfate ion removed from the samples using barium sulfate precipitation method
CFC-11, CFC-12, CFC-113	GC	0.5-1.0 picogram/kilogram	Shimadzu GC-8AIE gas chromatograph (GC) with an electron capturedetector (ECD), Agilent model 6890A GC with an ECD	U.S. Geological Survey (2004b)
Dissolved gases (CH_4, N_2, O_2, Ar)	Quadrupole-MS	0.005 cc/kg	Prisma quadrupole mass spectrometer	Solomon and others (1996)
Dissolved gas isotopes (^{3}He, ^{4}He, Ne)	Magnetic sector-field MS	^{3}He: 0.07 µcc/kg	Mass Analyzer Products 215-50 mass spectrometer	Bayer and others (1989); Solomon and others (1996)
Tritium (^{3}H)	^{3}He in-growth technique	0.05 tritium unit	Mass Analyzer Products 215-50 mass spectrometer	Clark and others (1976); Bayer and others (1989)

[1] Some samples were diluted for ICP-MS analysis; reported detection limits must be multiplied by the dilution factor for these samples.

[2] These values are expressions of precision or range, rather than relative standard deviation, for pH and isotope determinations.

[3] Percent relative standard deviation

[4] GFAAS was used when the concentration of the constituent was below or near the ICP-OES detection limit.

[5] ICP-MS was used for a selected subset of samples.

GROUND-WATER GEOCHEMISTRY

Water analyses are reported in tables 4 and 5. Table 4 includes routine analyses performed for nearly every sampling event, analyses performed for only selected sampling events including mercury and isotope analyses, and charge imbalance (C.I.) calculations. Table 5 is composed of ICP-MS analyses for the February and May, 2003, samples. Sample identification numbers in tables 4 and 5 for ground-water samples are the well numbers (figures 1 – 5) and for surface-water samples are by catchment plus an 'SW' and 'high' for high altitude and 'low' for low altitude position in the catchment. Samples having an 'R' represent duplicates.

Charge imbalances were calculated using the program WATEQ4F (Ball and Nordstrom, 1991) according to the following equation:

$$\text{C.I.(percent)} = \frac{100 \text{ x (sum cations - sum anions)}}{(\text{sum cations} + \text{sum anions})/2} \tag{1}$$

where sum cations is the sum of the cations in milliequivalents per liter and sum anions is the sum of the anions in milliequivalents per liter. The C.I.s are twice the value normally reported because the denominator contains the average of the cation plus anion sum rather than just the cation plus anion sum. The frequency distribution of the C.I. is shown in figure 6A along with the normal (or Gaussian) distribution for 32 samples. All analyses have C.I. less than ± 11 percent, averaged +0.8 percent with a standard deviation of ± 5.8 percent, and are considered to be of sufficiently high quality for speciation calculations.

Speciation, ionic strength, saturation index, and redox potential calculations based on Fe(II)/Fe(III) determinations were obtained with the WATEQ4F code. The saturation index, SI, is defined as the logarithm of the ratio of the ion-activity product, IAP, to the solubility product constant, Ksp (Nordstrom and Munoz, 1994):

$$SI = \log\left[\frac{IAP}{K_{sp}}\right] \tag{2}$$

If the solution is in equilibrium with a mineral, the IAP=Ksp and the SI = 0. If the SI>0, the solution is supersaturated and the mineral would tend to precipitate; if the SI<0, the solution is undersaturated and the mineral, if present, would tend to dissolve.

The redox potential relative to the standard hydrogen electrode, or Eh, is calculated from the Fe(II/III) determinations after speciation with the Nernst electrochemical equilibrium equation:

$$Eh(T) = E^{o}(T) - \frac{2.303RT}{nF}\log\frac{a_{Fe^{2+}}}{a_{Fe^{3+}}} \tag{3}$$

where E° is the standard electrode potential of the Fe(II)- Fe(III) redox couple, in volts, at temperature, T, in degrees Celsius; R is the ideal gas constant; n is the number of electrodes transferred in the redox reaction; F is the Faraday constant; and $a_{Fe^{2+}}$ and $a_{Fe^{3+}}$ are the activities of the free ferrous (Fe(II)) and ferric ions (Fe(III)) in solution, respectively (Nordstrom and Munoz, 1994).

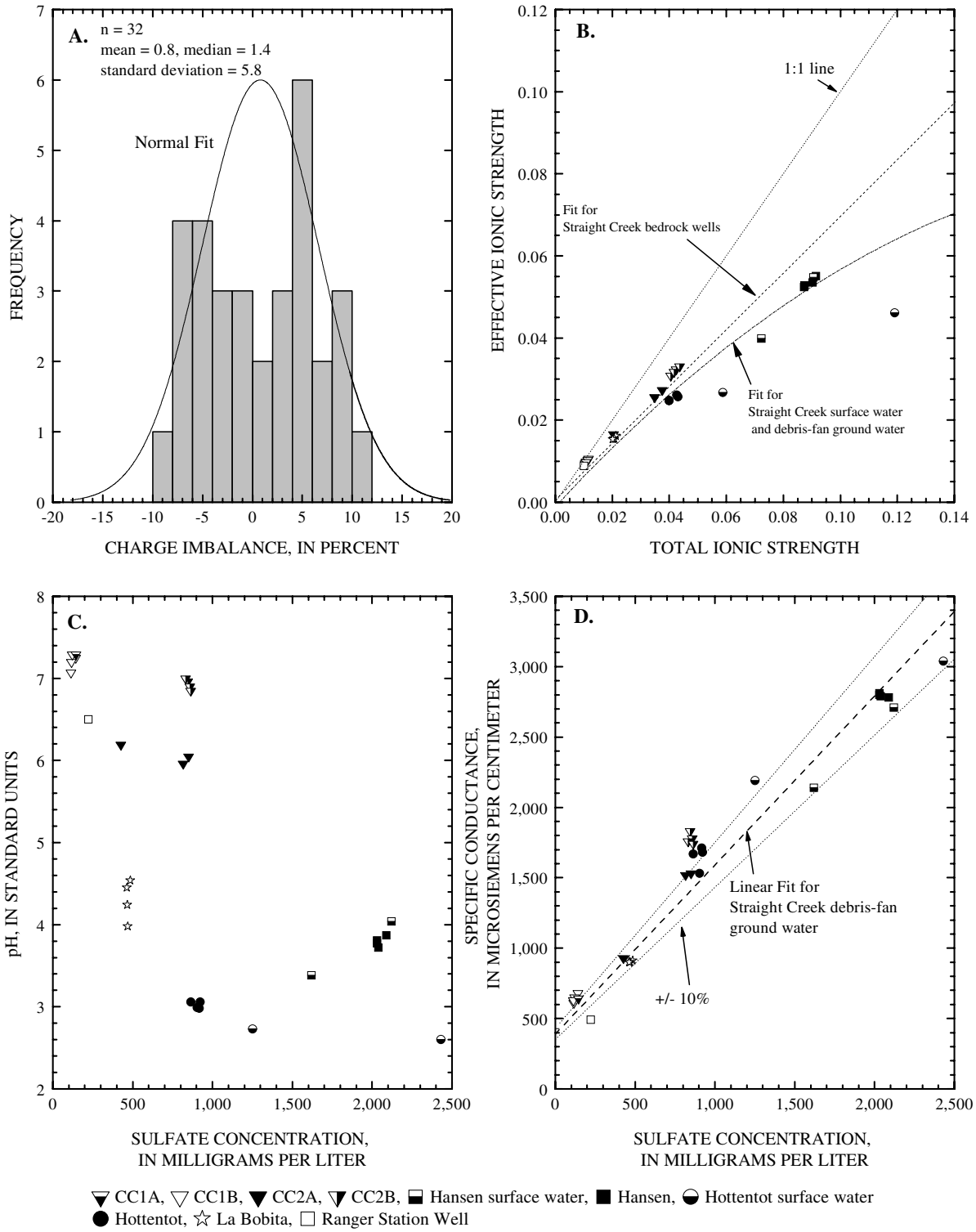

Figure 6. A. Frequency distribution of charge imbalance in percent using equation 1. **B.** Effective molal ionic strength in relation to total molal ionic strength. **C.** pH in relation to sulfate concentration. **D.** Specific conductance in relation to sulfate concentration with linear fit for Straight Creek debris-fan ground-water data.

A considerable range of dissolved solids concentrations and ionic strengths were encountered in these ground waters. Figure 6B shows the range in both total and effective ionic strength for these waters. Only 29 data points are plotted because constituents were averaged for duplicate samples. Effective ionic strength is the computed ionic strength after speciation using WATEQ4F, and total ionic strength is the computed ionic strength before speciation. Both are computed according to the following formula:

$$I = \frac{1}{2}\sum_i m_i z_i^2 \tag{4}$$

where I is the ionic strength, m_i is the molality of the i^{th} ion, and z_i is the electronic charge on the i^{th} ion.

Figure 6B exhibits a range of total ionic strength from 0 to 0.12 molal, but the effective ionic strength does not increase at the same rate as the total ionic strength. The effective ionic strength ranges from 0.01 to 0.055 molal for these waters, about half of the total ionic strength. The decrease in the effective ionic strength relative to the total ionic strength is caused by complexing of sulfate with polyvalent cations such as calcium, iron, and aluminum. These waters are much lower in total or effective ionic strength than sea water, considered to be the upper limit for application of the ion association model for speciation (Nordstrom and Munoz, 1994). Hence, the ion association model should be applicable for these waters.

Figure 6C plots the pH values of ground waters for phase II wells as a function of sulfate concentration to show the range in these parameters. The pH values (2.6 to 7.3) and sulfate concentrations (100 to 2,400 mg/L) cover similar ranges as those found in the Straight Creek ground waters (Naus and others, 2005). The lowest pH values are found in the Hottentot surface waters and the Hottentot ground water, whereas the highest pH values are found in the Capulin Canyon wells. The general trend of values in figure 6C demonstrates lower pH with increasing sulfate concentration that reflects increasing contribution of acid sulfate waters from pyrite oxidation.

Figure 6D is a plot of specific conductance in relation to sulfate concentration with a dashed line showing the linear fit from the Straight Creek alluvial ground water values. All the phase II data are consistent with the linear correlation from the Straight Creek data and demonstrates that not only is there nothing unusual or anomalous about the phase II data, but a sample's sulfate concentration could be estimated from a measure of its specific conductance. The linear least-squares fit equation for the Straight Creek data is:

$$\text{sulfate concentration (mg/L)} = 0.83\left(\frac{\text{mg/L}}{\mu\text{S/cm}}\right) \times \text{specific conductance } (\mu\text{S/cm}) - 390(\text{mg/L}) \tag{5}$$

When the specific conductance is above 600 µS/cm, the sulfate concentration for ground waters in the Red River Valley can be estimated to within 10 percent of its actual value from the specific conductance measurement.

The equations of best fit from the Straight Creek data (Naus and others, 2005) are reproduced in table 6 because they are used in most of the following diagrams to compare the trends in ground- and surface-water chemistry data for Straight Creek with those for other Phase II observation wells and surface water from Hottentot Creek and Hansen Creek.

Table 4. Water analyses for Phase II wells and Hottentot Creek and Hansen Creek surface waters

[DIW, deionized water; ID, identification; GW, ground water; µm, micrometer; µS/cm, microsiemens per centimeter; mg/L, milligrams per liter; R, replicate; RA, raw-acidified; SW, surface water; <, less than; ---, not analyzed; °C, degrees Celsius]

Sample ID	**CC1A**	**CC1A**	**CC1A**	**CC1A**	**CC1B**
Collection Date	**2/5/2003**	**2/5/2003**	**5/14/2003**	**5/14/2003**	**2/5/2003**
Treatment	**Filtered - 0.45 µm**	**RA**	**Filtered - 0.45 µm**	**RA**	**Filtered - 0.45 µm**
Specific conductance (field / laboratory), µS/cm	640 / 463	640 / 463	680 / 436	680 / 436	680 / 443
pH (field / laboratory)	7.29 / 8.02	7.29 / 8.02	5.65 / 8.41	5.65 / 8.41	7.25 / 7.88
Temperature, °C	---	---	16.9	16.9	6.2
Eh, volts	---	---	0.256	0.256	0.300
Dissolved oxygen, mg/L	---	---	6.12	6.12	3.00
Constituents, mg/L [1]					
Calcium (Ca)	82.7	85.5	---	59.2	96.5
Magnesium (Mg)	14.1	22.2	---	10.3	14.2
Sodium (Na)	22.8	24.7	---	24.1	24.9
Potassium (K)	2.81	4.11	---	2.53	2.68
Alkalinity (as HCO_3)	180	---	---	---	244
Sulfate (SO_4)	146	---	98.5	---	143
Chloride (Cl)	7.50	---	6.92	---	7.20
Fluoride (F)	0.720	---	1.64	---	0.770
Bromide (Br)	<0.1	---	<0.1	---	<0.1
Silica (SiO_2)	21.2	137	---	38.2	13.4
Aluminum (Al)	0.009	16.6	---	0.853	0.008
Arsenic (As)	0.0002	<0.04	<0.04	<0.04	<0.0001
Arsenite (As(III))	---	---	---	---	---
Barium (Ba)	0.027	0.237	---	0.034	0.036
Beryllium (Be)	<0.001	0.002	---	<0.001	<0.001
Boron (B)	<0.01	0.015	---	0.020	0.013
Cadmium (Cd)	0.0010	0.0007	---	0.0011	<0.0002
Cobalt (Co)	0.002	0.014	---	<0.0007	<0.0007
Copper (Cu)	0.0007	0.0469	---	0.0046	0.0013
Chromium (Cr)	0.0033	0.077	---	0.0039	<0.0005
Iron Total (Fe(T))	0.015	23.8	0.006	1.07	<0.001
Ferrous Iron (Fe(II))	0.008	---	<0.001	---	<0.001
Lead (Pb)	<0.0003	0.063	---	0.0040	<0.0003
Lithium (Li)	0.011	0.030	---	0.010	0.022
Mercury (Hg), ng/L	---	---	---	---	---
Manganese (Mn)	0.350	0.693	---	0.102	0.441
Molybdenum (Mo)	0.007	<0.007	---	0.008	<0.007
Nickel (Ni)	0.0044	0.0522	---	0.0057	0.0051
Selenium (Se)	<0.04	<0.04	---	<0.04	<0.04
Strontium (Sr)	0.865	0.954	---	0.586	1.37
Vanadium (V)	<0.002	0.021	---	<0.002	<0.002
Zinc (Zn)	0.009	0.136	---	0.024	0.026
Dissolved Organic Carbon (DOC)	3.4	---	---	---	2.0
δ^2H, per mil	-94.57	---	---	---	-84.77
$\delta^{18}O$, per mil	-12.65	---	---	---	-11.74
$\delta^{34}S_{SO4}$, per mil	-0.4	---	---	---	-3.4
$\delta^{18}O_{SO4}$, per mil	-0.4	---	---	---	-4.2
Sum cations (meq/L)	5.91	---	---	---	6.62
Sum anions (meq/L)	5.76	---	---	---	6.66
C.I. (percent)	2.5	---	---	---	-0.5

[1]Except for mercury (ng/L)

Table 4. Water analyses for Phase II wells and Hottentot Creek and Hansen Creek surface waters - Continued

[DIW, deionized water; ID, identification; GW, ground water; µm, micrometer; µS/cm, microsiemens per centimeter; mg/L, milligrams per liter; R, replicate; RA, raw-acidified; SW, surface water; <, less than; ---, not analyzed; °C, degrees Celsius]

Sample ID	**CC1B**	**CC1B**	**CC1B**	**CC1B**	**CC1B**
Collection Date	**2/5/2003**	**6/4/2003**	**6/4/2003**	**8/19/2003**	**8/19/2003**
Treatment	**RA**	**Filtered - 0.45 µm**	**RA**	**Filtered - 0.45 µm**	**RA**
Specific conductance (field / laboratory), µS/cm	680 / 443	610 / 409	610 / 409	650 / 485	650 / 485
pH (field / laboratory)	7.25 / 7.88	7.20 / 8.21	7.20 / 8.21	7.29 / 8.22	7.29 / 8.22
Temperature, °C	6.2	10.4	10.4	13.4	13.4
Eh, volts	0.300	0.458	0.458	0.502	0.502
Dissolved oxygen, mg/L	3.00	0.43	0.43	0.10	0.10
Constituents, mg/L [1]					
Calcium (Ca)	94.9	95.5	94.9	99.9	101
Magnesium (Mg)	14.1	13.2	13.6	13.7	14.2
Sodium (Na)	24.1	23.8	23.1	21.7	21.4
Potassium (K)	2.66	1.90	1.86	1.69	1.66
Alkalinity (as HCO_3)	---	239	---	250	---
Sulfate (SO_4)	---	116	---	122	---
Chloride (Cl)	---	5.91	---	6.57	---
Fluoride (F)	---	1.35	---	1.35	---
Bromide (Br)	---	0.23	---	0.25	---
Silica (SiO_2)	13.8	14.7	14.3	13.7	14.0
Aluminum (Al)	0.208	0.005	0.013	0.004	0.020
Arsenic (As)	<0.04	<0.0001	<0.04	<0.0001	<0.04
Arsenite (As(III))	---	---	---	---	---
Barium (Ba)	0.040	0.027	0.027	0.023	0.024
Beryllium (Be)	<0.001	<0.001	<0.001	<0.001	<0.001
Boron (B)	0.013	<0.01	<0.01	0.011	0.011
Cadmium (Cd)	0.0004	<0.0002	0.0003	<0.0002	<0.0002
Cobalt (Co)	0.002	<0.0007	<0.0007	<0.0007	0.001
Copper (Cu)	0.0026	<0.0005	0.0015	<0.0005	0.0010
Chromium (Cr)	0.0010	<0.0005	<0.0005	<0.0005	0.0024
Iron Total (Fe(T))	0.343	0.024	<0.007	0.039	<0.007
Ferrous Iron (Fe(II))	---	0.016		0.037	---
Lead (Pb)	0.0015	<0.0003	<0.0003	0.0011	<0.0003
Lithium (Li)	0.021	0.018	0.017	0.023	0.021
Mercury (Hg), ng/L	---	---	---	---	---
Manganese (Mn)	0.393	0.221	0.224	0.183	0.241
Molybdenum (Mo)	<0.007	<0.007	<0.007	<0.007	<0.007
Nickel (Ni)	0.0052	<0.0005	0.0012	0.0034	0.0047
Selenium (Se)	<0.04	<0.04	<0.04	<0.04	<0.04
Strontium (Sr)	1.33	1.28	1.28	1.15	1.24
Vanadium (V)	<0.002	<0.002	<0.002	<0.002	<0.002
Zinc (Zn)	0.009	<0.005	<0.005	<0.005	<0.005
Dissolved Organic Carbon (DOC)	---	2.2	---	2.2	---
δ^2H, per mil	---	---	---	---	---
$\delta^{18}O$, per mil	---	---	---	---	---
$\delta^{34}S_{SO4}$, per mil	---	---	---	---	---
$\delta^{18}O_{SO4}$, per mil	---	---	---	---	---
Sum cations (meq/L)	---	6.51	---	6.59	---
Sum anions (meq/L)	---	6.09	---	6.35	---
C.I. (percent)	---	6.8	---	3.7	---

[1]Except for mercury (ng/L)

Table 4. Water analyses for Phase II wells and Hottentot Creek and Hansen Creek surface waters - Continued

[DIW, deionized water; ID, identification; GW, ground water; µm, micrometer; µS/cm, microsiemens per centimeter; mg/L, milligrams per liter; R, replicate; RA, raw-acidified; SW, surface water; <, less than; ---, not analyzed; °C, degrees Celsius]

Sample ID	**CC1B**	**CC1B**	**CC2A**	**CC2A**	**CC2A**
Collection Date	**10/22/2003**	**10/22/2003**	**5/14/2003**	**5/14/2003**	**5/14/2003**
Treatment	**Filtered - 0.45 µm**	**RA**	**Filtered - 0.45 µm**	**RA**	**Filtered - 0.45 µm**
Specific conductance (field / laboratory), µS/cm	630 / 490	630 / 490	930 / 878	930 / 878	930 / 974
pH (field / laboratory)	7.07 / 7.9	7.07 / 7.9	6.19 / 7.7	6.19 / 7.7	6.19 / 7.63
Temperature, °C	9.1	9.1	6.9	6.9	6.9
Eh, volts	0.440	0.440	0.348	0.348	0.348
Dissolved oxygen, mg/L	0.23	0.23	5.05	5.05	5.05
Constituents, mg/L [1]					
Calcium (Ca)	93.7	95.9	159	158	171
Magnesium (Mg)	13.1	13.7	11.3	14.6	11.6
Sodium (Na)	22.2	21.4	28.9	29.4	27.6
Potassium (K)	1.90	1.45	5.23	5.22	4.98
Alkalinity (as HCO_3)	241	---	63.6	---	102
Sulfate (SO_4)	113	---	408	---	446
Chloride (Cl)	5.85	---	5.20	---	3.61
Fluoride (F)	1.65	---	8.63	---	8.19
Bromide (Br)	0.17	---	<0.1	---	<0.1
Silica (SiO_2)	14.6	14.4	28.6	33.0	23.9
Aluminum (Al)	0.006	0.013	2.07	3.17	1.00
Arsenic (As)	<0.04	<0.04	<0.0001	<0.04	<0.0001
Arsenite (As(III))	---	---	---	---	---
Barium (Ba)	0.024	0.025	0.004	0.014	0.005
Beryllium (Be)	<0.001	<0.001	0.021	0.020	0.015
Boron (B)	0.016	0.014	0.018	0.018	0.014
Cadmium (Cd)	<0.0002	0.0010	0.0032	0.0034	0.0018
Cobalt (Co)	<0.0007	<0.0007	0.002	0.003	0.004
Copper (Cu)	0.0009	<0.0005	0.0011	0.0043	0.0008
Chromium (Cr)	<0.0005	<0.0005	0.0016	0.0044	0.0010
Iron Total (Fe(T))	0.042	0.042	5.91	7.07	1.80
Ferrous Iron (Fe(II))	0.039	---	5.91	---	1.74
Lead (Pb)	<0.0003	<0.0003	<0.0003	0.0037	0.0005
Lithium (Li)	0.024	0.039	0.038	0.037	0.036
Mercury (Hg), ng/L	0.7	---	---	---	---
Manganese (Mn)	0.216	0.179	10.0	9.59	8.78
Molybdenum (Mo)	<0.007	<0.007	0.012	0.014	0.011
Nickel (Ni)	<0.0005	0.0012	0.0021	0.0052	<0.0005
Selenium (Se)	<0.04	<0.04	<0.04	<0.04	<0.04
Strontium (Sr)	1.26	1.18	0.625	0.636	0.692
Vanadium (V)	<0.002	<0.002	<0.002	<0.002	<0.002
Zinc (Zn)	<0.005	<0.005	0.907	0.857	0.589
Dissolved Organic Carbon (DOC)	2.1	---	1.2	---	---
δ^2H, per mil	---	---	---	---	---
$\delta^{18}O$, per mil	---	---	---	---	---
$\delta^{34}S_{SO4}$, per mil	---	---	-3.1	---	---
$\delta^{18}O_{SO4}$, per mil	---	---	-4.0	---	---
Sum cations (meq/L)	6.34	---	9.21	---	9.35
Sum anions (meq/L)	6.08	---	8.24	---	9.52
C.I. (percent)	4.1	---	11.1	---	-1.8

[1]Except for mercury (ng/L)

Table 4. Water analyses for Phase II wells and Hottentot Creek and Hansen Creek surface waters - Continued

[DIW, deionized water; ID, identification; GW, ground water; µm, micrometer; µS/cm, microsiemens per centimeter; mg/L, milligrams per liter; R, replicate; RA, raw-acidified; SW, surface water; <, less than; ---, not analyzed; °C, degrees Celsius]

Sample ID	**CC2A**	**CC2A**	**CC2A_R**	**CC2A**	**CC2A**
Collection Date	**5/14/2003**	**8/19/2003**	**8/19/2003**	**8/19/2003**	**10/22/2003**
Treatment	**RA**	**Filtered - 0.45 µm**	**Filtered - 0.45 µm**	**RA**	**Filtered - 0.45 µm**
Specific conductance (field / laboratory), µS/cm	930 / 974	1530 / 1430	1530 / 1440	1530 / 1440	1520 / 1400
pH (field / laboratory)	6.19 / 7.63	6.05 / 4.94	6.05 / 4.82	6.05 / 4.82	5.96 / 4.87
Temperature, °C	6.9	16.6	16.6	16.6	16.0
Eh, volts	0.348	0.467	0.467	0.467	0.274
Dissolved oxygen, mg/L	5.05	5.66	5.66	5.66	3.90
Constituents, mg/L [1]					
Calcium (Ca)	178	246	251	255	225
Magnesium (Mg)	12.2	15.9	14.7	19.9	13.2
Sodium (Na)	28.9	34.5	39.1	38.6	35.9
Potassium (K)	5.12	7.56	6.87	6.60	7.21
Alkalinity (as HCO_3)	---	66.0	57.0	---	45.4
Sulfate (SO_4)	---	844	850	---	816
Chloride (Cl)	---	2.98	2.81	---	2.79
Fluoride (F)	---	19.9	20.1	---	19.1
Bromide (Br)	---	0.14	0.14	---	<0.1
Silica (SiO_2)	31.3	26.8	24.1	28.8	26.7
Aluminum (Al)	3.20	5.50	5.42	6.07	5.51
Arsenic (As)	<0.04	<0.0001	<0.0001	<0.04	<0.04
Arsenite (As(III))	---	---	---	---	---
Barium (Ba)	0.015	0.005	0.006	0.008	0.006
Beryllium (Be)	0.015	0.083	0.084	0.089	0.078
Boron (B)	0.014	<0.01	<0.01	<0.01	0.018
Cadmium (Cd)	0.0020	0.0026	0.0028	0.0028	0.0025
Cobalt (Co)	0.004	0.018	0.018	0.017	0.016
Copper (Cu)	0.0042	<0.0005	0.0027	0.0013	<0.0005
Chromium (Cr)	0.0058	0.0006	0.0007	<0.0005	<0.0005
Iron Total (Fe(T))	4.65	36.3	36.3	37.6	33.6
Ferrous Iron (Fe(II))	---	36.3	36.3	---	33.6
Lead (Pb)	0.0047	0.0006	0.0007	0.0006	0.0007
Lithium (Li)	0.038	0.094	0.088	0.093	0.039
Mercury (Hg), ng/L	---	---	---	---	0.9
Manganese (Mn)	8.78	46.9	47.4	49.0	40.9
Molybdenum (Mo)	0.010	0.077	0.055	0.064	0.089
Nickel (Ni)	0.0035	0.0310	0.0302	0.0282	0.0277
Selenium (Se)	<0.04	<0.04	<0.04	<0.04	<0.04
Strontium (Sr)	0.710	0.924	0.893	0.842	0.825
Vanadium (V)	<0.002	<0.002	<0.002	<0.002	<0.002
Zinc (Zn)	0.643	5.46	4.95	5.23	3.96
Dissolved Organic Carbon (DOC)	---	1.1	2.3	---	1.5
δ^2H, per mil	---	---	---	---	---
$\delta^{18}O$, per mil	---	---	---	---	---
$\delta^{34}S_{SO4}$, per mil	---	-3.2	-3.2	---	---
$\delta^{18}O_{SO4}$, per mil	---	-4.3	-4.5	---	---
Sum cations (meq/L)	---	14.1	14.3	---	12.9
Sum anions (meq/L)	---	14.8	14.7	---	14.2
C.I. (percent)	---	-4.8	-2.5	---	-9.6

[1]Except for mercury (ng/L)

Table 4. Water analyses for Phase II wells and Hottentot Creek and Hansen Creek surface waters - Continued

[DIW, deionized water; ID, identification; GW, ground water; µm, micrometer; µS/cm, microsiemens per centimeter; mg/L, milligrams per liter; R, replicate; RA, raw-acidified; SW, surface water; <, less than; ---, not analyzed; °C, degrees Celsius]

Sample ID	**CC2A**	**CC2B**	**CC2B**	**CC2B**	**CC2B**
Collection Date	**10/22/2003**	**2/5/2003**	**2/5/2003**	**6/4/2003**	**6/4/2003**
Treatment	**RA**	**Filtered - 0.45 µm**	**RA**	**Filtered - 0.45 µm**	**RA**
Specific conductance (field / laboratory), µS/cm	1520 / 1400	1830 / 1530	1830 / 1530	1780 / 1480	1780 / 1480
pH (field / laboratory)	5.96 / 4.87	6.96 / 7.82	6.96 / 7.82	6.90 / 7.88	6.90 / 7.88
Temperature, °C	16.0	7.8	7.8	8.7	8.7
Eh, volts	0.274	0.360	0.360	0.297	0.297
Dissolved oxygen, mg/L	3.90	1.72	1.72	1.62	1.62
Constituents, mg/L [1]					
Calcium (Ca)	232	388	379	391	390
Magnesium (Mg)	13.0	20.8	20.1	27.8	75.6
Sodium (Na)	37.8	45.3	46.0	43.6	43.5
Potassium (K)	7.70	4.68	4.73	4.43	4.51
Alkalinity (as HCO_3)	---	287	---	305	---
Sulfate (SO_4)	---	846	---	858	---
Chloride (Cl)	---	2.20	---	2.68	---
Fluoride (F)	---	2.00	---	1.93	---
Bromide (Br)	---	<0.1	---	0.12	---
Silica (SiO_2)	27.7	23.2	22.8	22.9	23.1
Aluminum (Al)	6.38	0.009	0.048	0.007	0.012
Arsenic (As)	<0.04	<0.0001	<0.04	<0.0001	<0.04
Arsenite (As(III))	---	---	---	---	---
Barium (Ba)	0.007	0.012	0.012	0.014	0.014
Beryllium (Be)	0.083	<0.001	<0.001	<0.001	<0.001
Boron (B)	0.015	<0.01	0.021	0.013	0.013
Cadmium (Cd)	0.0025	<0.0002	<0.0002	<0.0002	0.0002
Cobalt (Co)	0.018	<0.0007	0.002	0.002	<0.0007
Copper (Cu)	0.0008	<0.0005	<0.0005	<0.0005	<0.0005
Chromium (Cr)	<0.0005	<0.0005	0.0006	0.0013	0.0010
Iron Total (Fe(T))	38.4	0.105	0.219	0.911	1.16
Ferrous Iron (Fe(II))	---	0.102	---	0.878	---
Lead (Pb)	0.0007	0.0009	<0.0003	<0.0003	<0.0003
Lithium (Li)	0.033	0.061	0.063	0.074	0.080
Mercury (Hg), ng/L	---	---	---	---	---
Manganese (Mn)	43.7	4.92	4.91	5.43	5.37
Molybdenum (Mo)	0.105	<0.007	<0.007	<0.007	0.008
Nickel (Ni)	0.0277	0.0033	0.0035	0.0011	0.0016
Selenium (Se)	<0.04	<0.04	<0.04	<0.04	<0.04
Strontium (Sr)	0.837	4.79	4.95	4.71	4.95
Vanadium (V)	<0.002	<0.002	0.006	<0.002	<0.002
Zinc (Zn)	4.06	0.082	0.073	0.009	0.011
Dissolved Organic Carbon (DOC)	---	0.8	---	2.0	---
δ^2H, per mil	---	-94.19	---	---	---
$\delta^{18}O$, per mil	---	-12.64	---	---	---
$\delta^{34}S_{SO4}$, per mil	---	---	---	---	---
$\delta^{18}O_{SO4}$, per mil	---	---	---	---	---
Sum cations (meq/L)	---	18.4	---	19.0	---
Sum anions (meq/L)	---	17.5	---	17.8	---
C.I. (percent)	---	5.3	---	6.1	---

[1]Except for mercury (ng/L)

Table 4. Water analyses for Phase II wells and Hottentot Creek and Hansen Creek surface waters - Continued

[DIW, deionized water; ID, identification; GW, ground water; µm, micrometer; µS/cm, microsiemens per centimeter; mg/L, milligrams per liter; R, replicate; RA, raw-acidified; SW, surface water; <, less than; ---, not analyzed; °C, degrees Celsius]

Sample ID	**CC2B**	**CC2B**	**CC2B**	**CC2B**	**Hansen**
Collection Date	**8/19/2003**	**8/19/2003**	**10/22/2003**	**10/22/2003**	**2/7/2003**
Treatment	**Filtered - 0.45 µm**	**RA**	**Filtered - 0.45 µm**	**RA**	**Filtered - 0.45 µm**
Specific conductance (field / laboratory), µS/cm	1760 / 1530	1760 / 1530	1740 / 1520	1740 / 1520	2780 / 2730
pH (field / laboratory)	7.00 / 7.82	7.00 / 7.82	6.85 / 7.74	6.85 / 7.74	3.87 / 3.75
Temperature, °C	11.0	11.0	8.7	8.7	6.6
Eh, volts	0.430	0.430	0.044	0.044	0.740
Dissolved oxygen, mg/L	0.12	0.12	0.44	0.44	4.99
Constituents, mg/L [1]					
Calcium (Ca)	355	346	365	370	499
Magnesium (Mg)	20.7	22.2	19.7	22.0	97.3
Sodium (Na)	36.2	38.5	38.0	40.0	17.9
Potassium (K)	4.32	4.29	4.93	5.16	3.79
Alkalinity (as HCO_3)	301	---	304	---	---
Sulfate (SO_4)	832	---	863	---	2090
Chloride (Cl)	2.70	---	2.49	---	2.90
Fluoride (F)	2.00	---	2.02	---	2.66
Bromide (Br)	0.14	---	<0.1	---	<0.1
Silica (SiO_2)	23.1	24.3	23.7	25.5	53.7
Aluminum (Al)	0.018	0.014	0.013	0.011	81.3
Arsenic (As)	0.0002	<0.04	<0.04	<0.04	<0.0001
Arsenite (As(III))	---	---	---	---	---
Barium (Ba)	0.013	0.011	0.013	0.014	0.003
Beryllium (Be)	<0.001	<0.001	<0.001	<0.001	0.016
Boron (B)	<0.01	<0.01	0.011	0.012	0.011
Cadmium (Cd)	<0.0002	0.0003	<0.0002	<0.0002	0.0059
Cobalt (Co)	0.002	<0.0007	0.002	0.001	0.179
Copper (Cu)	<0.0005	0.0127	0.0015	<0.0005	0.117
Chromium (Cr)	0.0008	0.0009	<0.0005	<0.0005	0.0025
Iron Total (Fe(T))	2.27	2.60	1.75	1.73	0.068
Ferrous Iron (Fe(II))	2.24	---	1.65	---	0.009
Lead (Pb)	<0.0003	<0.0003	<0.0003	<0.0003	<0.0003
Lithium (Li)	0.081	0.079	0.066	0.031	0.071
Mercury (Hg), ng/L	---	---	1.0	---	---
Manganese (Mn)	5.10	5.39	4.48	5.03	11.6
Molybdenum (Mo)	<0.007	<0.007	<0.007	<0.007	<0.007
Nickel (Ni)	0.0025	0.0023	<0.0005	<0.0005	0.562
Selenium (Se)	<0.04	<0.04	<0.04	<0.04	<0.04
Strontium (Sr)	4.74	4.46	4.52	4.74	2.79
Vanadium (V)	<0.002	<0.002	<0.002	<0.002	<0.002
Zinc (Zn)	<0.005	0.033	<0.005	<0.005	2.59
Dissolved Organic Carbon (DOC)	1.2	---	1.2	---	0.6
δ^2H, per mil	---	---	---	---	-90.96
$\delta^{18}O$, per mil	---	---	---	---	-12.55
$\delta^{34}S_{SO4}$, per mil	---	---	---	---	---
$\delta^{18}O_{SO4}$, per mil	---	---	---	---	---
Sum cations (meq/L)	16.6	---	17.0	---	27.9
Sum anions (meq/L)	17.6	---	18.2	---	28.0
C.I. (percent)	-5.5	---	-6.7	---	-0.4

[1]Except for mercury (ng/L)

Table 4. Water analyses for Phase II wells and Hottentot Creek and Hansen Creek surface waters - Continued

[DIW, deionized water; ID, identification; GW, ground water; µm, micrometer; µS/cm, microsiemens per centimeter; mg/L, milligrams per liter; R, replicate; RA, raw-acidified; SW, surface water; <, less than; ---, not analyzed; °C, degrees Celsius]

Sample ID	**Hansen**	**Hansen**	**Hansen**	**Hansen**	**Hansen**
Collection Date	**2/7/2003**	**5/13/2003**	**5/13/2003**	**8/19/2003**	**8/19/2003**
Treatment	**RA**	**Filtered - 0.45 µm**	**RA**	**Filtered - 0.45 µm**	**RA**
Specific conductance (field / laboratory), µS/cm	2780 / 2730	2800 / 2690	2800 / 2690	2810 / 2710	2810 / 2710
pH (field / laboratory)	3.87 / 3.75	3.77 / 3.76	3.77 / 3.76	3.81 / 3.75	3.81 / 3.75
Temperature, °C	6.6	8.5	8.5	8.2	8.2
Eh, volts	0.740	0.643	0.643	0.738	0.738
Dissolved oxygen, mg/L	4.99	5.38	5.38	5.65	5.65
Constituents, mg/L [1]					
Calcium (Ca)	493	457	469	456	446
Magnesium (Mg)	93.5	99	101	92.8	98.7
Sodium (Na)	19.0	19.5	19.7	14.3	14.6
Potassium (K)	3.74	4.42	4.61	3.35	3.28
Alkalinity (as HCO_3)	---	---	---	---	---
Sulfate (SO_4)	---	2030	---	2030	---
Chloride (Cl)	---	1.40	---	1.94	---
Fluoride (F)	---	3.69	---	3.55	---
Bromide (Br)	---	<0.1	---	<0.1	---
Silica (SiO_2)	54.4	60.4	63.1	55.4	56.7
Aluminum (Al)	80.6	76.7	77.7	79.8	80.0
Arsenic (As)	<0.04	<0.0001	<0.04	<0.0001	<0.04
Arsenite (As(III))	---	---	---	---	---
Barium (Ba)	0.003	0.003	0.006	0.002	0.003
Beryllium (Be)	0.011	0.019	0.017	0.014	0.012
Boron (B)	<0.01	<0.01	0.010	0.020	<0.01
Cadmium (Cd)	0.0056	0.0062	0.0059	0.0061	0.0058
Cobalt (Co)	0.162	0.211	0.215	0.158	0.181
Copper (Cu)	0.109	0.121	0.118	0.093	0.108
Chromium (Cr)	0.0025	0.0152	0.0154	0.0024	0.0032
Iron Total (Fe(T))	0.042	0.098	0.362	0.053	0.171
Ferrous Iron (Fe(II))	---	0.027	---	<0.001	---
Lead (Pb)	<0.0003	0.0009	<0.0003	<0.0003	<0.0003
Lithium (Li)	0.074	0.090	0.086	0.092	0.095
Mercury (Hg), ng/L	---	---	---	---	---
Manganese (Mn)	11.4	12.2	11.9	10.8	10.4
Molybdenum (Mo)	<0.007	<0.007	<0.007	<0.007	<0.007
Nickel (Ni)	0.564	0.613	0.613	0.587	0.605
Selenium (Se)	<0.04	<0.04	<0.04	<0.04	<0.04
Strontium (Sr)	2.75	2.85	2.93	2.61	2.55
Vanadium (V)	<0.002	<0.002	<0.002	<0.002	<0.002
Zinc (Zn)	2.58	2.83	2.88	2.80	2.88
Dissolved Organic Carbon (DOC)	---	0.6	---	0.8	---
δ^2H, per mil	---	-91.52	---	---	---
$\delta^{18}O$, per mil	---	-12.63	---	---	---
$\delta^{34}S_{SO4}$, per mil	---	-7.0	---	---	---
$\delta^{18}O_{SO4}$, per mil	---	-7.5	---	---	---
Sum cations (meq/L)	---	26.3	---	25.8	---
Sum anions (meq/L)	---	27.5	---	27.5	---
C.I. (percent)	---	-4.4	---	-6.4	---

[1]Except for mercury (ng/L)

Table 4. Water analyses for Phase II wells and Hottentot Creek and Hansen Creek surface waters - Continued

[DIW, deionized water; ID, identification; GW, ground water; µm, micrometer; µS/cm, microsiemens per centimeter; mg/L, milligrams per liter; R, replicate; RA, raw-acidified; SW, surface water; <, less than; ---, not analyzed; °C, degrees Celsius]

Sample ID	**Hansen**	**Hansen**	**Hansen SW - low**	**Hansen SW - low**	**Hansen SW - high**
Collection Date	**10/21/2003**	**10/21/2003**	**9/11/2001**	**9/11/2001**	**9/11/2001**
Treatment	**Filtered - 0.45 µm**	**RA**	**Filtered - 0.1 µm**	**RA**	**Filtered - 0.1 µm**
Specific conductance (field / laboratory), µS/cm	2790 / 2690	2790 / 2690	2710	2710	2140
pH (field / laboratory)	3.72 / 3.75	3.72 / 3.75	4.04	4.04	3.38
Temperature, °C	8.7	8.7	6.5	6.5	12.1
Eh, volts	0.724	0.724	0.527	0.527	0.705
Dissolved oxygen, mg/L	4.96	4.96	---	---	---
Constituents, mg/L [1]					
Calcium (Ca)	448	445	530	530	290
Magnesium (Mg)	113	107	72.0	72.0	50.0
Sodium (Na)	14.6	15.7	13.0	13.0	11.0
Potassium (K)	3.81	3.80	6.80	7.00	6.70
Alkalinity (as HCO_3)	---	---	---	---	---
Sulfate (SO_4)	2040	---	2100	---	1600
Chloride (Cl)	1.8	---	2.0	---	2.0
Fluoride (F)	3.64	---	3.00	---	2.00
Bromide (Br)	<0.1	---	<0.1	---	<0.1
Silica (SiO_2)	55.3	50.0	48.0	46.0	49.0
Aluminum (Al)	87.9	78.7	76.0	81.0	100
Arsenic (As)	<0.0001	<0.04	<0.0001	<0.05	<0.0001
Arsenite (As(III))	---	---	<0.001	---	<0.001
Barium (Ba)	0.003	0.004	0.007	0.007	0.005
Beryllium (Be)	0.016	0.015	0.015	0.015	0.015
Boron (B)	<0.01	0.015	0.007	0.007	0.007
Cadmium (Cd)	0.0059	0.0056	0.008	0.009	0.006
Cobalt (Co)	0.175	0.243	0.210	0.330	0.150
Copper (Cu)	0.111	0.138	0.190	0.190	0.087
Chromium (Cr)	0.0028	0.0036	0.002	0.002	0.004
Iron Total (Fe(T))	0.059	0.120	0.279	0.280	24.3
Ferrous Iron (Fe(II))	0.009	---	0.038	---	5.98
Lead (Pb)	0.0008	<0.0003	<0.008	<0.008	<0.008
Lithium (Li)	0.095	0.098	0.077	0.073	0.075
Mercury (Hg), ng/L	0.9	---	---	---	---
Manganese (Mn)	13.4	12.3	14.2	14.4	7.70
Molybdenum (Mo)	<0.007	<0.007	<0.007	<0.007	<0.007
Nickel (Ni)	0.581	0.535	0.550	0.550	0.370
Selenium (Se)	<0.04	<0.04	<0.05	<0.05	<0.05
Strontium (Sr)	3.09	3.07	2.60	2.50	1.30
Vanadium (V)	<0.002	<0.002	<0.005	<0.005	<0.005
Zinc (Zn)	2.65	2.23	2.86	2.92	2.90
Dissolved Organic Carbon (DOC)	1.1	---	---	---	---
δ^2H, per mil	---	---	-88.74	---	-93.97
$\delta^{18}O$, per mil	---	---	-11.87	---	-12.70
$\delta^{34}S_{SO4}$, per mil	---	---	-8.0	---	-6.5
$\delta^{18}O_{SO4}$, per mil	---	---	-6.9	---	-8.6
Sum cations (meq/L)	27.4	---	26.9	---	19.9
Sum anions (meq/L)	26.9	---	28.5	---	20.8
C.I. (percent)	1.6	---	-5.5	---	-4.5

[1]Except for mercury (ng/L)

Table 4. Water analyses for Phase II wells and Hottentot Creek and Hansen Creek surface waters - Continued

[DIW, deionized water; ID, identification; GW, ground water; µm, micrometer; µS/cm, microsiemens per centimeter; mg/L, milligrams per liter; R, replicate; RA, raw-acidified; SW, surface water; <, less than; ---, not analyzed; °C, degrees Celsius]

Sample ID	**Hansen SW - high**	**Hottentot**	**Hottentot**	**Hottentot**	**Hottentot**
Collection Date	**9/11/2001**	**2/5/2003**	**2/5/2003**	**5/12/2003**	**5/12/2003**
Treatment	**RA**	**Filtered - 0.45 µm**	**RA**	**Filtered - 0.45 µm**	**RA**
Specific conductance (field / laboratory), µS/cm	2140	1670 / 1960	1670 / 1960	1680 / 2000	1680 / 2000
pH (field / laboratory)	3.38	3.06 / 2.61	3.06 / 2.61	3.06 / 2.57	3.06 / 2.57
Temperature, °C	12.1	7.3	7.3	11.0	11.0
Eh, volts	0.705	0.630	0.630	0.629	0.629
Dissolved oxygen, mg/L	---	0.00	0.00	0.59	0.59
Constituents, mg/L [1]					
Calcium (Ca)	290	82.6	80.9	87.2	90.3
Magnesium (Mg)	50.0	36.6	35.5	40.2	42.0
Sodium (Na)	11.0	9.02	9.13	8.14	8.29
Potassium (K)	6.70	2.06	2.13	2.16	2.25
Alkalinity (as HCO_3)	---	---	---	---	---
Sulfate (SO_4)	---	864	---	922	---
Chloride (Cl)	---	3.20	---	2.82	---
Fluoride (F)	---	3.62	---	4.14	---
Bromide (Br)	---	<0.1	---	<0.1	---
Silica (SiO_2)	48.0	92.1	87.7	95.5	96.6
Aluminum (Al)	110	60.3	64.0	70.4	69.9
Arsenic (As)	<0.05	0.0001	<0.04	0.0004	<0.04
Arsenite (As(III))	---	---	---	---	---
Barium (Ba)	0.007	0.001	0.002	0.001	0.001
Beryllium (Be)	0.015	0.011	0.011	0.011	0.011
Boron (B)	0.007	0.011	0.016	0.012	0.021
Cadmium (Cd)	0.006	0.0019	0.0021	0.0040	<0.0002
Cobalt (Co)	0.200	0.136	0.128	0.134	0.142
Copper (Cu)	0.087	0.118	0.119	0.118	0.118
Chromium (Cr)	0.005	0.0120	0.0116	0.0114	0.0108
Iron Total (Fe(T))	25.0	93.4	91.0	85.1	85.2
Ferrous Iron (Fe(II))	---	92.1	---	84.0	---
Lead (Pb)	<0.008	<0.0003	<0.0003	<0.0003	<0.0003
Lithium (Li)	0.073	0.074	0.069	0.063	0.063
Mercury (Hg), ng/L	---	---	---	---	---
Manganese (Mn)	7.70	8.51	7.90	7.99	8.04
Molybdenum (Mo)	<0.007	<0.007	0.010	<0.007	<0.007
Nickel (Ni)	0.380	0.352	0.344	0.345	0.354
Selenium (Se)	<0.05	<0.04	<0.04	<0.04	<0.04
Strontium (Sr)	1.40	<0.0003	<0.0003	0.015	0.037
Vanadium (V)	<0.005	0.011	0.011	0.010	0.010
Zinc (Zn)	2.90	3.63	3.33	3.91	3.84
Dissolved Organic Carbon (DOC)	---	1.1	---	1.1	---
δ^2H, per mil	---	-97.37	---	-96.13	---
$\delta^{18}O$, per mil	---	-13.35	---	-13.39	---
$\delta^{34}S_{SO4}$, per mil	---	---	---	-5.8	---
$\delta^{18}O_{SO4}$, per mil	---	---	---	-6.5	---
Sum cations (meq/L)	---	13.3	---	13.8	---
Sum anions (meq/L)	---	12.3	---	12.7	---
C.I. (percent)	---	8.1	---	8.6	---

[1]Except for mercury (ng/L)

Table 4. Water analyses for Phase II wells and Hottentot Creek and Hansen Creek surface waters - Continued

[DIW, deionized water; ID, identification; GW, ground water; µm, micrometer; µS/cm, microsiemens per centimeter; mg/L, milligrams per liter; R, replicate; RA, raw-acidified; SW, surface water; <, less than; ---, not analyzed; °C, degrees Celsius]

Sample ID	Hottentot	Hottentot	Hottentot	Hottentot	Hottentot_R
Collection Date	8/20/2003	8/20/2003	10/24/2003	10/24/2003	10/24/2003
Treatment	Filtered - 0.45 µm	RA	Filtered - 0.45 µm	RA	Filtered - 0.45 µm
Specific conductance (field / laboratory), µS/cm	1710 / 1930	1710 / 1930	1530 / 1900	1530 / 1900	1530 / 1920
pH (field / laboratory)	2.98 / 2.58	2.98 / 2.58	2.99 / 2.6	2.99 / 2.6	2.99 / 2.59
Temperature, °C	7.5	7.5	7.5	7.5	7.5
Eh, volts	0.556	0.556	0.634	0.634	0.634
Dissolved oxygen, mg/L	0.25	0.25	0.21	0.21	0.21
Constituents, mg/L [1]					
Calcium (Ca)	86.9	87.5	76.8	80.5	88.4
Magnesium (Mg)	41.9	42.5	36.1	37.9	39.9
Sodium (Na)	8.42	7.66	6.90	7.46	7.76
Potassium (K)	1.74	1.65	1.94	1.91	2.36
Alkalinity (as HCO_3)	---	---	---	---	---
Sulfate (SO_4)	918	---	903	---	913
Chloride (Cl)	1.81	---	1.67	---	1.65
Fluoride (F)	4.10	---	4.04	---	4.10
Bromide (Br)	<0.1	---	<0.1	---	<0.1
Silica (SiO_2)	91.2	95.6	86.0	85.0	92.6
Aluminum (Al)	66.2	67.5	59.1	59.7	62.3
Arsenic (As)	0.0002	<0.04	<0.0001	<0.04	<0.0001
Arsenite (As(III))	---	---	---	---	---
Barium (Ba)	<0.0008	<0.0008	<0.0008	0.001	0.001
Beryllium (Be)	0.007	0.007	0.010	0.009	0.011
Boron (B)	<0.01	<0.01	0.018	0.016	<0.01
Cadmium (Cd)	0.0046	<0.0002	0.0047	0.0012	0.0045
Cobalt (Co)	0.107	0.108	0.122	0.141	0.123
Copper (Cu)	0.074	0.073	0.122	0.138	0.113
Chromium (Cr)	0.0120	0.0109	0.0119	0.0118	0.0129
Iron Total (Fe(T))	89.4	88.2	87.7	86.3	87.5
Ferrous Iron (Fe(II))	87.3	---	85.6	---	83.3
Lead (Pb)	<0.0003	<0.0003	<0.0003	<0.0003	<0.0003
Lithium (Li)	0.091	0.086	0.062	0.068	0.080
Mercury (Hg), ng/L	---	---	0.8	---	0.9
Manganese (Mn)	8.19	8.20	6.61	6.86	6.81
Molybdenum (Mo)	<0.007	<0.007	<0.007	0.008	<0.007
Nickel (Ni)	0.339	0.345	0.314	0.347	0.351
Selenium (Se)	<0.04	<0.04	<0.04	<0.04	<0.04
Strontium (Sr)	0.006	0.006	0.010	0.010	0.011
Vanadium (V)	0.007	0.006	0.008	0.011	0.011
Zinc (Zn)	4.15	4.23	3.41	3.60	3.70
Dissolved Organic Carbon (DOC)	1.5	---	1.1	---	1.1
δ^2H, per mil	---	---	---	---	---
$\delta^{18}O$, per mil	---	---	---	---	---
$\delta^{34}S_{SO4}$, per mil	---	---	---	---	---
$\delta^{18}O_{SO4}$, per mil	---	---	---	---	---
Sum cations (meq/L)	14.2	---	12.7	---	13.7
Sum anions (meq/L)	12.8	---	13.1	---	12.9
C.I. (percent)	9.9	---	-2.7	---	5.9

[1]Except for mercury (ng/L)

Table 4. Water analyses for Phase II wells and Hottentot Creek and Hansen Creek surface waters - Continued

[DIW, deionized water; ID, identification; GW, ground water; µm, micrometer; µS/cm, microsiemens per centimeter; mg/L, milligrams per liter; R, replicate; RA, raw-acidified; SW, surface water; <, less than; ---, not analyzed; °C, degrees Celsius]

Sample ID	**Hottentot_R**	**Hottentot SW -low**	**Hottentot SW -low**	**Hottentot SW -high**	**Hottentot SW -high**
Collection Date	**10/24/2003**	**9/13/2001**	**9/13/2001**	**9/13/2001**	**9/13/2001**
Treatment	**RA**	**Filtered - 0.1 µm**	**RA**	**Filtered - 0.1 µm**	**RA**
Specific conductance (field / laboratory), µS/cm	1530 / 1920	2190	2190	3040	3040
pH (field / laboratory)	2.99 / 2.59	2.73	2.73	2.60	2.60
Temperature, °C	7.5	9.7	9.7	10.6	10.6
Eh, volts	0.634	0.824	0.824	0.784	0.784
Dissolved oxygen, mg/L	0.21	---	---	---	---
Constituents, mg/L [1]					
Calcium (Ca)	88.5	46.0	45.0	90.0	91.0
Magnesium (Mg)	34.3	41.0	41.0	68.0	67.0
Sodium (Na)	7.72	3.1	3.1	3.3	3.3
Potassium (K)	2.20	0.15	0.20	0.66	0.70
Alkalinity (as HCO_3)	---	---	---	---	---
Sulfate (SO_4)	---	1200	---	2400	---
Chloride (Cl)	---	2.0	---	3.0	---
Fluoride (F)	---	3.00	---	3.00	---
Bromide (Br)	---	<0.1	---	<0.1	---
Silica (SiO_2)	93.8	90.0	87.0	100	99.0
Aluminum (Al)	66.7	80.0	83.0	140	140
Arsenic (As)	<0.04	0.0040	<0.05	0.047	0.110
Arsenite (As(III))	---	<0.001	---	<0.001	---
Barium (Ba)	0.001	0.003	0.004	0.0006	0.002
Beryllium (Be)	0.010	0.011	0.011	0.023	0.023
Boron (B)	<0.01	0.005	0.006	0.006	0.007
Cadmium (Cd)	<0.0002	0.019	0.019	0.058	0.059
Cobalt (Co)	0.132	0.170	0.190	0.360	0.430
Copper (Cu)	0.116	0.540	0.530	2.30	2.40
Chromium (Cr)	0.0119	0.032	0.031	0.090	0.089
Iron Total (Fe(T))	88.6	151	151	399	400
Ferrous Iron (Fe(II))	---	0.251	---	4.12	---
Lead (Pb)	<0.0003	<0.008	<0.008	0.018	0.017
Lithium (Li)	0.077	0.074	0.074	0.095	0.093
Mercury (Hg), ng/L	---	---	---	---	---
Manganese (Mn)	6.93	5.80	5.80	16.1	16.4
Molybdenum (Mo)	<0.007	<0.007	<0.007	0.044	0.050
Nickel (Ni)	0.328	0.400	0.390	0.800	0.790
Selenium (Se)	<0.04	<0.05	<0.05	<0.05	<0.05
Strontium (Sr)	0.010	0.081	0.079	0.093	0.087
Vanadium (V)	0.009	<0.005	<0.005	0.014	0.014
Zinc (Zn)	3.21	3.70	3.70	6.44	6.41
Dissolved Organic Carbon (DOC)	---	---	---	---	---
δ^2H, per mil	---	-90.36	---	-85.14	---
$\delta^{18}O$, per mil	---	-12.62	---	-12.00	---
$\delta^{34}S_{SO4}$, per mil	---	-7.6	---	-7.6	---
$\delta^{18}O_{SO4}$, per mil	---	-3.9	---	-4.6	---
Sum cations (meq/L)	---	14.4	---	26.0	---
Sum anions (meq/L)	---	13.9	---	24.3	---
C.I. (percent)	---	3.3	---	6.8	---

[1]Except for mercury (ng/L)

Table 4. Water analyses for Phase II wells and Hottentot Creek and Hansen Creek surface waters - Continued

[DIW, deionized water; ID, identification; GW, ground water; µm, micrometer; µS/cm, microsiemens per centimeter; mg/L, milligrams per liter; R, replicate; RA, raw-acidified; SW, surface water; <, less than; ---, not analyzed; °C, degrees Celsius]

Sample ID	**La Bobita**	**La Bobita**	**La Bobita**	**La Bobita**	**La Bobita**
Collection Date	**2/5/2003**	**2/5/2003**	**5/15/2003**	**5/15/2003**	**8/20/2003**
Treatment	**Filtered - 0.45 µm**	**RA**	**Filtered - 0.45 µm**	**RA**	**Filtered - 0.45 µm**
Specific conductance (field / laboratory), µS/cm	910 / 853	910 / 853	900 / 846	900 / 846	900 / 874
pH (field / laboratory)	4.54 / 4.24	4.54 / 4.24	3.98 / 4.24	3.98 / 4.24	4.24 / 4.26
Temperature, °C	4.7	4.7	9.1	9.1	12.2
Eh, volts	0.620	0.620	0.535	0.535	0.723
Dissolved oxygen, mg/L	4.33	4.33	3.16	3.16	3.59
Constituents, mg/L [1]					
Calcium (Ca)	117	119	108	108	114
Magnesium (Mg)	31.2	33.6	32.5	28.9	33.2
Sodium (Na)	13.4	13.1	13.1	13.0	11.3
Potassium (K)	1.66	1.63	2.19	2.17	1.95
Alkalinity (as HCO_3)	<1.0	---	---	---	---
Sulfate (SO_4)	486	---	468	---	466
Chloride (Cl)	5.80	---	2.40	---	5.18
Fluoride (F)	2.45	---	2.55	---	2.75
Bromide (Br)	<0.1	---	<0.1	---	<0.1
Silica (SiO_2)	33.7	34.9	33.7	33.2	33.1
Aluminum (Al)	12.8	13.1	12.7	12.6	11.6
Arsenic (As)	<0.0001	<0.04	<0.0001	<0.04	<0.0001
Arsenite (As(III))	---	---	---	---	---
Barium (Ba)	0.023	0.023	0.021	0.021	0.020
Beryllium (Be)	0.006	0.006	0.005	0.005	0.005
Boron (B)	<0.01	<0.01	<0.01	<0.01	0.022
Cadmium (Cd)	0.0041	0.0041	0.0036	0.0035	0.0042
Cobalt (Co)	0.018	0.018	0.019	0.018	0.020
Copper (Cu)	0.0331	0.0269	0.0248	0.0254	0.0309
Chromium (Cr)	0.0005	0.0007	0.0101	0.0125	0.0108
Iron Total (Fe(T))	0.037	0.050	0.072	0.147	0.037
Ferrous Iron (Fe(II))	0.006	---	0.039	---	0.010
Lead (Pb)	0.0009	<0.0003	0.0009	0.0011	0.0009
Lithium (Li)	0.033	0.032	0.027	0.027	0.034
Mercury (Hg), ng/L	---	---	---	---	---
Manganese (Mn)	2.62	2.66	2.71	2.63	2.75
Molybdenum (Mo)	<0.007	<0.007	<0.007	<0.007	<0.007
Nickel (Ni)	0.143	0.142	0.131	0.130	0.134
Selenium (Se)	<0.04	<0.04	<0.04	<0.04	<0.04
Strontium (Sr)	0.806	0.793	0.821	0.798	0.888
Vanadium (V)	<0.002	<0.002	<0.002	<0.002	<0.002
Zinc (Zn)	1.00	1.07	0.929	0.919	0.925
Dissolved Organic Carbon (DOC)	0.9	---	2.0	---	1.1
δ^2H, per mil	-96.03	---	-97.88	---	---
$\delta^{18}O$, per mil	-13.46	---	-13.5	---	---
$\delta^{34}S_{SO4}$, per mil	-3.6	---	---	-3.4	---
$\delta^{18}O_{SO4}$, per mil	-5.6	---	---	-6.0	---
Sum cations (meq/L)	8.37	---	8.13	---	8.15
Sum anions (meq/L)	8.14	---	7.69	---	7.69
C.I. (percent)	2.8	---	5.7	---	5.9

[1]Except for mercury (ng/L)

Table 4. Water analyses for Phase II wells and Hottentot Creek and Hansen Creek surface waters - Continued

[DIW, deionized water; ID, identification; GW, ground water; µm, micrometer; µS/cm, microsiemens per centimeter; mg/L, milligrams per liter; R, replicate; RA, raw-acidified; SW, surface water; <, less than; ---, not analyzed; °C, degrees Celsius]

Sample ID	La Bobita	La Bobita	La Bobita	Ranger Station	Ranger Station
Collection Date	8/20/2003	10/23/2003	10/23/2003	2/7/2003	2/7/2003
Treatment	RA	Filtered - 0.45 µm	RA	Filtered - 0.45 µm	RA
Specific conductance (field / laboratory), µS/cm	900 / 874	900 / 858	900 / 858	490 / ---	490 / ---
pH (field / laboratory)	4.24 / 4.26	4.45 / 4.24	4.45 / 4.24	6.5 / ---	6.5 / ---
Temperature, °C	12.2	8.1	8.1	8.8	8.8
Eh, volts	0.723	0.530	0.530	0.450	0.450
Dissolved oxygen, mg/L	3.59	3.71	3.71	5.55	5.55
Constituents, mg/L [1]					
Calcium (Ca)	117	108	109	71.8	71.9
Magnesium (Mg)	33.4	31.6	29.5	14.7	14.9
Sodium (Na)	11.2	12.8	12.8	8.45	7.99
Potassium (K)	2.01	1.37	1.62	1.32	6.89
Alkalinity (as HCO_3)	---	---	---	45.8	---
Sulfate (SO_4)	---	465	---	223	---
Chloride (Cl)	---	4.81	---	5.00	---
Fluoride (F)	---	2.87	---	0.920	---
Bromide (Br)	---	<0.1	---	<0.1	---
Silica (SiO_2)	32.9	32.9	32.8	17.6	20.1
Aluminum (Al)	11.7	11.8	12.1	0.087	1.38
Arsenic (As)	<0.04	<0.0001	<0.04	<0.0001	<0.04
Arsenite (As(III))	---	---	---	---	---
Barium (Ba)	0.017	0.025	0.022	0.048	0.059
Beryllium (Be)	0.004	0.006	0.006	<0.001	<0.001
Boron (B)	<0.01	<0.01	<0.01	<0.01	<0.01
Cadmium (Cd)	0.0040	0.0040	0.0042	0.0002	0.0003
Cobalt (Co)	0.019	0.016	0.016	<0.0007	<0.0007
Copper (Cu)	0.0341	0.0307	0.0265	0.0010	0.0101
Chromium (Cr)	0.0083	0.0009	0.0009	<0.0005	0.0014
Iron Total (Fe(T))	0.055	0.011	0.015	0.142	4.78
Ferrous Iron (Fe(II))	---	---	---	0.135	---
Lead (Pb)	0.0011	0.0008	0.0006	<0.0003	0.040
Lithium (Li)	0.039	0.042	0.040	0.004	0.005
Mercury (Hg), ng/L	---	0.8	---	---	---
Manganese (Mn)	2.83	2.35	2.41	0.014	0.105
Molybdenum (Mo)	<0.007	<0.007	<0.007	0.008	0.014
Nickel (Ni)	0.130	0.131	0.131	0.0048	0.0083
Selenium (Se)	<0.04	<0.04	<0.04	<0.04	<0.04
Strontium (Sr)	0.883	0.805	0.806	0.509	0.398
Vanadium (V)	<0.002	<0.002	<0.002	<0.002	<0.002
Zinc (Zn)	1.04	1.03	0.962	0.035	0.046
Dissolved Organic Carbon (DOC)	---	1.4	---	0.9	---
δ^2H, per mil	---	---	---	---	-96.28
$\delta^{18}O$, per mil	---	---	---	---	-13.25
$\delta^{34}S_{SO4}$, per mil	---	---	---	---	---
$\delta^{18}O_{SO4}$, per mil	---	---	---	---	---
Sum cations (meq/L)	---	7.89	---	4.55	---
Sum anions (meq/L)	---	7.80	---	4.91	---
C.I. (percent)	---	1.1	---	-7.6	---

[1]Except for mercury (ng/L)

Table 5. ICP-MS analyses for selected sampling events for Phase II wells

[ID, identification; FA, filtered-acidified; µg/L, micrograms per liter; <, less than]

Sample ID	CC2A	CC1B	CC2B	HANSEN	HANSEN	HOTTENTOT	HOTTENTOT	LA BOBITA	LA BOBITA	RANGER STATION
Date	5/14/2003	2/5/2003	2/5/2003	2/7/2003	5/13/2003	2/5/2003	5/12/2003	2/5/2003	5/15/2003	2/7/2003
Treatment	FA	FA	FA	FA	FA	FA	FA	FA	FA	FA
Constituent, µg/L										
Arsenic (As)	< 0.2	< 0.2	< 0.2	2.4	2.1	0.7	0.8	0.6	0.5	0.06
Bismuth (Bi)	< 0.01	< 0.01	< 0.01	< 0.01	< 0.01	< 0.01	< 0.01	< 0.01	< 0.01	< 0.001
Cerium (Ce)	5.6	0.10	0.28	343	347	20	22	88	69	0.008
Cesium (Cs)	< 0.2	< 0.2	< 0.2	< 0.2	< 0.2	< 0.2	< 0.2	< 0.2	< 0.2	< 0.02
Dysprosium (Dy)	1.00	0.017	0.040	30	29	13	13	11	8.9	0.028
Erbium (Er)	0.55	0.019	0.029	9.5	8.9	4.3	4.5	4.1	3.3	0.014
Europium (Eu)	0.020	< 0.002	0.006	11	11	3.0	3.0	4.7	3.9	0.0081
Gadolinium (Gd)	0.74	0.019	0.039	64	63	20	20	20	15	0.047
Holmium (Ho)	0.22	0.0052	0.0091	4.5	4.4	2.1	2.1	1.8	1.5	0.0057
Lanthanum (La)	1.5	0.070	0.17	113	110	2.2	2.8	30	23	0.17
Lutetium (Lu)	0.046	0.002	0.004	0.82	0.81	0.39	0.39	0.35	0.28	0.0020
Molybdenum (Mo)	0.9	9.9	2.6	< 0.6	< 0.6	< 0.6	< 0.6	< 0.6	0.6	13
Neodymium (Nd)	1.0	0.06	0.17	306	296	61	61	94	76	0.22
Lead (Pb)	< 0.08	< 0.08	< 0.08	0.11	< 0.08	< 0.08	0.28	0.58	0.35	0.043
Praseodymium (Pr)	0.23	0.013	0.032	61	60	8.1	8.4	18	15	0.043
Rubidium (Rb)	9.8	2.0	4.8	7.8	7.6	3.5	3.9	2.9	3.1	1.1
Rhenium (Re)	0.020	0.015	0.003	0.016	0.015	0.048	0.042	0.099	0.084	0.73
Antimony (Sb)	0.30	0.08	0.10	< 0.03	< 0.03	< 0.03	0.40	0.18	0.03	0.62
Selenium (Se)	< 2	< 2	< 2	7	7	4	5	< 2	< 2	0.5
Samarium (Sm)	0.28	0.010	0.029	75	73	18	18	22	18	0.040
Terbium (Tb)	0.15	0.002	0.007	7.2	7.2	2.5	2.7	2.4	1.9	0.0052
Tellurium (Te)	0.07	< 0.07	< 0.07	< 0.07	< 0.07	0.09	0.16	< 0.07	< 0.07	0.009
Thorium (Th)	0.032	< 0.008	< 0.008	0.063	0.059	0.83	0.81	< 0.008	< 0.008	0.0051
Thallium (Tl)	< 0.07	< 0.07	< 0.07	< 0.07	< 0.07	< 0.07	< 0.07	< 0.07	< 0.07	< 0.007
Thulium (Tm)	0.062	0.002	0.004	1.1	1.1	0.53	0.51	0.47	0.39	0.0017
Uranium (U)	1.3	4.2	4.5	5.0	4.8	2.3	2.4	1.4	1.2	0.46
Vanadium (V)	1	< 1	< 1	< 1	< 1	9	10	< 1	< 1	< 0.1
Tungsten (W)	< 0.02	0.23	0.04	< 0.02	0.04	< 0.02	< 0.02	0.02	< 0.02	0.007
Yttrium (Y)	7.7	0.26	0.51	119	117	58	59	47	37	0.38
Ytterbium (Yb)	0.31	0.012	0.024	6.1	6.0	3.1	2.9	2.6	2.2	0.011
Zirconium (Zr)	0.12	0.03	0.03	0.01	0.02	0.05	0.12	< 0.01	< 0.01	0.033

Table 6. The equations of best fit from the Straight Creek data

[a, activity; dis., dissolved; SW, surface water; TR, total recoverable; R^2, correlation coefficient; vs., versus; <, less than]

plot (y vs. x)	Linear equation	R^2	Note
log a(Al^{3+}) vs. pH	y = -0.27x - 2.8	0.59	For pH < 5, Straight Creek SW not included
Al vs. Al(TR)	y = 0.99x + 0.25	0.99	All wells and Straight Creek SW
Al vs. SO_4	y = 0.036x + 19.0	0.97	SC1A, 6A, 3A, 5A only
Be vs. Al	y = 0.0004x - 0.0112	0.84	SC1A, 6A, 3A, 5A only
Be vs. F	y = 0.0024x + 0.0008	0.73	SC1A, 6A, 3A, 5A only
Be vs. SO_4	y = 0.000014x - 0.0046	0.84	SC1A, 6A, 3A, 5A only
Ca vs.SO_4	y = 0.19x - 10.9	0.98	Straight Creek debris-fan ground waters
Cd vs. Zn	y = 0.0056x - 0.0032	0.92	Straight Creek SW, SC1A, 3A, 6A, 5A, 7A, 8A, AWWT1
Co vs. Ni	y = 0.45x - 0.0069	0.98	Straight Creek SW, SC1A, 6A, 5A, 7A, 8A, AWWT1
Cu vs. SO_4	y = 0.0006x - 0.29	0.82	SC1A, 6A, 3A, 5A only
Cu vs. SO_4	y = 0.001x - 0.095	0.85	Straight Creek SW
Cu vs. Zn	y = 0.15x - 0.14	0.84	SC1A, 6A, 3A, 5A only
Cu vs. Zn	y = 0.21x + 0.25	0.78	Straight Creek SW
F vs. Ca	y = 0.024x - 0.26	0.87	SC1A, 6A, 3A, 5A only
F vs. SO_4	y = 0.0049x - 0.97	0.85	SC1A, 6A, 3A, 5A only
Fe(II) vs. Fe(T)	y = 1.0x - 0.52	1.00	Straight Creek ground water
Li vs. SO_4	y = 0.0001x - 0.041	0.84	SC1A, 6A, 3A, 5A only
Mg vs. Ca	y = 0.27x + 14.0	0.95	SC1A, 6A, 3A, 5A only
Mg vs.SO_4	y = 0.056x + 4.3	0.98	Straight Creek debris- fan wells, except 4A
Mg vs.SO_4	y = 0.055x - 12.2	0.74	Straight Creek SW
SC vs. SO_4	y = 1.2x + 390	0.97	Straight Creek SW, SC1A, 3A, 6A, 5A, 7A, 8A, AWWT1
SiO_2 vs. SO_4	y = 0.042x - 17.5	0.76	Straight Creek SW
SiO_2 vs. SO_4	y = 0.016x + 63.8	0.75	SC1A, 6A, 3A, 5A only
Zn vs. Mn	y = 0.37x - 0.16	0.99	Straight Creek SW, SC1A, 3A, 6A, 5A, 7A, 8A, AWWT1
Zn vs. SO_4	y = 0.0042x - 1.3	0.96	Straight Creek SW, SC1A, 3A, 6A, 5A, 7A, 8A, AWWT1
Mn vs. SO_4	y = 0.011x - 3.3	0.97	Straight Creek SW, SC1A, 3A, 6A, 5A, 7A, 8A, AWWT1
Ni vs. SO_4	y = 0.00039x - 0.070	0.96	Straight Creek SW, SC1A, 3A, 6A, 5A, 7A, 8A, AWWT1
Fe(dis.) vs. Fe(TR)	y = 0.96x - 0.59	0.99	Straight Creek ground water

Redox Potentials and Iron Chemistry

Redox potential measurements and their relation with the Fe(II/III) determinations through the equilibrium Nernst equation were evaluated for the data from the Straight Creek well waters (Naus and others, 2005). The same evaluation was performed with the current data from the phase II well-water samples and the results are shown in figures 7A-D. Figure 7A shows the redox potential, or Eh measured in the field with a platinum electrode plotted in relation to the calculated Eh based on the iron redox determinations and speciation computed with WATEQ4F. Only those samples for which both iron determinations and redox potential measurements were made are included, although some of the Fe(II/III) determinations were below detection. The solid diagonal line indicates exact correspondence between measured and calculated Eh. The dotted lines (±35 mV) show the range for one standard deviation developed from the Straight Creek well data (Naus and others, 2005). Several data points fall within the standard deviation and several others fall outside. In figure 7B the same data are plotted as the difference between measured and calculated Eh values in relation to the Fe(II) to total dissolved iron weight ratio for samples that are above the method detection limits for Fe(II) and total dissolved iron (Fe(T)). The Fe(III) is below the detection limit for samples containing more than 97 percent of the total dissolved iron as Fe(II) (Naus and others, 2005). Such samples have been excluded from figures 7C and 7D.

The platinum electrode that measures the redox potential also has detection limits that would depend on the lower limit of electroactivity of iron for these waters. In a laboratory study, Morris and Stumm (1967) showed that the lower limit of electroactivity is about 10^{-5} molar for Fe(II) or Fe(III). Our field studies (such as Naus and others, 2005) indicate that the platinum electrode can often approximate equilibrium potentials for solutions that are as low as 10^{-6} molar in Fe(II) or Fe(III) concentration. Hence we have designated a transition zone from 0.02 to 0.2 mg/L in Fe(III) concentration (about 0.46 to 4.6 micromolar) where the equilibrium Nernstian response of the electrode ceases. This transition zone is shown in figure 7C that plots the difference in the Eh (measured-calculated) in relation to the Fe(III) concentration. The Fe(III) concentration is used because it is more frequently present at the lowest concentrations. Data that fall below the concentration range of the transition zone should be, and are, excluded from the redox potential comparison shown in figure 7D. Our field work indicates that the field measurement of Eh is more likely to be in error than the determination of Fe(II/III) or the speciation calculation. Precautions were taken to carefully measure Eh and to collect samples for redox species determinations after field parameters and iron redox chemistry had stabilized. Nonetheless there may have been some lapse of time between the platinum electrode measurement and collection of the water sample; consequently, some difference in sample water chemistry may have occurred.

Samples that have an acceptable comparison between measured and calculated redox potential (within 2 standard deviations, that is ±70 mV) are considered reliable for calculations of ferrihydrite (or other Fe(III) mineral) saturation indices. Ferrihydrite saturation indices for phase II well water samples that met this criterion are plotted in relation to pH in figure 8. As shown previously by Naus and others (2005), the phase II well water data also demonstrated that ferrihydrite solubility provides an upper limit to the concentration of Fe(III).

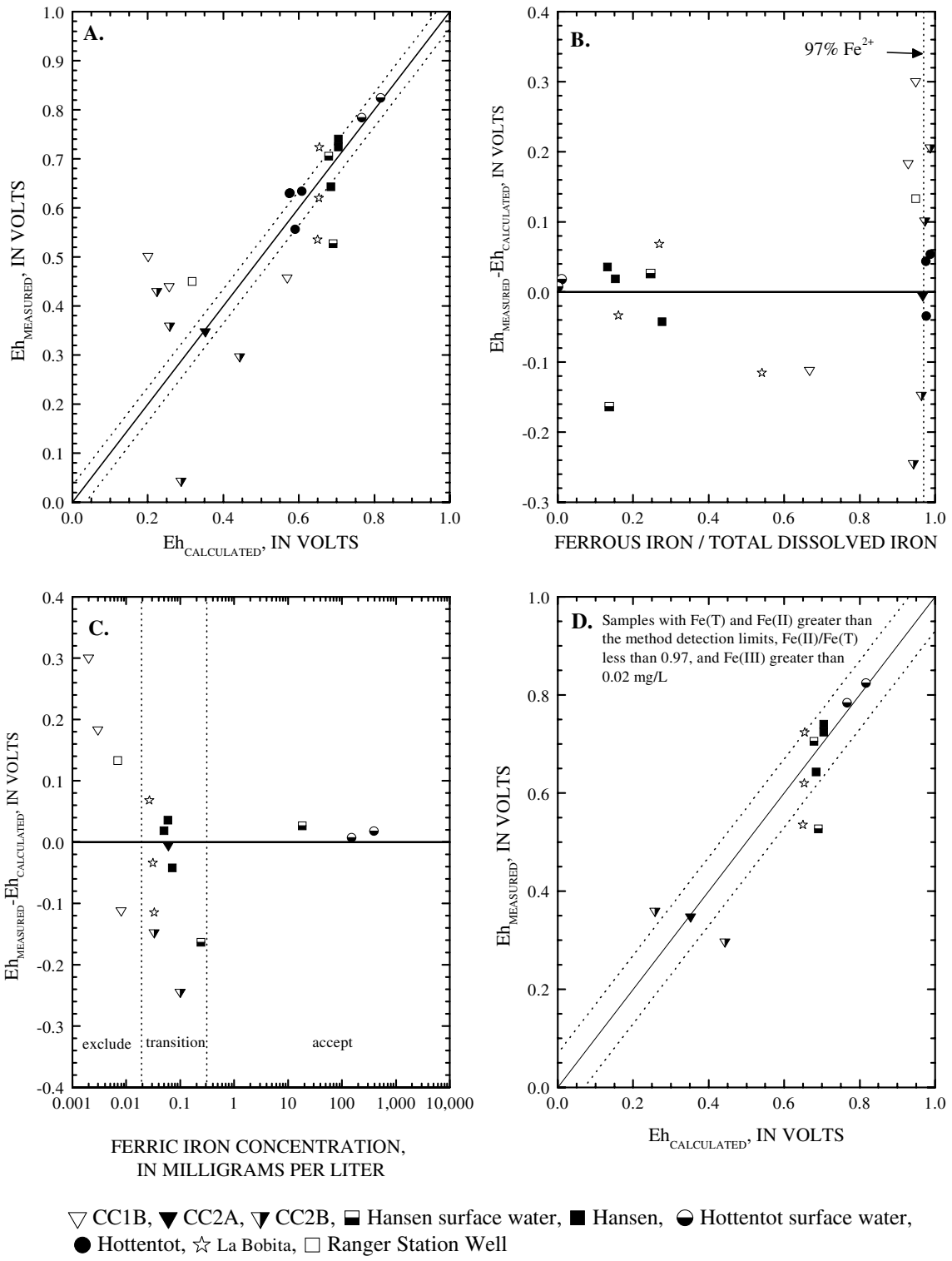

Figure 7. A. Measured Eh in relation to calculated Eh for all samples. Solid line indicates the 1:1 correspondence; the dotted lines show ±35 mV error range. **B.** The difference between measured and calculated Eh in relation to Fe(II)/Fe(T) ratio for samples with Fe(T) and Fe(II) above method detection limits. **C.** The difference between measured and calculated Eh in relation to Fe(III) concentration. The vertical dotted lines show the lower limit range over which Fe(III) concentration is expected to be electroactive. **D.** Revised plot of figure 7A excluding data points containing non-detectable and non-electroactive ferric iron concentrations. Solid line indicates the 1:1 correspondence; the dotted lines show ±70 mV error range.

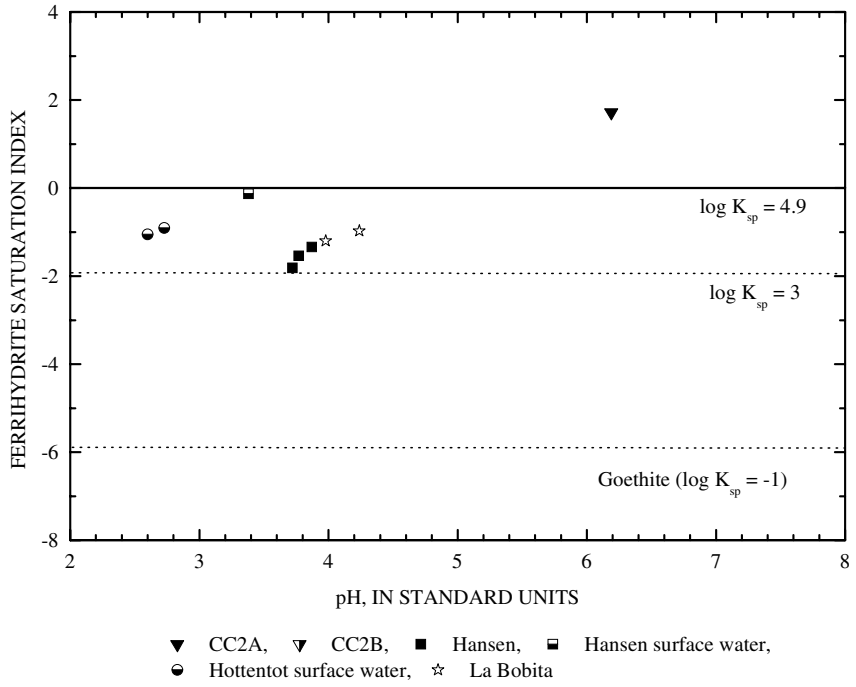

Figure 8. Saturation index for hydrous ferric oxides (ferrihydrite and goethite) as a function of pH.

Figures 9A and 9B demonstrate the general lack of correlation of iron concentrations with sulfate concentrations, similar to the Straight Creek data of Naus and others (2005). This result is expected from the reactive nature of iron geochemistry as a function of redox chemistry and pH. As with the Straight Creek data, the iron concentrations in Hottentot surface waters are sufficient to account for the iron concentrations in the Hottentot well water. No addition of iron is needed but attenuation or, more likely, dilution of iron sometimes occurs, as shown by the trend in figure 9A.

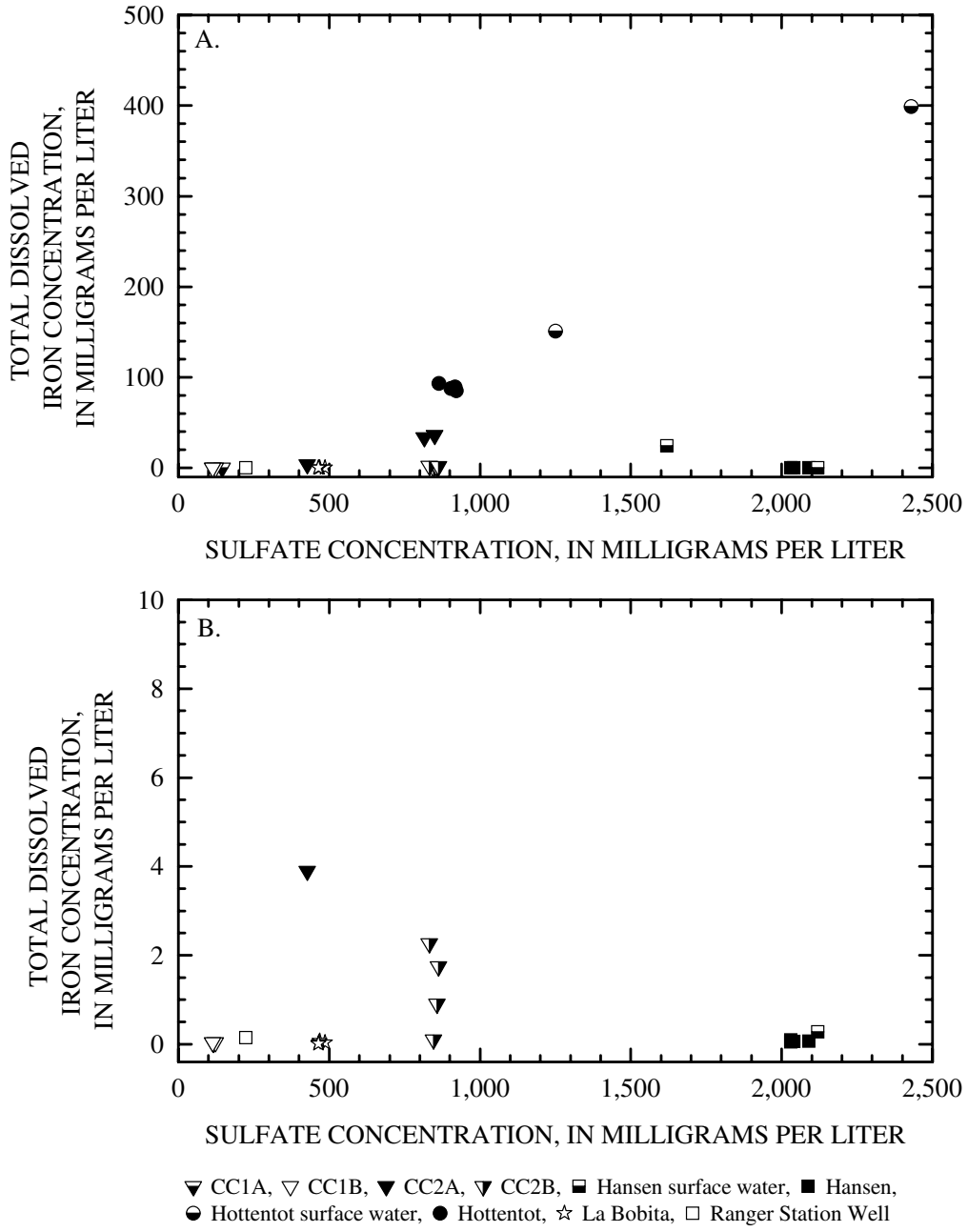

Figure 9. A. Total dissolved iron concentration plotted in relation to sulfate concentration. **B.** Total dissolved iron concentration plotted in relation to sulfate concentration for the low concentration range (0 – 10 mg/L iron).

The close equivalency of the dissolved iron concentrations to the total recoverable iron concentrations (fig. 10) indicates the general lack of particulate iron in these samples except for samples from wells CC1A and the Ranger Station. Waters from wells CC1A and CC2A were noted to be turbid during sampling. The silica and aluminum concentrations for total recoverable samples were much higher in waters from well CC2A than those for the other ground waters, consistent with high turbidity.

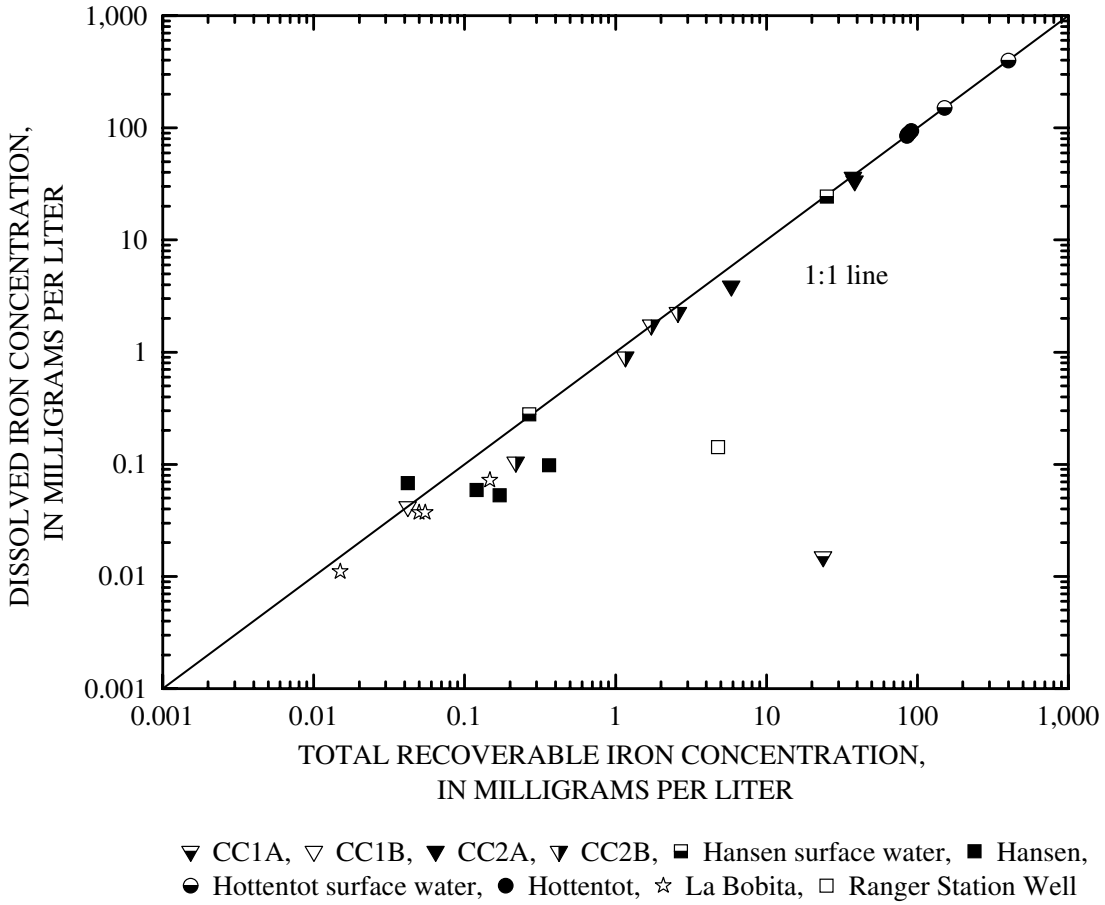

Figure 10. Dissolved iron concentration in relation to total recoverable iron concentration.

Figures 11A-C demonstrate the same trends as the Straight Creek data (Naus and others, 2005) in that the surface waters contain nearly all oxidized iron and the well waters contain nearly all reduced iron. The Hottentot well waters contains some Fe(III) that is probably dissolved, because figure 10 reflects very small differences between dissolved iron and total recoverable iron for these samples, but is still about 97% Fe(II). Hansen well waters are unusual because the Fe concentrations are very low and only 13 to 28% Fe(II). The high percentage of Fe(III), however, is clearly caused by particulate or colloidal Fe (fig. 10).

Figure 12A depicts siderite saturation indices for the circumneutral pH well waters as a function of pH. The saturation indices for the acid ground-water samples are not shown because they are substantially undersaturated for all carbonate minerals. The trend is the same as that for the Straight Creek waters (Naus and others, 2005) in that siderite saturation is maintained and appears to control the Fe(II) concentrations for these waters. The siderite saturation indices also are plotted in figure 12B as a function of the calcium concentrations to show that the trend to approach siderite saturation apparently is driven by the dissolution of a soluble calcium mineral, probably calcite. This calcium trend is much more apparent for the phase II data than for the Straight Creek phase I data. The samples with the highest siderite saturation indices are from well CC2B and, as will be shown in the next section for the manganese data, these same samples have the highest dissolved inorganic carbon concentrations.

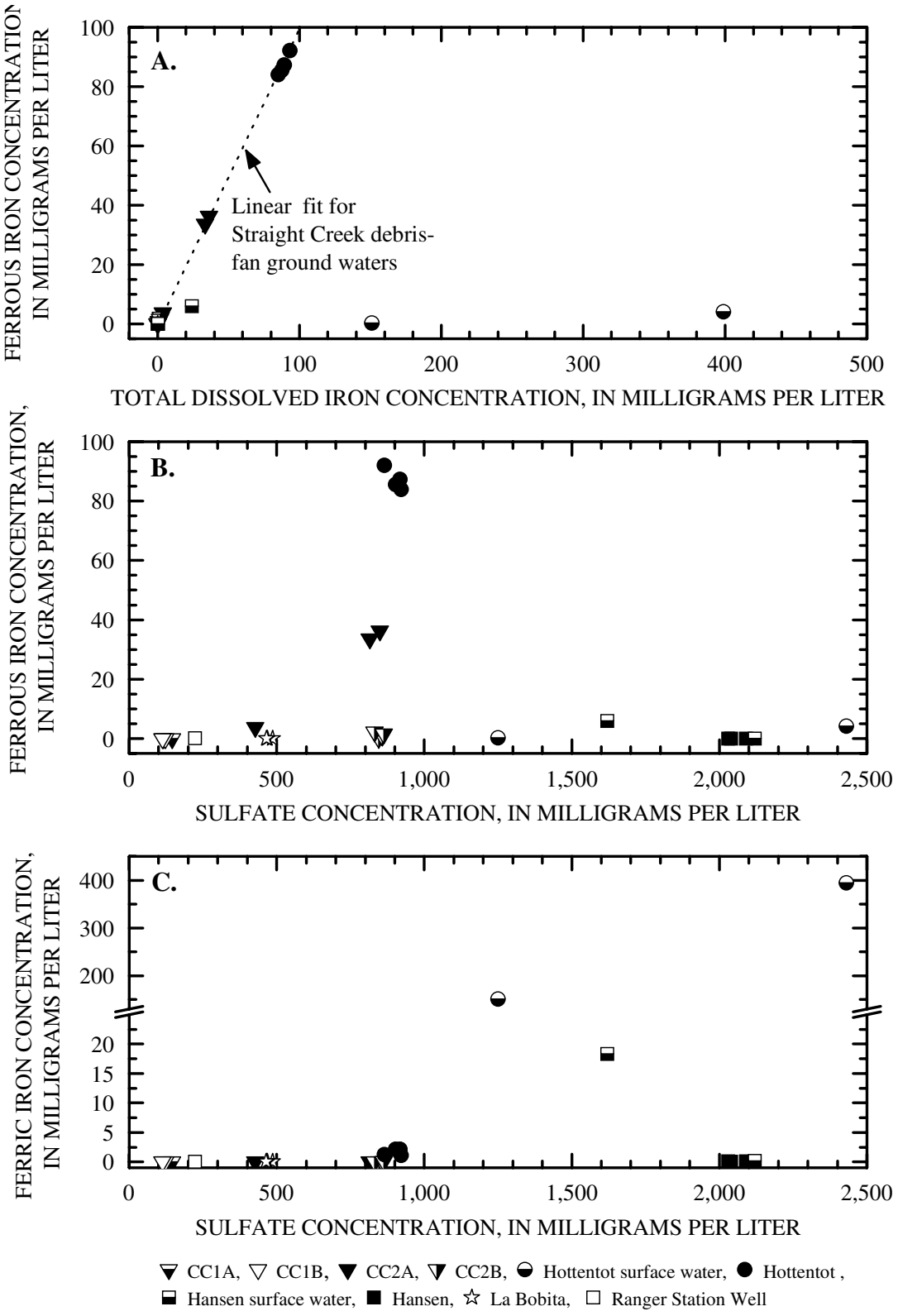

Figure 11. A. Ferrous iron concentration in relation to total dissolved iron concentration. **B.** Ferrous iron concentration plotted in relation to sulfate concentration. **C.** Ferric iron concentration in relation to sulfate concentration.

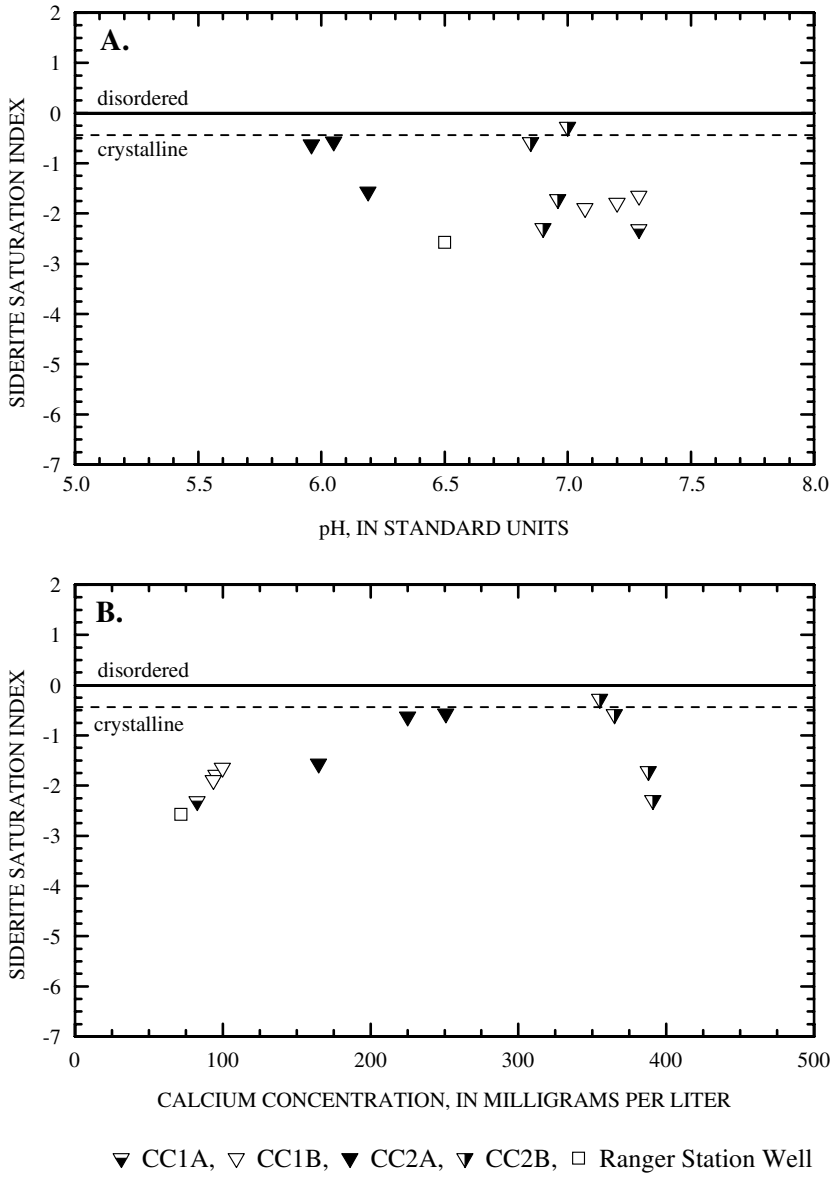

Figure 12. A. Saturation indices for crystalline and disordered siderite as a function of pH for wells of circumneutral pH. **B.** Siderite saturation indices as a function of calcium concentration for wells of circumneutral pH.

Manganese Chemistry

The relation between manganese and sulfate concentrations is shown in figure 13. Up to about 1,000 mg/L sulfate, the manganese concentrations closely follow the linear best-fit trend for the Straight Creek data. At higher sulfate concentrations the manganese concentrations tend to be slightly lower than the concentrations observed for Straight Creek data, except for samples from well CC2A, which increased substantially in manganese concentration for the last two samples collected. The high concentrations in samples from well CC2A are consistent with the trend seen for other elements with anomalously high concentrations. These results indicate that well CC2A may have been drilled into a mineralized section of andesite. This well water also contains elevated sulfate concentration (850 mg/L).

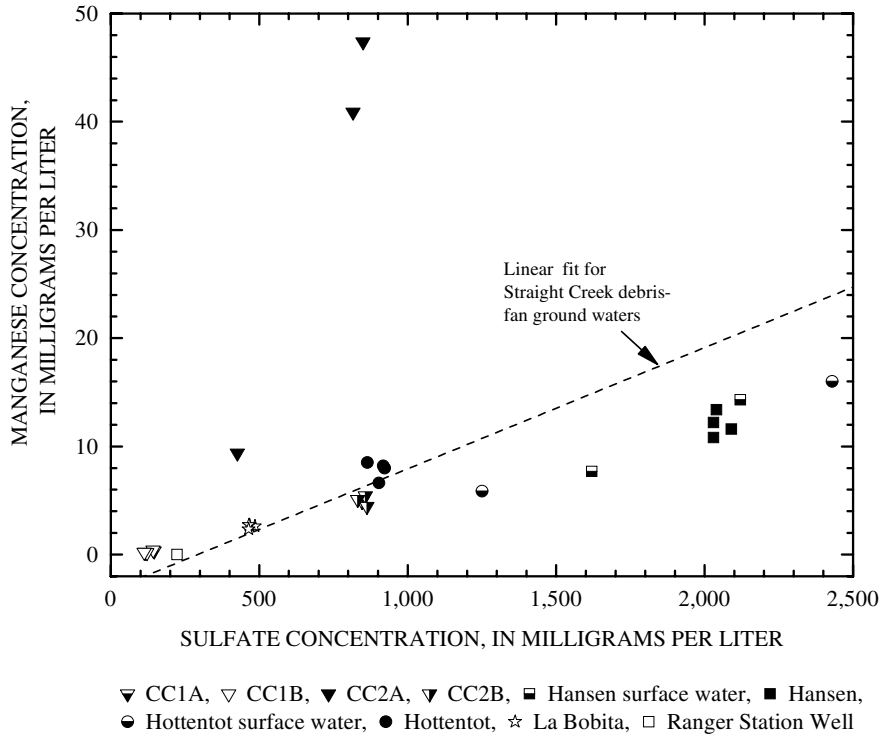

Figure 13. Manganese concentration in relation to sulfate concentration. Dashed line is the best fit of Straight Creek debris-fan well waters (except SC4A).

Rhodochrosite saturation indices are plotted as a function of dissolved inorganic carbon molality and pH in figures 14A and 14B, respectively. Consistent with the results from the Straight Creek data, the phase II data reflect an equilibrium solubility control by rhodochrosite that limits the maximum concentrations of manganese under circumneutral-pH conditions. Samples with lower pH values were not plotted because they are substantially undersaturated with respect to rhodochrosite. It is noteworthy that while acid ground waters have no apparent upper solubility limit to manganese concentrations, they have substantially lower Mn concentrations than do CC2A samples. This difference is likely related to the relative abundance of soluble manganese minerals. Typical QSP alteration zones contains little manganese compared to deeper alteration zones (Ludington and others, 2004).

Aluminum Chemistry

The trends in the aluminum concentrations are comparable to the results from the Straight Creek data. Total recoverable aluminum is comparable to dissolved aluminum for all waters except for CC1A, which was observed to be turbid (fig. 15A). Acid ground waters have high aluminum concentrations, generally following a dilution trend but with greater variability than the Straight Creek samples (fig. 15B). Neutral-pH ground waters have low aluminum concentrations (generally less than 1 mg/L), substantially lower than concentrations for the Straight Creek dilution trend but similar to those found in Straight Creek neutral-pH bedrock ground waters. Aluminum concentrations are limited by microcrystalline gibbsite to amorphous $Al(OH)_3$ solubility (figs. 15C and 15D). Ground waters from CC2A seem to be anomalous in that they are substantially undersaturated with respect to gibbsite-like phases for a circumneutral pH water. These samples also contain anomalously high fluoride concentrations. Fluoride forms strong complexes with aluminum and substantially lowers the aluminum free-ion activity and the gibbsite saturation indices. Thus, the elevated fluoride concentrations seem to be the main reason for the undersaturation effect.

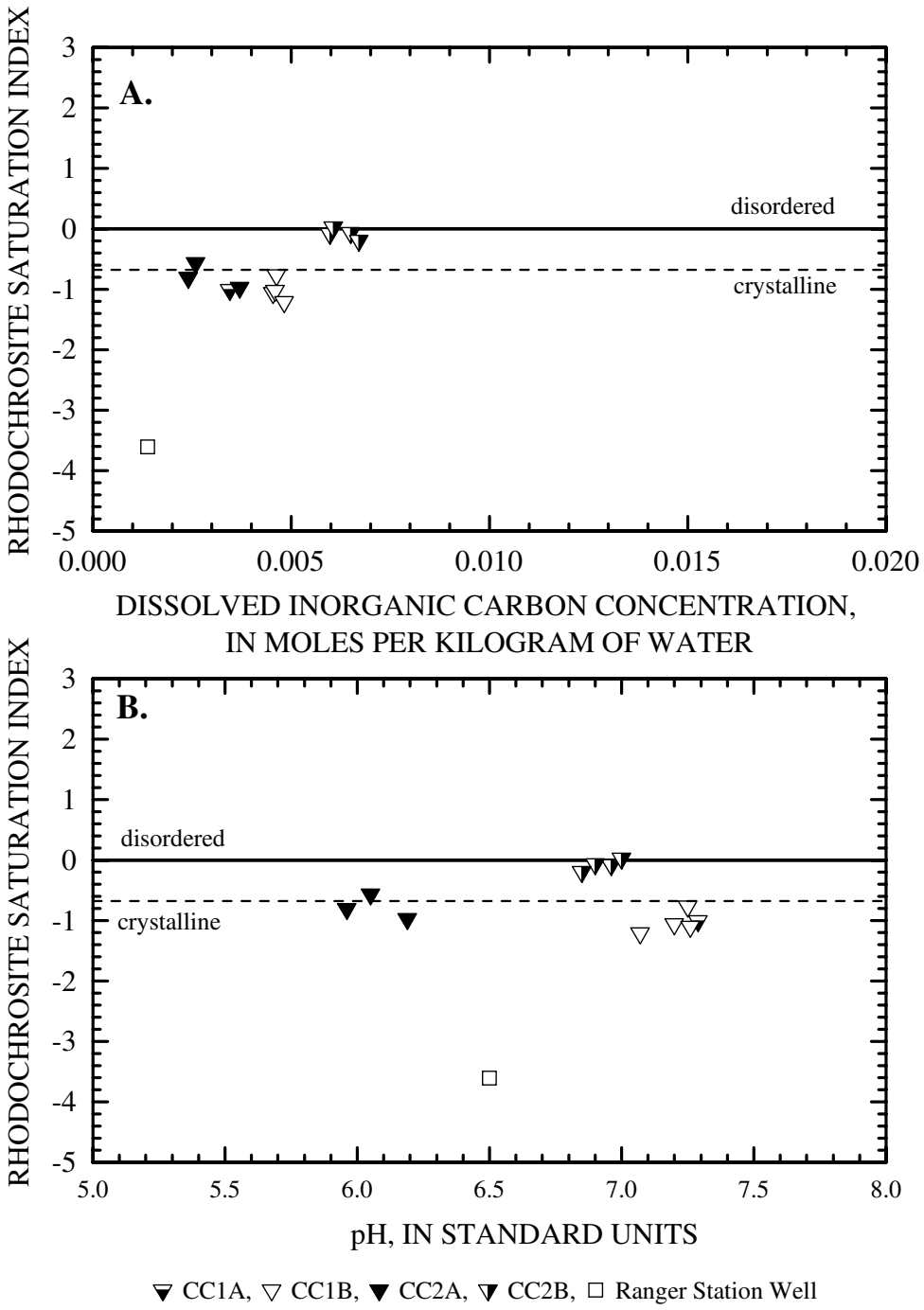

Figure 14. A. Saturation indices for rhodochrosite in relation to dissolved inorganic carbon. **B.** Saturation indices for rhodochrosite in relation to pH. Solid horizontal line represents the solubility-product constant for poorly crystalline, disordered rhodochrosite and the dashed line represents the solubility-product constant for well-crystallized rhodochrosite.

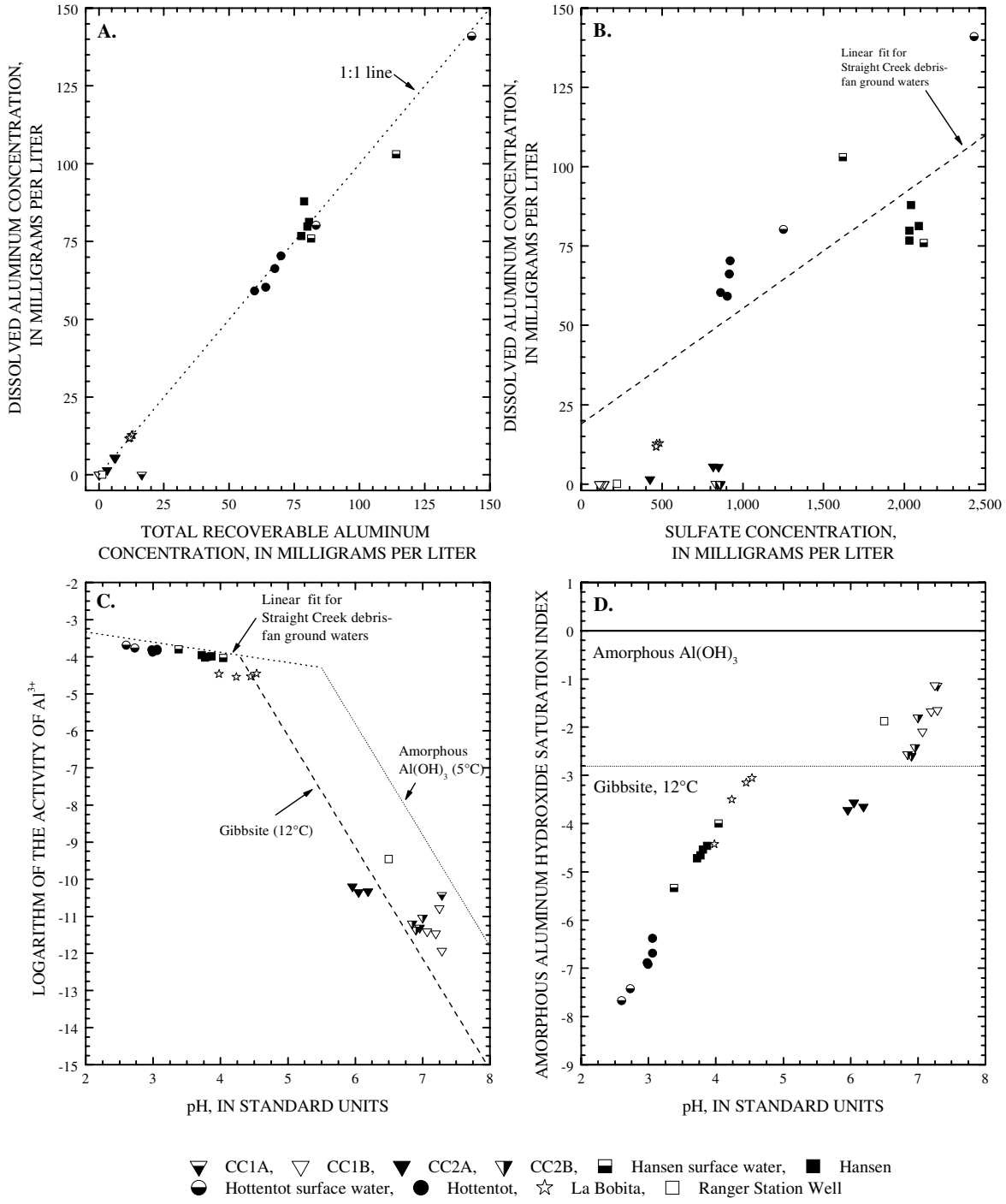

Figure 15. A. Dissolved aluminum concentration plotted in relation to total recoverable aluminum concentrations along with linear fit. **B.** Dissolved aluminum concentration in relation to dissolved sulfate concentration showing linear fit for selected Straight Creek debris-fan ground water. **C.** The logarithm of the free aluminum ion activity in relation to the pH with the degree of fit for low pH waters (pH < 5) and the range of solubility limits for gibbsite to amorphous $Al(OH)_3$ for the temperature of the ground-water samples. **D.** Amorphous aluminum hydroxide and gibbsite saturation indices in relation to pH.

Calcium Chemistry and Solubilities of Gypsum, Calcite, and Fluorite

Gypsum and Calcite Solubilities

The ground waters in the Red River Valley can be categorized as calcium-sulfate type waters because of the preponderance of calcium as the main cation and sulfate as the main anion. Dissolved calcium has two main sources: weathering of gypsum and weathering of calcite. Dissolved sulfate also has two main sources: weathering of gypsum and weathering of pyrite. In previous reports (Maest and others, 2004; Naus and others, 2005) plots of these two constituents indicated the relative (and qualitative) proportions of pyrite and calcite weathering relative to pure gypsum weathering. Figure 16A shows a plot of calcium in relation to sulfate concentrations for the phase II ground waters with the gypsum congruent dissolution line, the equilibrium solubility limit of gypsum in pure water (based on Lilley and Briggs, 1976), and the equilibrium solubility range for these ground waters. Most of the ground waters are enriched in sulfate relative to the gypsum dissolution line, indicating the contribution of pyrite weathering to the ground waters. The surface and ground waters from Hottentot are substantially more enriched in sulfate than the waters from Straight Creek. The reason for this anomaly is that much of the scar weathering at Hottentot is within a rhyolite porphyry that contains abundant pyrite and low calcium. This difference is an important lithologic change that also may affect other dissolved constituents.

Another anomaly is the calcium and sulfate concentrations found in ground waters from wells CC1A and CC1B, which reflect enrichment of calcium relative to sulfate and indicate the contribution of calcite weathering. The preponderance of calcite over gypsum and pyrite weathering for CC1A and CC1B can be seen more clearly in figure 16B in which the calcium:sulfate molar ratio has been plotted in relation to pH. The two dashed lines that outline the area of predominance of gypsum dissolution are based on the qualitative evaluation of pyrite-gypsum-calcite weathering reactions by Nordstrom and others (2005) for the Animas River watershed study. When pyrite weathering dominates the sulfate concentrations, the pH values should be acid and figure 16B shows that the lowest calcium:sulfate ratios occur at the lowest pH values (Hottentot and Hansen surface and ground waters). For the range of pH 4 to 7 the calcium:sulfate ratios are nearly constant, in the range of 0.6 to 1.1. The higher ratios above pH 7 are consistent with calcite dissolution dominating the weathering reactions and providing a buffered pH value above neutral pH. Water from wells CC1A and CC1B is dominated by calcite and gypsum dissolution, whereas water from wells CC2A, CC2B, and the Questa Ranger Station is dominated by gypsum dissolution, and water from Hansen and Hottentot wells is dominated by pyrite and gypsum dissolution. The La Bobita well waters are close to the gypsum dissolution line but some low acidity reflects the influence of some pyrite weathering.

Saturation indices for gypsum are shown in figures 17A and 17B as a function of calcium concentrations and sulfate concentrations, respectively. These data reflect trends similar to those found in the Straight Creek data. The approach to gypsum saturation appears to be driven more consistently by increasing calcium concentrations than by increasing sulfate concentrations. This pattern would be expected in an environment where gypsum precipitation is governed by calcite dissolution that neutralizes the acidity developed by pyrite oxidation and dissolution. The isotopic and mineralogical data indicate that all the gypsum occurring in the weathering zone is secondary gypsum formed from reaction of primary calcite and pyrite found in hydrothermal veins (Ludington and others, 2004). Thus, conditions inferred for the weathering zone support the results of the geochemical relations.

Calcite saturation indices as a function of pH are plotted in figure 18 and show that the circumneutral pH ground waters are at or close to calcite saturation. Low-pH waters are not shown because they are substantially undersaturated. These results are consistent with the hypothesis of calcite dissolution as an important source of calcium and the main driver for neutralizing the acidity from pyrite oxidation. The waters from well CC2A are noticeably undersaturated with respect to calcite,

relative to the other circumneutral pH waters, and this undersaturation and pH of about 6 suggests that this water may be on the verge of going acidic because it is losing its neutralizing capacity from calcite. The opposite trend — it has been acid and is now being neutralized by increased calcite dissolution — is unlikely because it would be the opposite of weathering trends observed by Ludington and others (2004). Waters from well CC2A also are anomalous with respect to several other constituents.

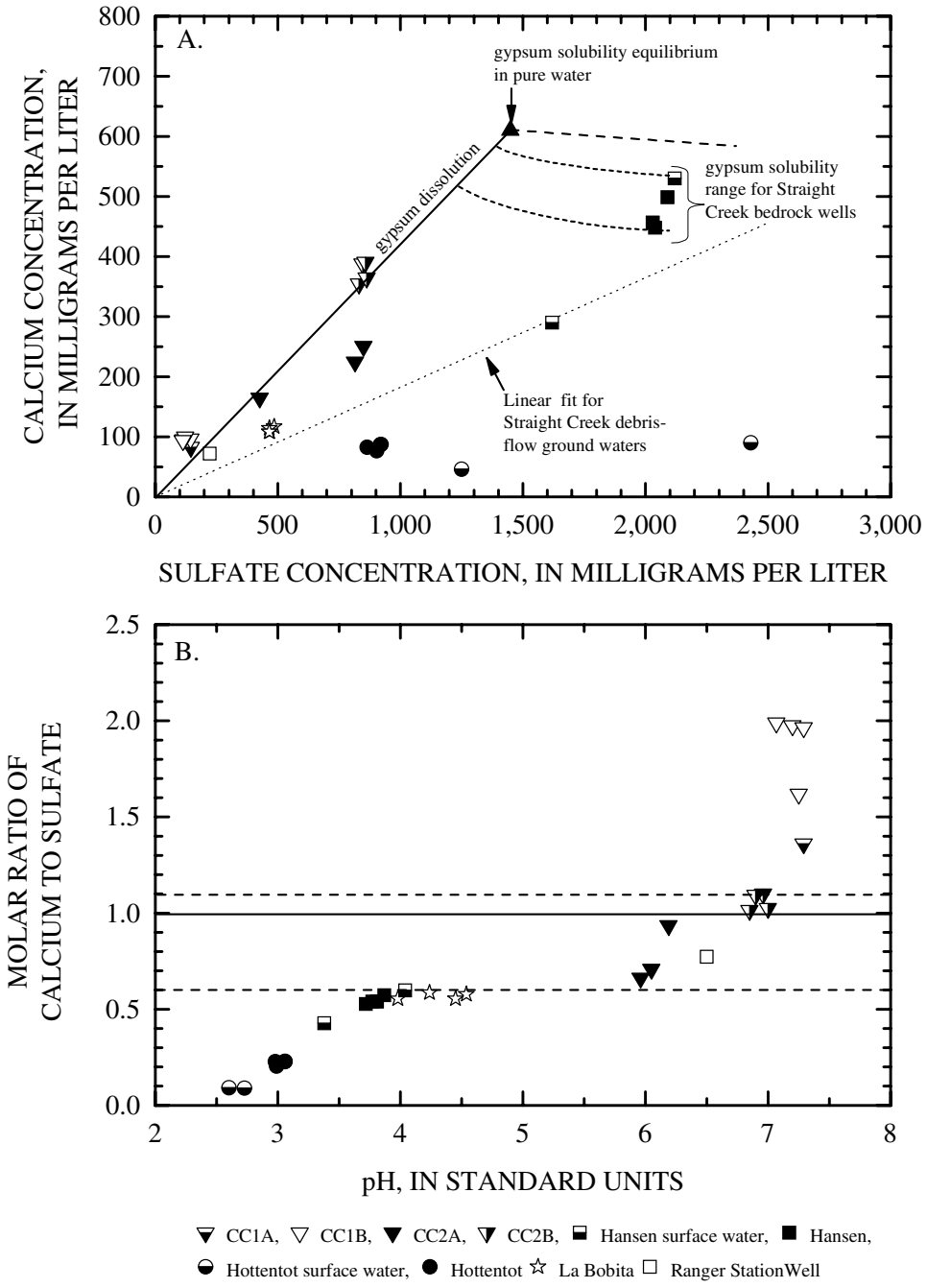

Figure 16. A. Calcium concentration in relation to sulfate concentration. Solid line shows stoichiometric gypsum dissolution ending at solubility equilibrium for gypsum in pure water. **B.** Plot of calcium: sulfate molar ratio in relation to pH. Solid line reflects 1:1 ratio of $Ca:SO_4$ and the dashed lines represents the region where gypsum dissolution is predominant.

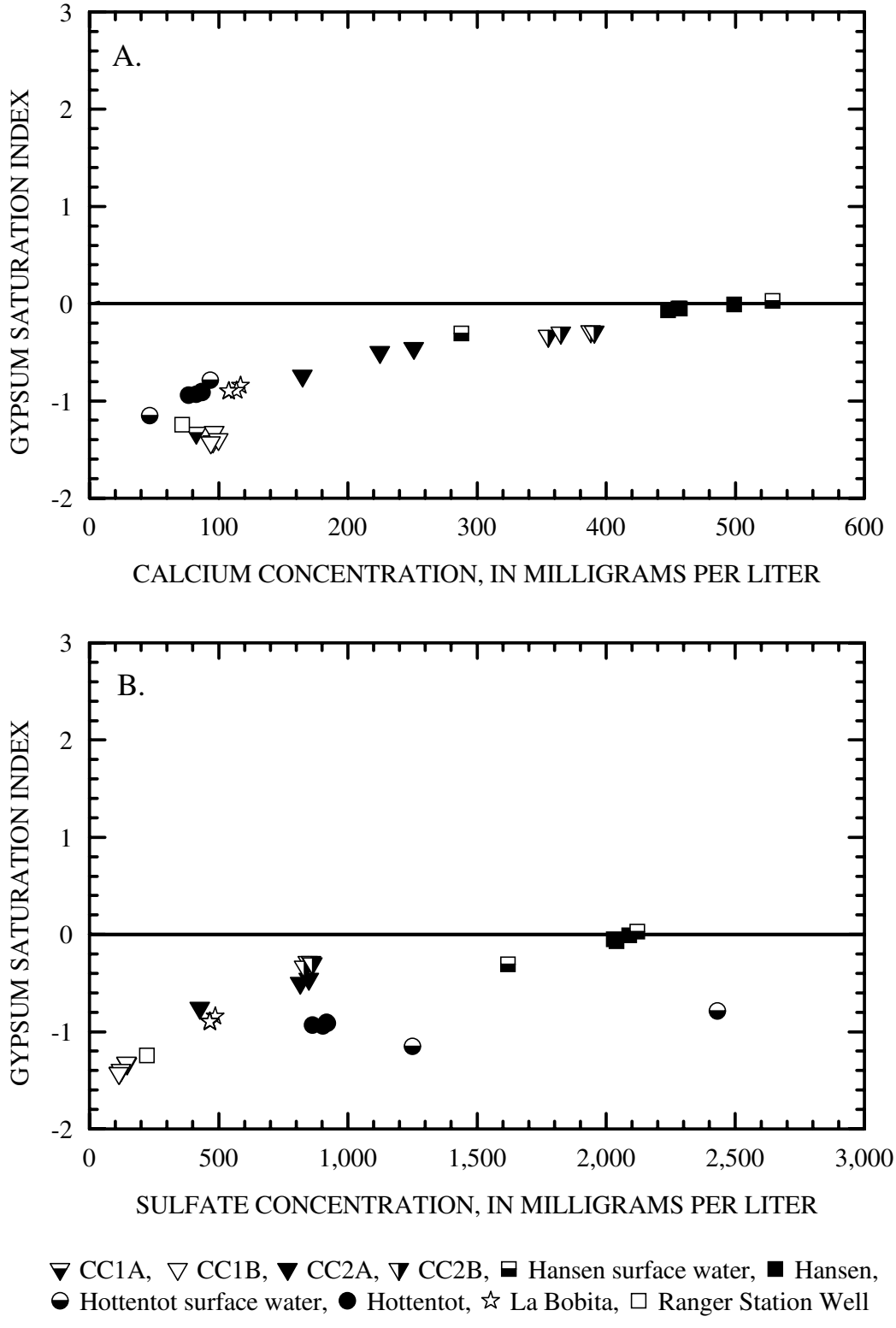

Figure 17. A. Saturation indices for gypsum in relation to calcium concentration. **B.** Saturation indices for gypsum in relation to sulfate concentration.

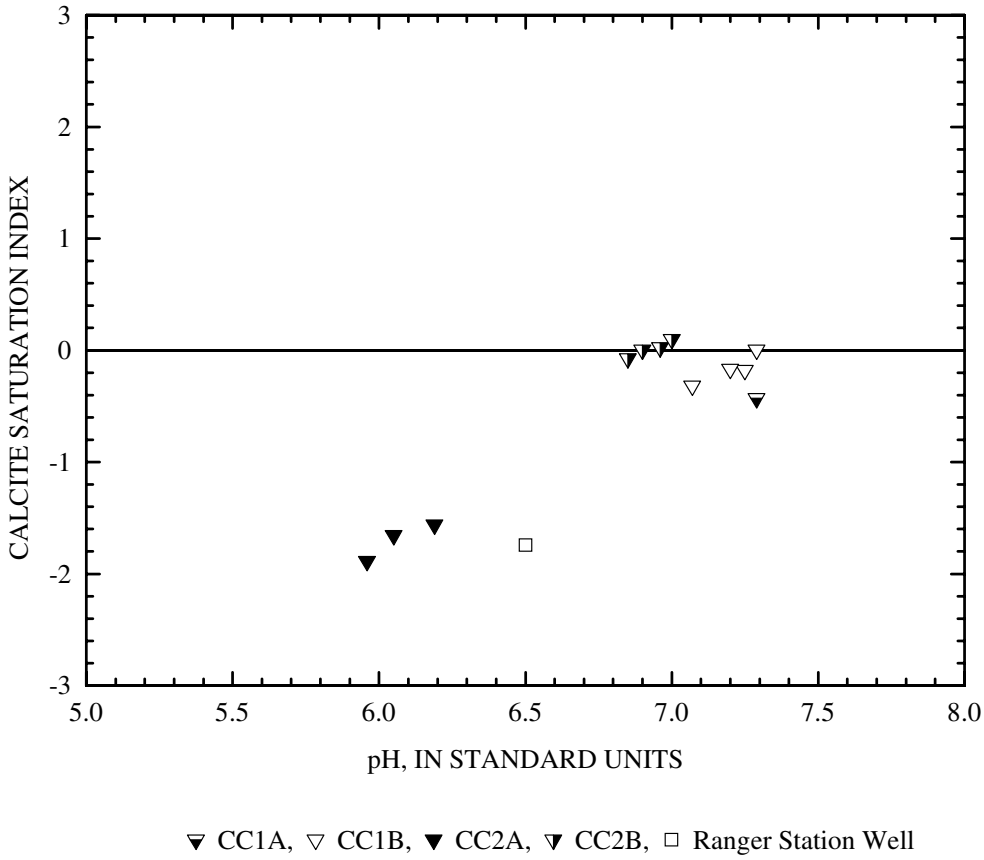

Figure 18. Calcite saturation indices in relation to pH.

Fluoride Chemistry and Fluorite Solubility

Fluoride concentrations can vary widely in ground waters of the Red River Valley depending on the type and degree of mineralization of the aquifer material (LoVetere and others, 2004; Naus and others, 2005). The most readily available source of fluoride from weathering processes is dissolution of fluorite, CaF_2, a common gangue mineral. Plots of fluoride concentration in relation to calcium concentration and sulfate concentration are shown in figures 19A and 19B, respectively, to compare to the same plots for the Straight Creek data (Naus and others, 2005). Fluoride does not follow the dilution trend found in the Straight Creek catchment except at sulfate concentrations below 1,000 mg/L. Fluoride concentrations in waters from phase II wells are nearly constant in the range of 1 to 4 mg/L with the one exception of waters from well CC2A for which concentrations as high as 20 mg/L have been determined. Figure 19A indicates that increasing fluoride in CC2A is consistent with increasing calcium. Furthermore, the increase in fluoride for CC2A (high minus low concentration) is about 0.6 millimole for a 1.5 millimole increase in calcium. If fluorite were the only calcium-bearing mineral dissolving, 3 millimoles of fluoride would be produced for every 1.5 millimoles of calcium. Thus, there is no mass balance constraint on fluorite dissolution to account for the increased fluoride concentration. Equilibrium fluorite solubility would be a constraint, and figures 19C and 19D show the fluorite saturation indices plotted in relation to calcium concentration and pH, respectively. At low pH the waters are substantially undersaturated, but at circumneutral pH fluorite saturation is reached for all waters except those from well CC2A which are about an order of magnitude supersaturated. The result for CC2A is similar to that for SC2B from the Straight Creek catchment. These two wells have similar pH values and fluoride concentrations for SC2B are similar to the lower fluoride concentration in

CC2A. Fluoride speciation and fluorite saturation indices have been shown to be sensitive to aluminum concentrations (Naus and others, 2005). The waters from well CC2A contain aluminum concentrations of about 1 to 6 mg/L. These aluminum concentrations are high enough that they should have complexed most of the fluoride and kept the saturation indices of fluorite closer to saturation. Another possible source of apparent supersaturation would be errors in the analytical determination of fluoride. However, the analyses have been carefully checked by two independent techniques (ion chromatography and ion-selective electrode potentiometry) with excellent agreement so that analytical error is an unlikely possibility. Whether this supersaturation is an artifact of speciation calculations or a real effect that may indicate kinetic inhibition to fluorite solubility equilibrium is difficult to determine at this time. What can be stated is that fluorite supersaturation is observed for samples that have pH values of 5 to 7, fluoride concentrations above 5 mg/L, and low aluminum concentrations. Compositions other than those found in waters from well CC2A reach fluorite solubility equilibrium at neutral pH values without achieving supersaturation.

Magnesium Chemistry

The three predominant mineral sources of magnesium in ground waters of the Red River Valley are dolomite, magnesium-rich carbonates (calcite and rhodochrosite), and chlorite (Ludington and others, 2004). Carbonates weather faster than silicates so that dolomite and magnesium-rich carbonates should be more important sources of magnesium than chlorite, but chlorite is abundant in most of the rocks and it is fine-grained, increasing its reactivity.

Figures 20A portray the concentrations of magnesium relative to those of sulfate. There is a general tendency for these constituents to follow a dilution trend but the trend does not fit the Straight Creek trend particularly closely. Data from the La Bobita, CC1B, and Questa Ranger Station wells follow the Straight Creek alluvial well trend, whereas data from the Hansen and Hottentot wells fall on the Straight Creek surface-water trend and CC2A and CC2B wells have Mg concentrations that are depleted with respect to the Straight Creek surface-water trend. The one feature comparable to Straight Creek is that the Hansen and Hottentot ground waters are enriched in magnesium relative to sulfate compared to their surface water counterparts. The relation of magnesium to calcium (fig. 20B) shows that only Hottentot and La Bobita data are near the Straight Creek trend and the remaining data are either enriched in calcium or depleted in magnesium relative to the Straight Creek trend. Wells CC1A and CC1B are enriched in calcium from calcite weathering (figure 16B and accompanying text), whereas wells CC2A, CC2B, and Hansen are more influenced by gypsum dissolution without as much magnesium carbonates or silicates.

Figures 20C and 20D indicate that all samples are undersaturated with respect to dolomite. Thus, dolomite solubility does not provide a constraint on magnesium concentrations.

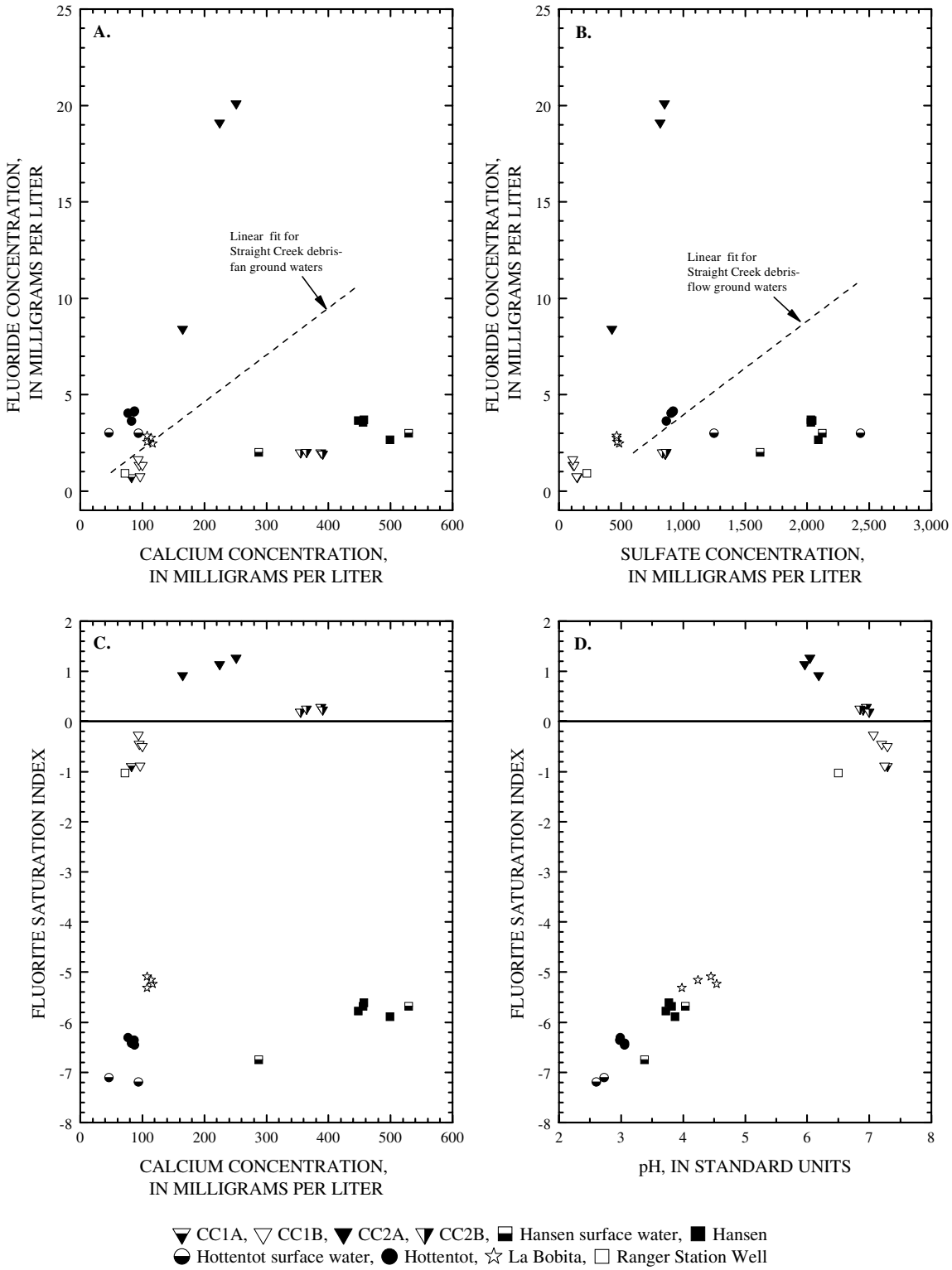

Figure 19. A. Fluoride concentration in relation to calcium concentration. Dashed line represents a linear fit of Straight Creek debris-fan wells. **B.** Fluoride concentration in relation to sulfate concentration. Dashed line represents a linear fit of Straight Creek debris-fan wells. **C.** Fluorite saturation indices in relation to calcium concentration. **D.** Fluorite saturation indices in relation to pH.

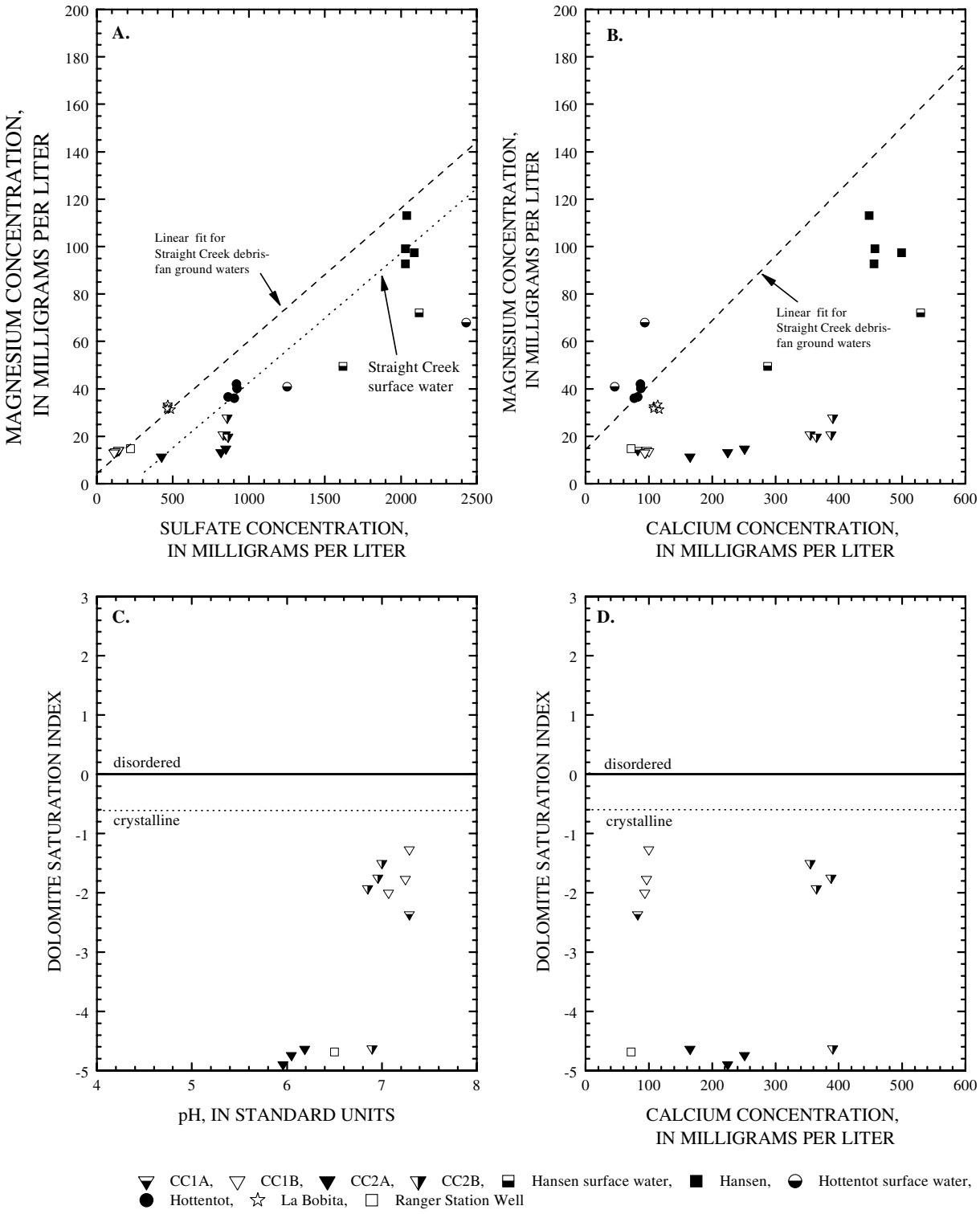

Figure 20. A. Magnesium concentration in relation to sulfate concentration. Dashed line represents a linear fit of Straight Creek debris-fan wells. Dotted line represents a linear fit of Straight Creek surface water. **B**. Magnesium concentration in relation to calcium concentrations. Dashed line represents a linear fit of Straight Creek debris-fan wells. **C**. Dolomite saturation indices in relation to pH. **D**. Dolomite saturation indices in relation to calcium concentration.

Strontium Chemistry

Strontium concentrations in ground waters of the Red River Valley do not follow the simple dilution trends that exemplify most constituents. Instead, they show a pattern of markedly increased concentration only at the highest calcium concentrations. The plot of strontium in relation to calcium concentrations for the Straight Creek data (Naus and others, 2005) showed that strontium concentrations did not exceed 1.5 mg/L until calcium concentrations reached about 400 mg/L, and then strontium increased to 12 mg/L. A similar plot for the phase II well data is shown in figure 21A. Strontium concentrations do not exceed 1.5 mg/L until calcium concentrations reach 350 mg/L, indicating that dissolution of calcite is a primary source of strontium. Mineralogical data with trace-element compositions for calcites support this hypothesis. Up to 0.6 percent SrO has been found in calcite from Straight Creek rock samples (G.S. Plumlee, oral commun., 2004). Figure 21B, a plot of strontium relative to sulfate concentrations, shows no dilution trend.

Saturation indices for celestite and strontianite as a function of calcium concentration are shown in figures 21C and 21D, respectively. Although celestite saturation is reached at high calcium concentrations for the Straight Creek data, the saturation indices remain about 0.5 log units below saturation for the phase II well data. Strontianite saturation indices remain at least an order of magnitude undersaturated because of the Gibbs phase rule constraint (Naus and others, 2005; Plummer and others, 1990).

Silica Chemistry

The range of silica concentrations from the phase II data is in the same general range as those from the Straight Creek study but there are some important differences. Silica concentrations are plotted relative to sulfate concentrations in figure 22. The silica concentrations in the Hottentot surface and ground waters are comparable to those from the Straight Creek alluvial ground waters; however, silica concentrations from Hottentot surface waters are elevated substantially above those from Straight Creek surface waters. Silica concentrations in the Hottentot surface waters are likely to be elevated because the Hottentot surface waters have longer residence times in the debris fan than the Straight Creek surface waters. The increased residence time of acid water with aluminosilicate minerals should result in dissolution of more silica. Silica concentrations higher than the trend for Straight Creek alluvial well waters may reflect the increased silica content of the weathered rhyolite porphyry at Hottentot.

The silica concentrations in both surface and ground waters for Hansen are similar to those in the Straight Creek surface waters, because the Hansen waters have low residence times. The low silica concentrations in the remaining waters are typical of low-temperature circumneutral pH ground waters and show moderately increasing concentrations with decreasing pH (La Bobita waters have pH values of 4 to 4.5 and the highest silica concentrations, 33 to 35 mg/L, for this group of low silica waters).

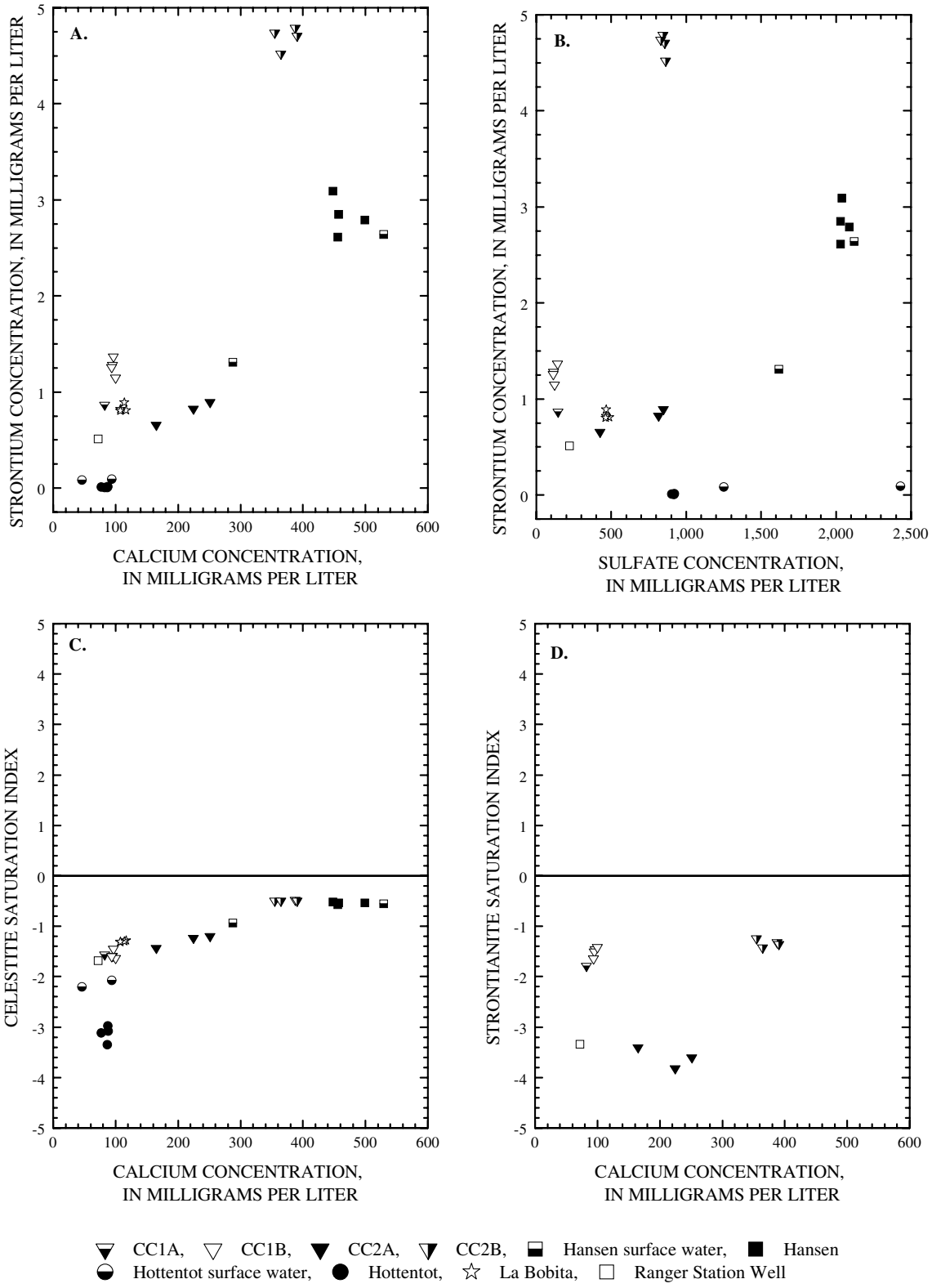

Figure 21. A. Strontium concentration in relation to calcium concentration. **B.** Strontium concentration in relation to sulfate concentration. **C.** Celestite saturation indices in relation to calcium concentration. **D.** Strontianite saturation indices in relation to calcium concentration.

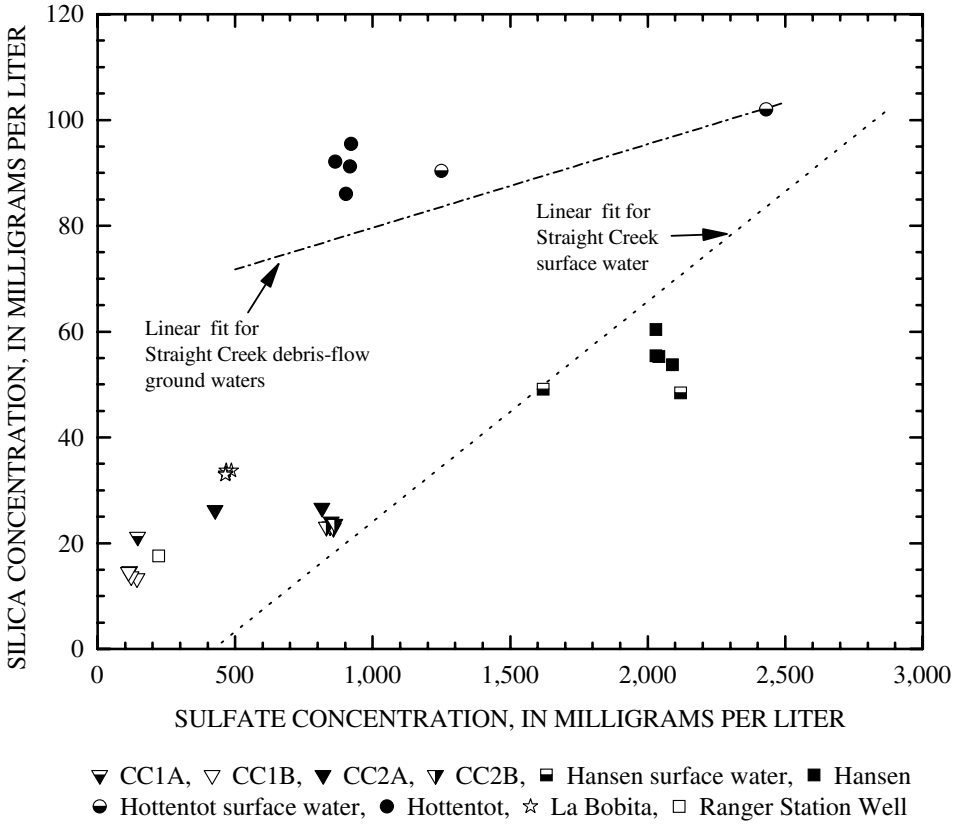

Figure 22. Silica concentration in relation to sulfate concentration. Linear fit lines are shown for the dilution of the Straight Creek debris-fan ground waters and the dilution of the Straight Creek surface waters.

Alkali Metal Chemistry

Lithium. Figure 23 depicts lithium concentrations relative to sulfate concentrations for the phase II data. The lithium concentrations generally follow the trend of Straight Creek alluvial well data except that Hottentot surface waters and all Hansen waters have lower lithium concentrations than the trend line. The lithium concentrations are less than 0.1 mg/L in all the phase II wells.

Sodium. Sodium concentrations in the Straight Creek waters did not follow an obvious dilution trend and the plot of sodium in relation to sulfate concentrations was unclear because of apparent contamination of wells SC1B and SC5B by additives (Naus and other, 2005). These additives resulted in sodium concentrations substantially greater than 40 mg/L. Concentrations in water from all the other wells were below 40 mg/L, and these values were considered to more accurately represent the sodium concentrations in the ground waters. The sodium concentrations for the phase II ground waters are plotted in relation to sulfate concentrations in figure 24A. The highest measured sodium concentration is 45 mg/L in well CC2B. These results support the hypothesis that concentrations greater than about 40 to 50 mg/L are likely a result of anthropogenic contamination (for example well drilling additives, road salt, septic tank leakage, treated sewage effluent). The primary source for sodium from weathering processes would be plagioclase feldspar, primarily oligoclase and albite.

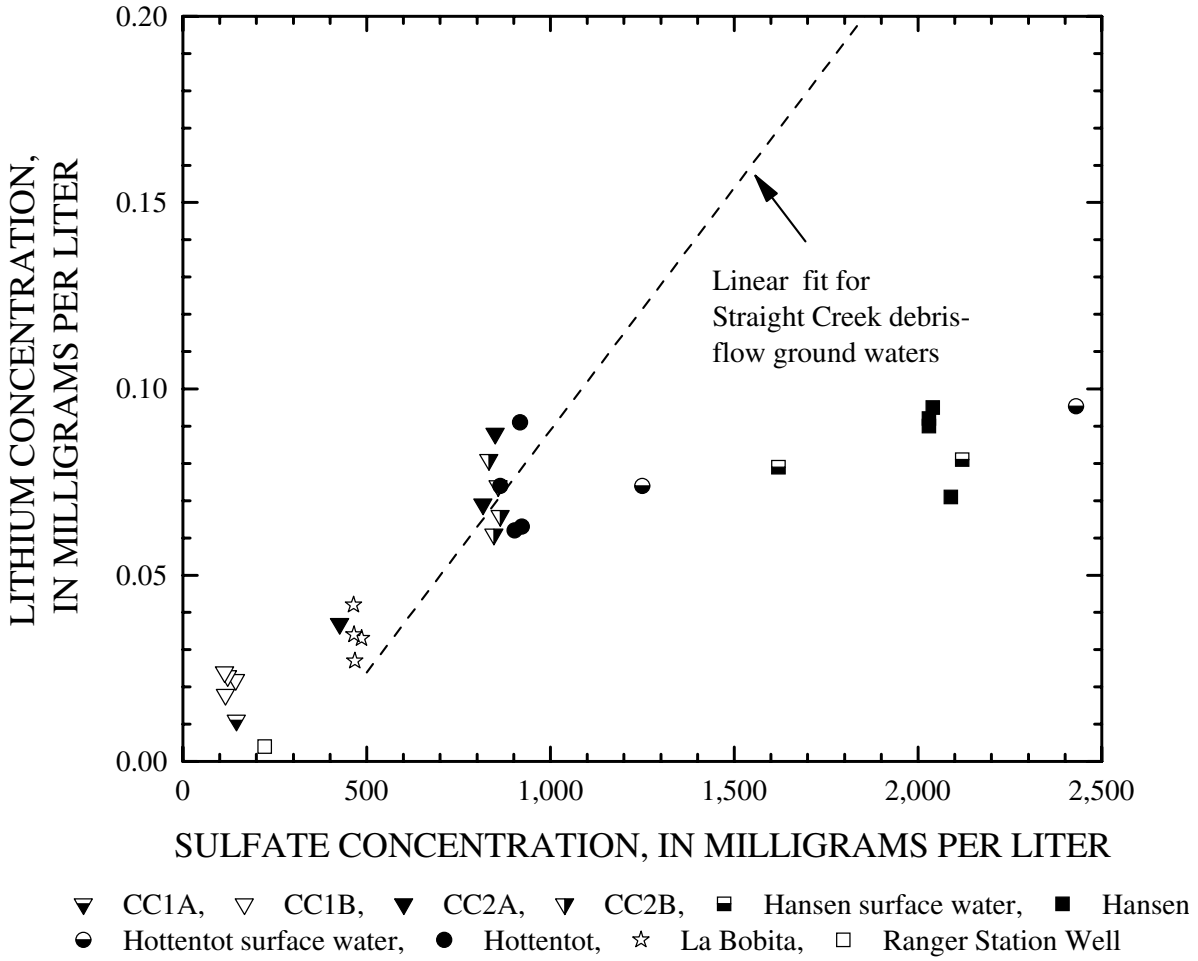

Figure 23. Lithium concentration in relation to sulfate concentration with the dashed line displaying the best fit for Straight Creek debris-fan wells.

Figure 24B shows the sodium concentrations relative to the chloride concentrations for samples from selected wells. The maximum chloride concentration is about 7 mg/L, whereas waters from wells SC1B and SC5B contained chloride concentrations in the range of 5 to 40 mg/L. These data further support the argument that uncontaminated ground waters in Red River aquifers are not likely to contain chloride concentrations greater than about 10 mg/L.

Figure 24C is a plot of lithium concentrations relative to sodium concentrations and demonstrates that lithium concentrations change little over a large range of sodium concentrations. The relation of the Li to Na provides additional evidence that lithium has limited abundance and lower solubility than sodium.

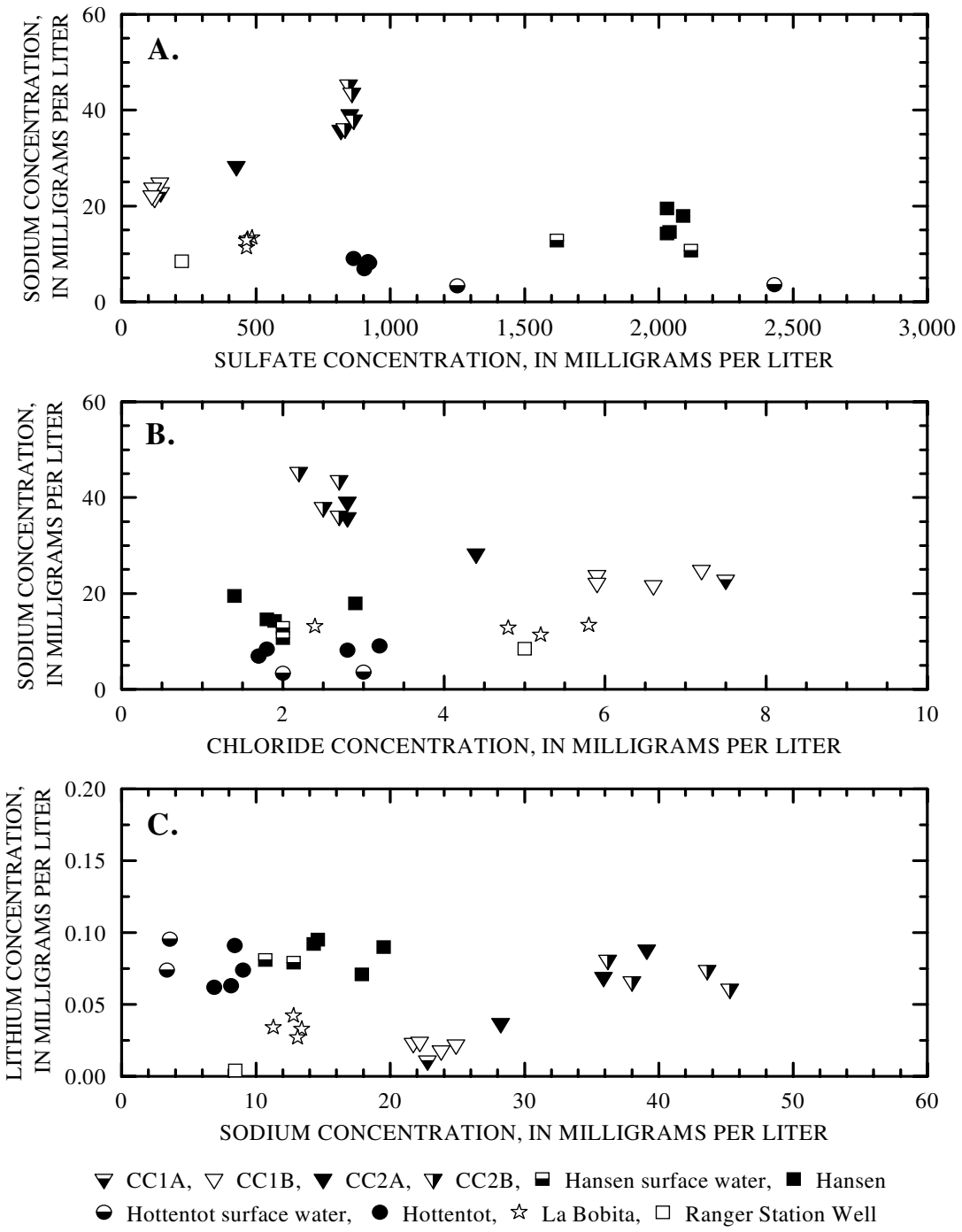

Figure 24. A. Plot of sodium concentration in relation to sulfate concentration. **B.** Sodium concentration plotted in relation to chloride concentration. **C.** Lithium concentration plotted in relation to sodium concentration.

Potassium. Potassium concentrations are plotted relative to sodium concentrations and sulfate concentrations in figures 25A and 25B, respectively. The trend of increasing potassium with increasing sodium is consistent with weathering of feldspars and some phyllosilicates. Potassium concentrations are always less than sodium concentrations for any given sample, reflecting the greater solubility of sodium minerals (such as albite or paragonite) relative to their potassium-rich equivalents (such as microcline or muscovite, respectively). Potassium concentrations do not exceed 8 mg/L for phase II ground waters, and these values confirm that this range is typical for weathering processes in the Red River Valley. Concentrations of 8 to 15 mg/L that were measured in wells SC1B and SC5B in the Straight Creek catchment are likely from contamination of the wells as suggested by Naus and others (2005).

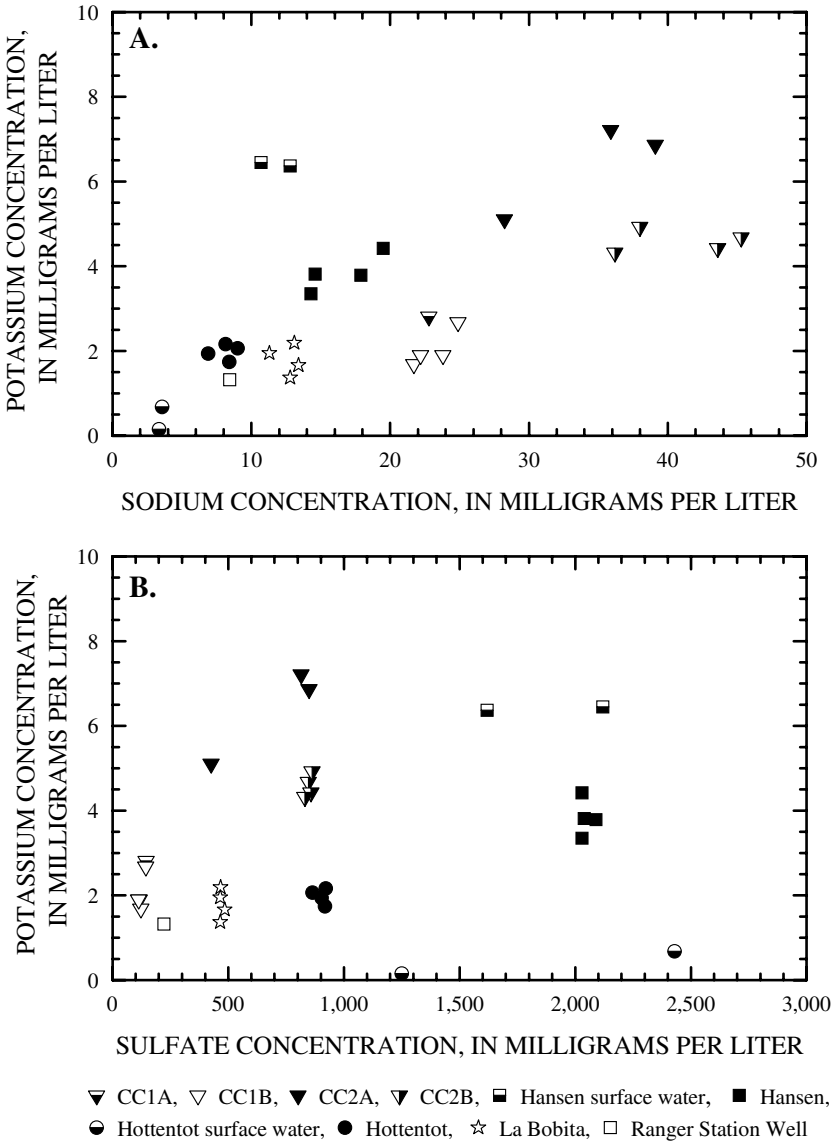

Figure 25. A. Potassium concentration in relation to sodium concentration. **B.** Potassium concentration in relation to sulfate concentration.

Trace Element Chemistry

Zinc and Cadmium. The plot of zinc concentrations relative to sulfate concentrations shown in figure 26A has some similarity to the trend from the Straight Creek alluvial wells (Naus and others, 2005), but some notable differences are also apparent. Two samples from CC2A are enriched in zinc, whereas Hansen samples and CC2B samples are depleted in zinc relative to sulfate compared to the Straight Creek trend line for alluvial ground waters. The Hansen samples may be low in zinc relative to those in the Straight Creek and Hottentot areas because of their more distal location from plutonic intrusions and the hydrothermal centers. The enrichment of zinc for samples from CC2A is unusual but is consistent with the elevated concentrations of manganese, fluoride, and beryllium that are found for these same samples. These anomalies indicate possible local hydrothermal mineralization in the vicinity of CC2A. The lack of elevated concentrations for these elements in nearby ground waters from wells CC1A, CC1B, and CC2B seems unusual unless there are substantial gradients in lithology and rock chemistry between these wells and well CC2A.

Figure 26B is a plot of zinc concentrations relative to manganese concentrations and reveals that the zinc:manganese ratios are similar to those for Straight Creek alluvial ground waters except for the two samples from CC2A that are substantially enriched in manganese relative to zinc. Cadmium and zinc concentrations are plotted in figure 26C. This figure shows that cadmium:zinc ratios vary substantially outside the Straight Creek catchment and could be a signature for individual catchments containing different mineral chemistry for trace elements. The source for most cadmium in waters infiltrating sulfide-mineralized areas is sphalerite, and these data indicate that different alteration zones may exhibit different cadmium:zinc ratios. The two Hottentot surface water samples differ substantially in trace-element concentrations. The sample with higher Zn and Cd concentrations were collected higher up in the catchment and contains substantially higher concentrations of iron and sulfate, indicating that oxidation of greater amounts of pyrite and other sulfide minerals could account for the higher trace element content. Concentrations of copper, zinc, cadmium, manganese, cobalt, chromium, nickel, lead, molybdenum, beryllium, and arsenic are elevated in concentration in the higher altitude sample relative to concentrations in the lower altitude sample. Copper enrichment in the higher altitude sample is illustrated in figure 26D that plots copper in relation to zinc concentrations.

Copper. Copper concentrations for the phase II ground-water data do not follow the trend found in the Straight Creek data. The concentrations of copper are plotted relative to sulfate in figure 27 along with the Straight Creek trend line for debris-fan ground waters. The Hansen waters are depleted in copper, and the upper altitude Hottentot surface water is enriched in copper relative to sulfate. The enrichment in several elements in the one Hottentot surface water was discussed in the zinc and cadmium – trace metal section. The depletion of copper in the Hansen waters is consistent with their relatively low zinc, manganese, and fluoride concentrations. This trend provides further evidence for the distal location of the Hansen area relative to centers of hydrothermal activity.

Nickel and cobalt. Concentrations of nickel and cobalt for the phase II ground waters are comparable to the dilution trends for the Straight Creek waters (Naus and others, 2005). Figure 28A shows the nickel concentrations relative to sulfate concentrations and figure 28B shows cobalt relative to nickel concentrations. Both plots correlate well with the Straight Creek trends and strongly indicate a single mineral source for these elements in the weathering environment with fairly constant cobalt:nickel ratios independent of alteration zone and lithology. Preliminary mineralogical data indicates that the main source of weatherable cobalt and nickel is pyrite (Plumlee, oral commun., 2004). Cobalt and nickel both occur in the pyrite from the area, but the Co:Ni ratio is very different than what is found in the water, indicating an attenuation process is taking place or another source of Ni. There is an indication of greater removal of cobalt relative to nickel for waters containing more oxidized iron and lower iron concentrations, such as Hansen and La Bobita well waters.

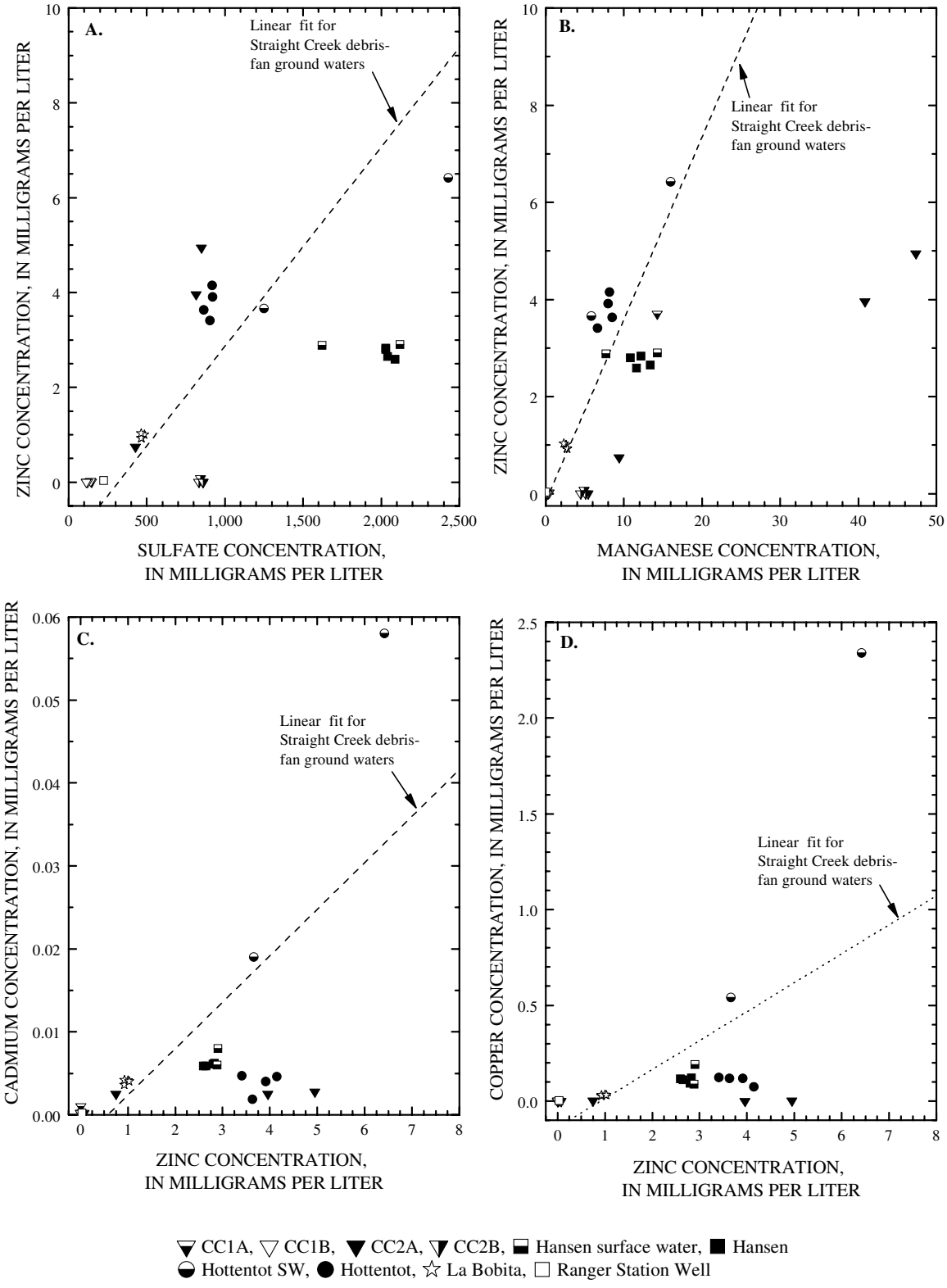

Figure 26. A. Zinc concentration in relation to sulfate concentration. **B.** Zinc concentration in relation to manganese concentration. **C.** Cadmium concentration in relation to zinc concentration. **D.** Copper concentration in relation to zinc concentration. Dashed line represents correlation of Straight Creek debris-fan ground waters.

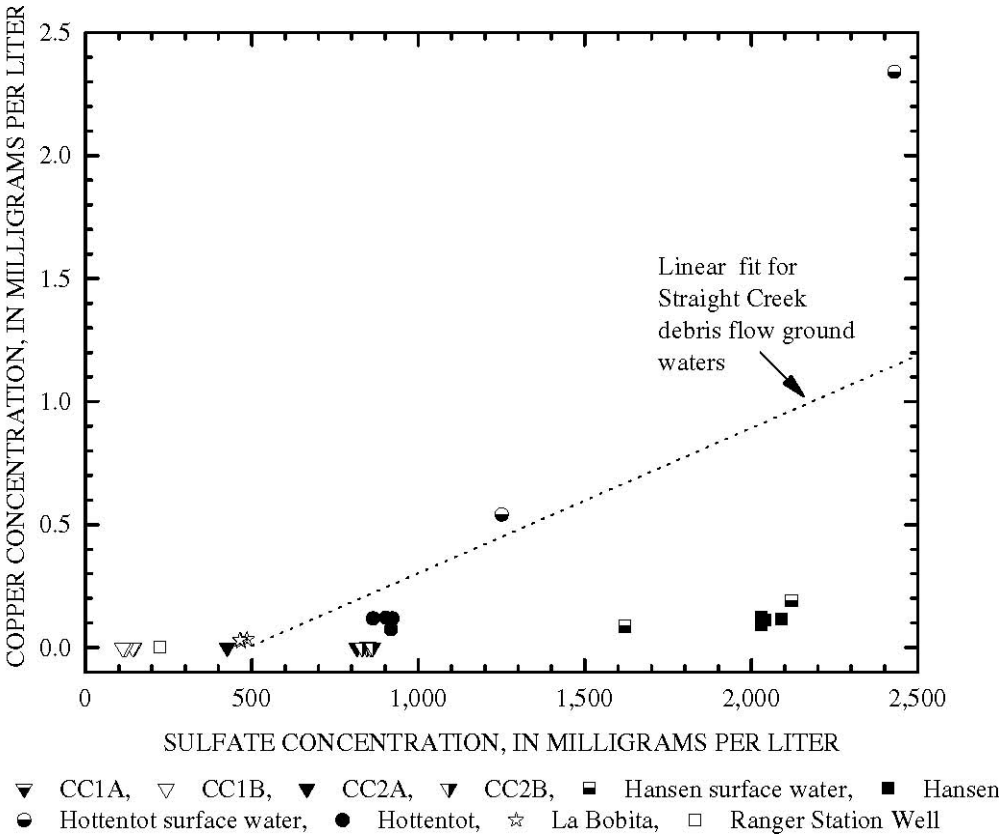

Figure 27. Copper concentration in relation to sulfate concentration. Dotted line shows correlation for Straight Creek debris-fan waters.

Barium. As mentioned in the previous report on the phase I ground-water data (Naus and others, 2005), barium concentrations are severely limited to concentrations of a few micrograms per liter or less because of the limiting solubility of barite and the high concentrations of sulfate from gypsum dissolution and pyrite oxidation. Instead of a dilution trend, an opposite trend is observed in the Straight Creek waters, with barium concentrations decreasing with increasing sulfate concentrations because of the common-ion effect. This same trend is seen in the phase II ground-water data shown in figure 29A, in which barium concentrations are plotted relative to sulfate concentrations. However, the anomalously high barium concentrations and supersaturated values for barite saturation indices observed for water from well SC5B are not seen in the phase II ground-water data. Figure 29B shows moderate supersaturation for samples of pH 4 or higher, and figure 29C shows little change in barite supersaturation as a function of barium concentration, unlike the Straight Creek data that show substantial and continuously increasing supersaturation with increasing barium concentrations (especially for waters from well SC5B) (Naus and others, 2005). The phase II data set appears to have less of a problem of fine-grained to colloidal barite getting through the filter units. The common occurrence of microscopic barite has been observed by Ludington and others (2004) and this result is consistent with the results from water chemistry given here. There appears to be few particles containing barium in these waters, as shown by the plot of dissolved barium in relation to total recoverable barium in figure 29D. Ground water from well CC2B, which is known to contain high turbidity, contains higher unfiltered barium concentrations than those that were filtered, but most of the other determinations were virtually equivalent within the analytical error.

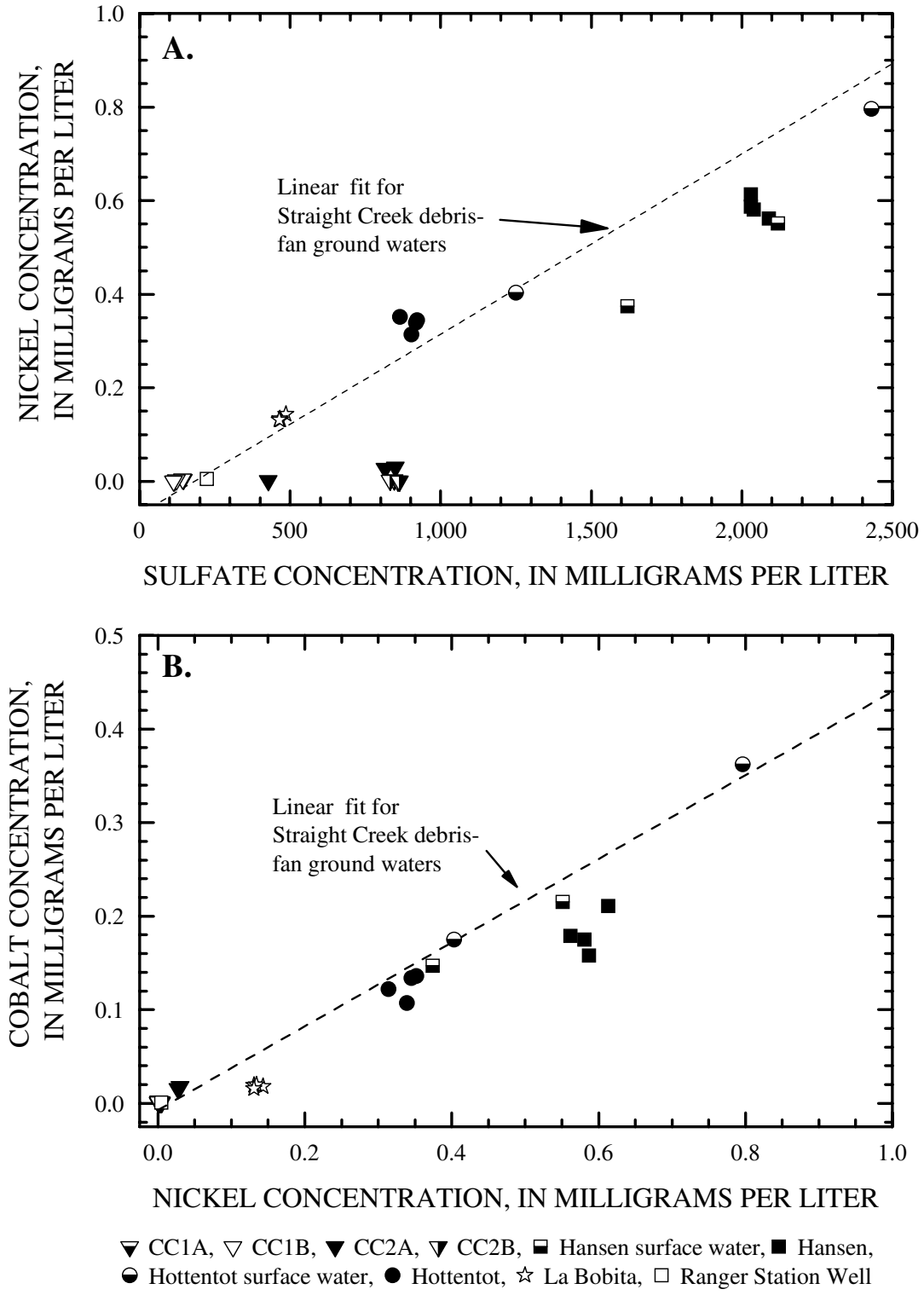

Figure 28. A. Nickel concentration in relation to sulfate concentration. **B.** Cobalt concentration in relation to nickel concentration. Dashed line shows correlation for Straight Creek debris-fan waters.

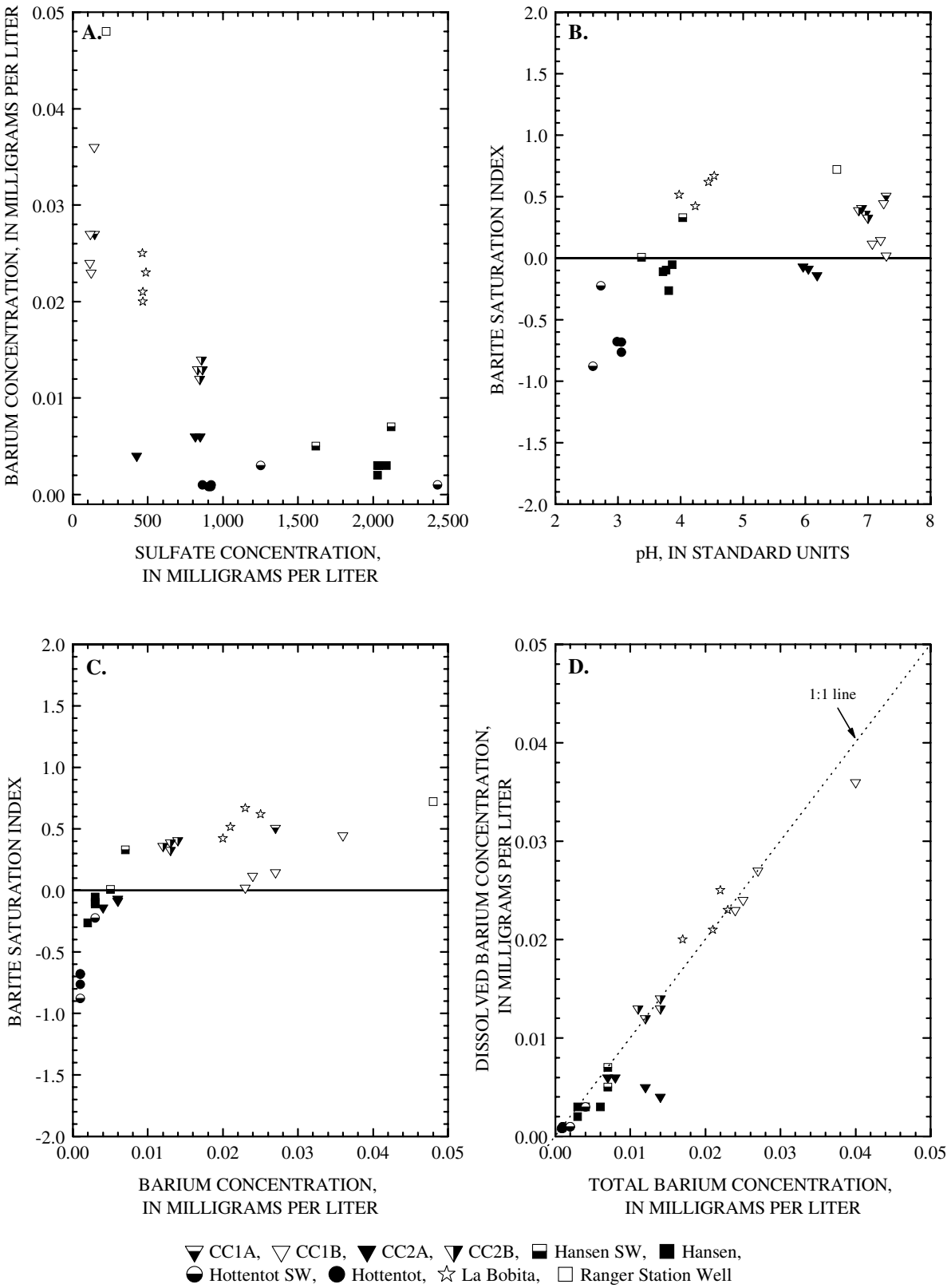

Figure 29. A. Barium concentration in relation to sulfate concentration. **B.** Barite saturation indices in relation to pH. **C.** Barite saturation indices in relation to barium concentration. **D.** Dissolved barium concentration in relation to total recoverable barium concentration.

Beryllium. Beryllium concentrations generally found near or below the ICP-OES detection limit of 0.001 mg/L in most ground waters, are present at tens to hundreds of µg/L in ground waters of the Red River Valley. Comparisons of the phase II samples in terms of beryllium and sulfate concentrations (fig. 30A) and beryllium and aluminum concentrations (fig. 30B) with the trends in the Straight Creek data (Naus and others, 2005) reveal a close correlation suggesting a similar dilution trend except for two anomalous samples from well CC2A. Furthermore, with the exception of well CC2A, the close association of lithium and beryllium mineralization that was noted for the Straight Creek ground waters in Naus and others (2005) also can be seen in the phase II ground-water data (fig. 31A). Figure 31A portrays a close correlation of lithium and beryllium concentrations with the trend lines from Straight Creek except for the beryllium-enriched values from CC2A. These enriched samples also are anomalously enriched in fluoride (fig. 31B). Complexing between beryllium and fluoride is strong and could account for the high concentrations of beryllium. The highest concentrations of beryllium in the historical ground-water quality data (LoVetere and others, 2004) also are those with the highest fluoride concentrations.

A potential solubility limiting phase for beryllium would be $Be(OH)_2$ (Langmuir and others, 2004). The highest beryllium concentration measured in ground waters from this study is 0.08 mg/L at a pH of 6. The solubility of $Be(OH)_2$ at 25°C is 0.1 to 1 mg/L (0.02 to 0.2 mg/L Be) at a pH of 6 depending on the degree of crystallinity of the precipitate. Hence, the ground-water composition approaches, but does not reach $Be(OH)_2$ saturation. Furthermore, the speciation of dissolved beryllium has not been calculated, and it would only make the dissolved beryllium appear more undersaturated with respect to $Be(OH)_2$.

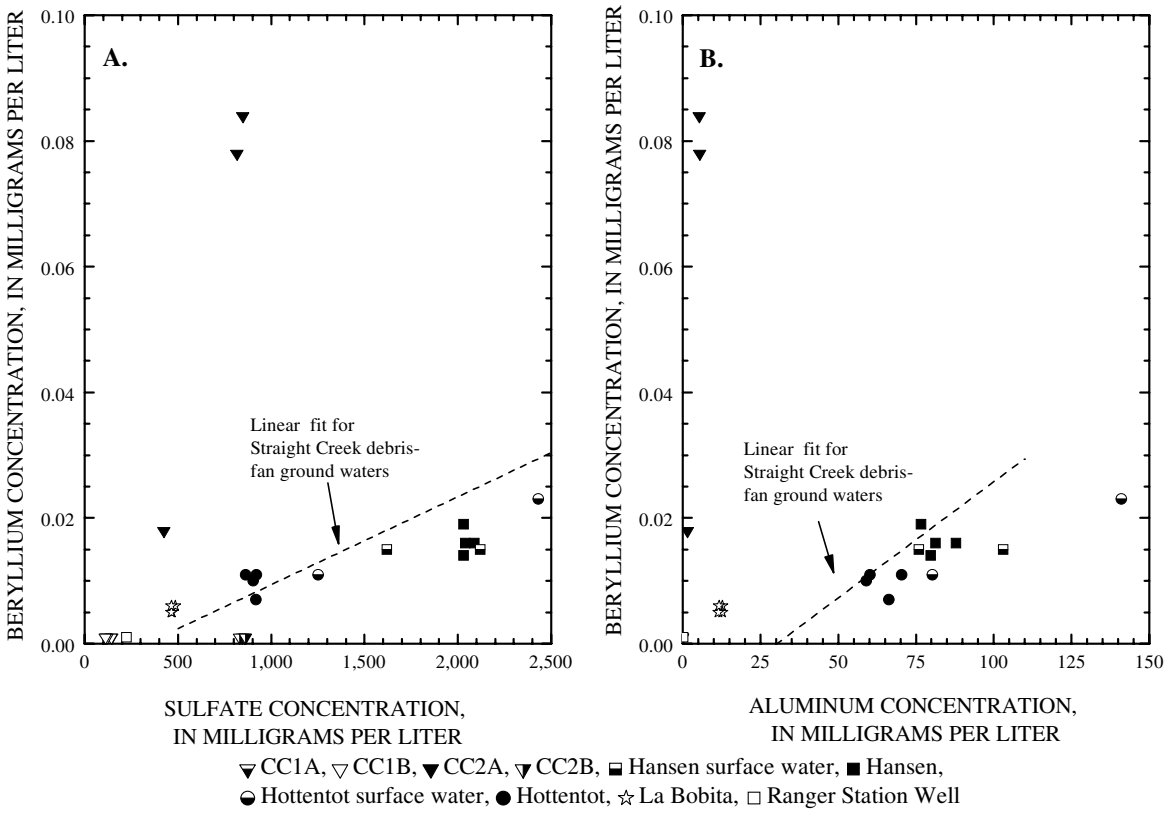

Figure 30. A. Beryllium concentration in relation to sulfate concentration. **B.** Beryllium concentration in relation to aluminum concentration. Dashed lines show correlation for Straight Creek debris-fan ground waters.

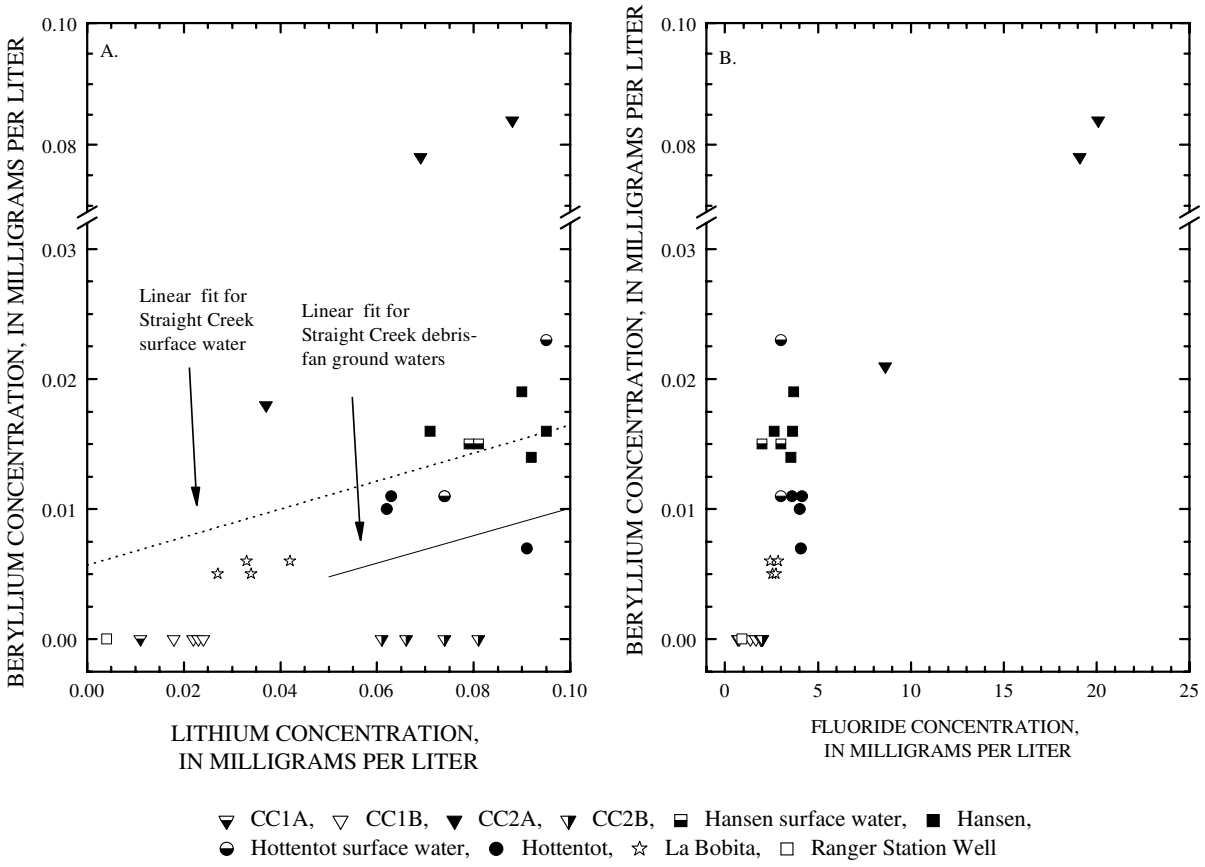

Figure 31. A. Beryllium concentration plotted in relation to lithium concentration with solid line showing correlation for debris-fan ground waters and the dotted line showing correlation for Straight Creek surface waters. **B.** Beryllium concentration plotted in relation to fluoride concentration.

Rare-Earth Elements

Rare-earth element (REE) concentrations were determined by ICP-MS for 10 phase II samples (fig. 32). The REE are normalized to chondrite values from Anders and Ebihara (1982) because of the Eu variations in the samples. The REE concentrations vary by over four orders of magnitude, and with the exception of samples from the Hottentot and Questa Ranger Station wells, have similar patters with a relatively flat light REE (La to Nd) portion, a negative Eu anomaly, and a slight negative slope or flat pattern for the heavy REE (Dy to Lu). The negative Eu anomaly is consistent with weathering of the Amalia Tuff (Johnson and Lipman, 1988; Lipman, 1988). The negative Ce anomaly found in the sample from the Questa Ranger Station well is consistent with oxidized waters.

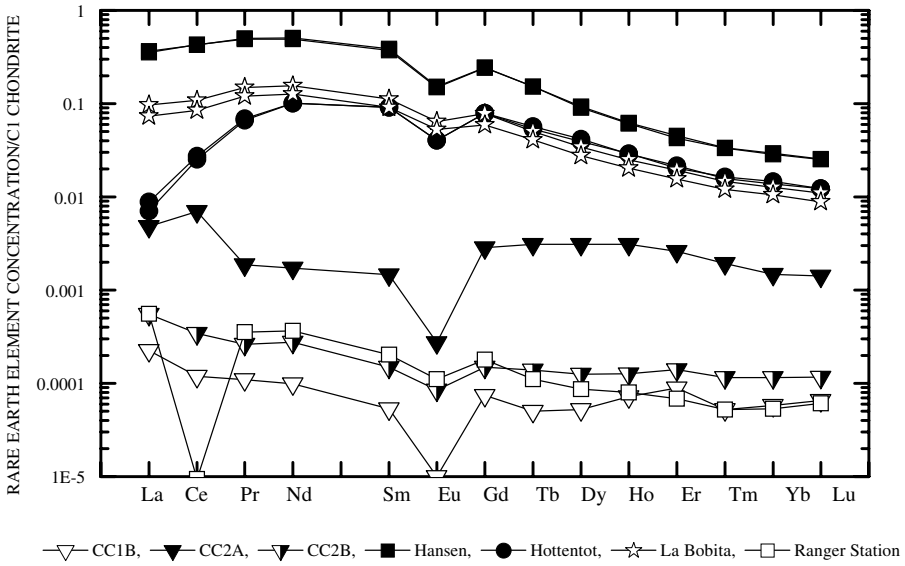

Figure 32. Rare-earth elements normalized against Chondrite for phase II wells.

Dissolved Organic Carbon and Hydrogen Sulfide

Dissolved organic carbon concentrations in the waters of this study are normal for ground waters, in the range of 0.5 to 3 mg/L (fig. 33). There is no obvious indication of well contamination by organic additives as was noted by Naus and others (2005) for wells SC1B and SC5B in the Straight Creek catchment. No hydrogen sulfide was detected for any phase II ground-water samples.

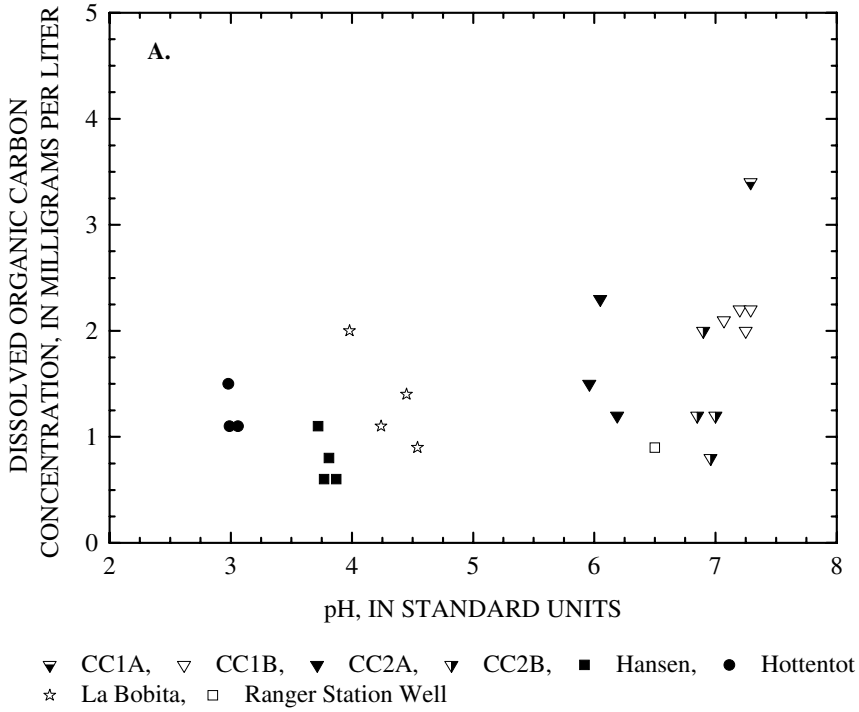

Figure 33. Dissolved organic carbon concentration in relation to pH.

Stable Isotopes

The oxygen and hydrogen isotopic compositions for selected sampling events, the global meteoric water line, the Rocky Mountain meteoric water line, and a Straight Creek rain and snow precipitation line are plotted in figure 34. Ground-water isotopic data are consistent with meteoric water as shown by local isotopic precipitation data in the Red River Valley, indicating ground are meteoric and show no significant indication of evaporation (fig. 34).

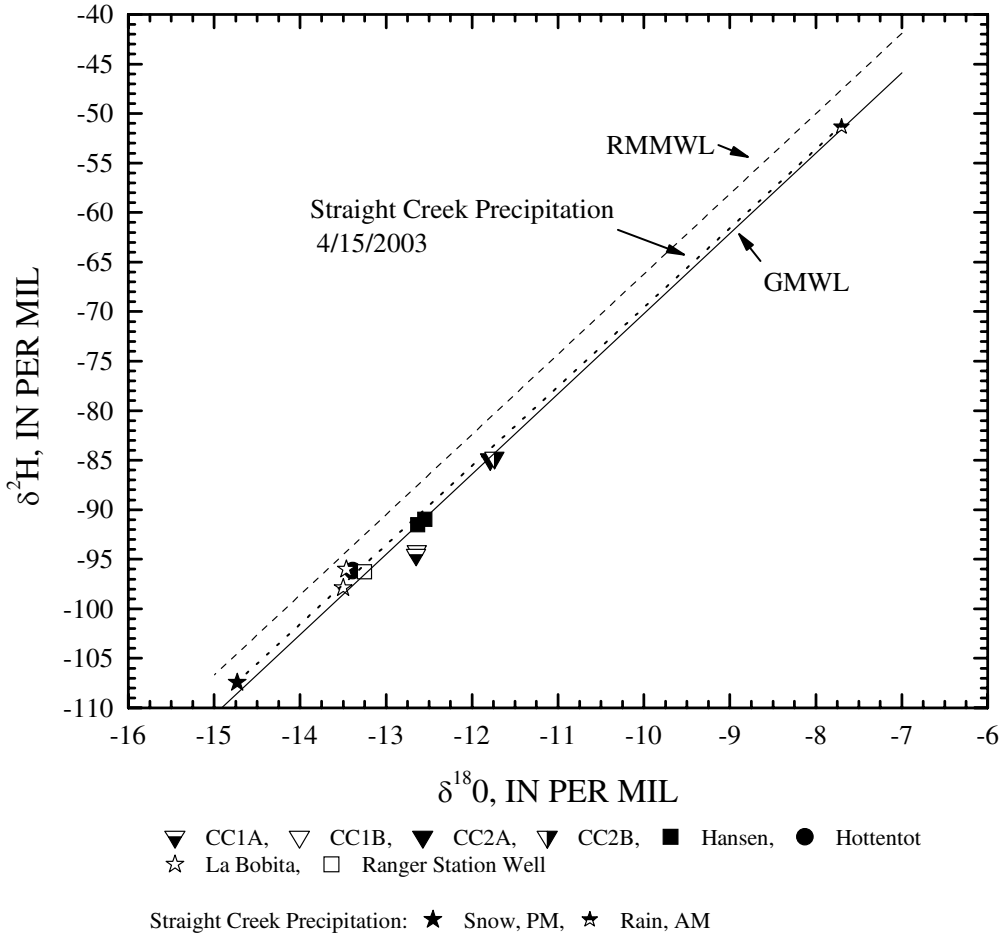

Figure 34. Hydrogen isotopic composition in relation to oxygen isotopic composition with a snow - rain line from Straight Creek, the Rocky Mountain meteoric water line, and the global meteoric water line.

The oxygen ($\delta^{18}O$) and sulfur ($\delta^{34}S$) isotopic composition of sulfate were determined for 13 phase II wells (fig. 35). With the exception of CC1A, the oxygen and sulfur isotopic composition of the phase II wells plot in the same region as the oxygen and sulfur isotopic composition of the phase I wells (except SC5B) (Naus and others, 2005). The $\delta^{34}S$ for well SC5B was much more positive, 4 to 5 per mil, than the other phase I and II well waters. The sulfur isotopic composition of well CC1A is consistent with the sulfur derived from ore-related FeS_2 or MoS_2.

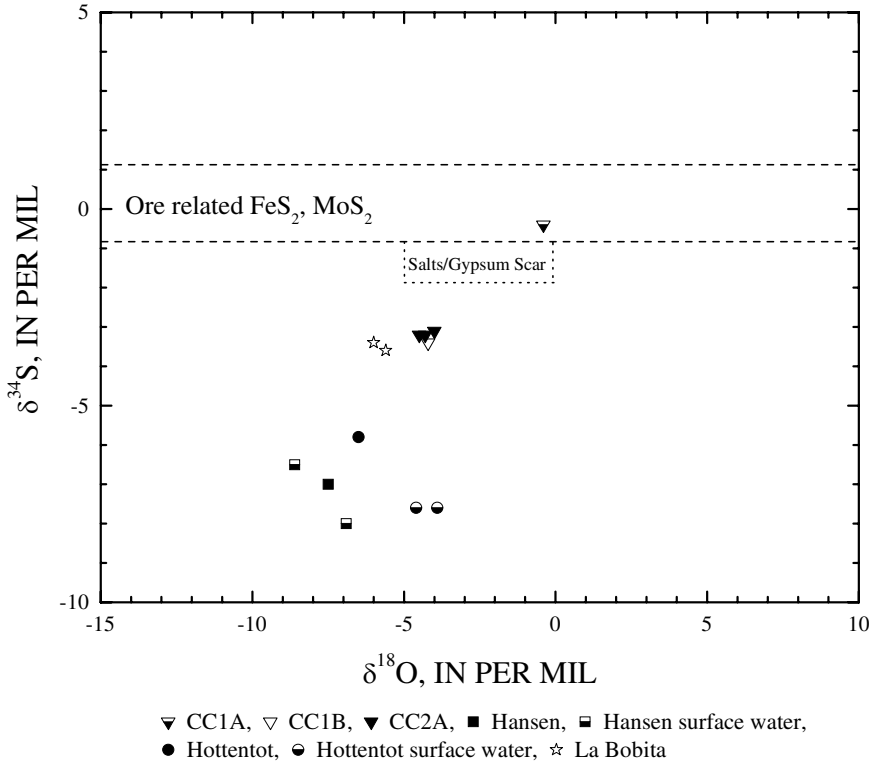

Figure 35. Sulfur isotopic composition of sulfate in relation to oxygen isotopic composition of sulfate with the region between the dashed lines showing sulfur composition related to ore FeS_2 and MoS_2.

Chlorofluorocarbons, Dissolved Gases, and Tritium

Samples were collected for determination of CFC, dissolved gas, and tritium concentrations for ground-water age-dating purposes. This section presents background information regarding ground-water age dating, analytical methods, and results.

Background

Ground-water age dating refers to the process of measuring the amount of time elapsed since a parcel of ground water became isolated from the atmosphere (residence time). The actual dating of water in almost all cases relies on the measurement of a specific tracer that is introduced to the ground water at the water table by a known physiochemical or biological process. The parcel of water then becomes isolated from the atmosphere with subsequent recharge and thus begins to "age" (Clark and Fritz, 1999). This measured time component should be considered a mean residence time for the ground water within an aquifer and can be used to determine recharge and discharge rates of water in the aquifer, horizontal and vertical flow velocities, or even the determination of kinetic reaction rates associated with bedrock weathering.

A simple system for classification of ages of ground water within a given flow system is commonly used. "Modern" ground waters are those waters considered to have been recharged within the past few decades and are considered part of the active hydrological cycle. "Sub-modern" waters are considerably older (pre-dating 1940s) and are characterized by the lack of measurable tritium (^3H) in the water.

Chlorofluorocarbons

Chlorofluorocarbons (CFCs) are stable synthetic organic compounds that were first produced in the 1930s and are purely of anthropogenic origin in the atmosphere. CFCs have accumulated in the atmosphere at a quantifiable rate since the 1930s, resulting in a relation between CFC concentration and age in modern ground water. Concentrations of CFCs in water are controlled by the partial pressure (altitude and mole fraction) of the constituent CFC (CFC-11, CFC-12, and CFC-113) and recharge temperature of the ground water. By measuring the concentration of a CFC in a sample, an atmospheric concentration can be computed and then compared to a known atmospheric concentration profile to define an age for the sample. This analysis ideally produces three complementary ages, each associated with a common CFC (CFC-11, CFC-12 or CFC-113). Strengths of the technique are the conservative nature of CFCs as ground-water tracers in aerobic conditions and the relative ease of analysis (Plummer and Busenberg, 2000). Drawbacks of the technique are the problems of age (concentration) being affected by mixing with other waters or the physical degradation of the CFCs in anaerobic conditions.

Helium-3 / Tritium Dating

Tritium, ^{3}H, the radioactive isotope of hydrogen, has a half-life of 12.43 years and undergoes beta decay to helium-3 (^{3}He). Tritium in the atmosphere is mainly associated with atmospheric testing of nuclear devices that began in 1952 and reached a maximum in 1963-1964. The nature of the ^{3}H input to the atmosphere produces a spike-like input associated with the nuclear testing maximum and a decay curve as the initial input undergoes radioactive decay. The ^{3}H age-dating technique is similar to CFC dating in that a measured concentration can be used to determine age through comparison to an historic input curve. The technique is improved by using a separate measurement of ^{3}He in the ground water to produce an absolute age, independent of the ^{3}H input curve, based on radioactive decay of ^{3}H to ^{3}He. This technique requires two separate samples, one for the measurement of tritiogenic ^{3}He (^{3}He from ^{3}H decay, denoted as $^{3}He^{*}$) contained as a dissolved gas in the ground water, and the other for the low-level measurement of ^{3}H by the ^{3}He in-growth method (Clark and others, 1976; Bayer and others, 1989).

Discrimination of $^{3}He^{*}$ from the total amount of ^{3}He in the dissolved gas samples requires not only the measurement of total amount of helium and its isotopic composition but also the measurement of Ne, Ar, and N_2. The data derived from these analyses facilitate the separation of the various sources of ^{3}He contained in the sample. Sources of helium within ground water include: ^{3}He associated with atmospheric solubility ($^{3}He_{solubility}$), He from excess air ($^{3}He_{exair}$), excess ^{3}He from primordial and nucleogenic sources ($^{3}He_{terrigenic}$), and ^{3}He from ^{3}H decay.

The solubility of ^{3}He is a function of the equilibrium solubility of ^{3}He in the atmosphere (temperature and pressure (altitude) related); however, the measured ^{3}He is frequently much higher than predicted by atmospheric solubility (along with other atmospherically derived gases (Ne, Ar and N_2)). The most common explanation for this supersaturation of gas within a sample is entrapment of air below wetting fronts during aquifer recharge. The entrapped air is forced into solution creating a gas component in excess above that of atmospheric solubility (excess air).

There is $^{3}He_{terrigenic}$ associated with an extrinsic source of helium that is migrating into the ground-water flow system; whether it comes from the rock the ground water flows through, or as a basal flux into the system, this excess component can be viewed as being derived from two sources; primordial and crustal. Primordial sources of ^{3}He include ^{3}He incorporated into the earth's mantle during planetary accretion (Clark and Fritz, 1999), while crustal He refers to He produced in the earth's crust by the decay of U-Th series elements. During U-Th series decay, ^{4}He is produced by alpha decay, while ^{3}He is produced as a result of fission reactions with ^{6}Li (nucleogenic production). The production ratio of ^{3}He to ^{4}He is typically on the order of 1.0×10^{-8} or 0.02 R/RA, where R is $^{3}He/^{4}He$ ratio in the sample and RA is the $^{3}He/^{4}He$ ratio in air ($R_{air} = 1.384 \times 10^{-6}$ (Ozima and Podosek, 1983)). For this investigation, the primary source of terrigenic He is assumed to be from crustal production (radiogenic/nucleogenic) not primordial (mantle derived).

Proper use of the $^3He/^3H$ age dating technique requires that the sources of ^3He be resolved. Accounting for these various sources, tritiogenic ^3He is calculated by:

$$^3He^* = {}^3He_{measured} - {}^3He_{solubility} - {}^3He_{exair} - {}^3He_{terrigenic} \quad (6)$$

where $^3He_{measured}$ is ^3He measured in the sample; $^3He_{solubility}$ is ^3He produced by atmospheric solubility, derived by using Ne, Ar, and N_2 concentrations; $^3He_{exair}$ is ^3He associated with excess air, calculated using Ne, Ar, and N_2 concentrations; and $^3He_{terrigenic}$ is associated with excess He, calculated using He, Ne, Ar, and N_2 concentrations.

The ^3He in-growth method of measuring ^3H allows for determinations as low as 0.05 tritium units (TU), where one TU equals 1 ^3H atom per 1018 hydrogen atoms. The method involves degassing a sample of water and sealing it off from the atmosphere in a measuring vessel for approximately 2 months. The sample is then analyzed for ^3He produced by ^3H decay over the 2-month period (^3He in-growth) and the amount of ^3H is then calculated.

Using the data from both the dissolved gas measurement and the tritium analysis (^3He in-growth method) the apparent age of the sample is derived from:

$$t = T_{1/2}/\ln 2 \times \ln(1 + (^3He^*/^3H)) \quad (7)$$

where t is apparent age, in years; $T_{1/2}$ is the half-life of ^3H, in years; and $^3He^*/^3H$ is the measured ratio of $^3He^*$ and ^3H.

The advantage of this technique is that the age determined for the sample is a function of the daughter-to-parent isotope ratio. This method is insensitive to mixing with sub-modern waters, and in the case of mixing of modern waters it produces an average age of the two mixing systems. Another advantage is the determination of the recharge temperature of and excess air in the sample by measuring the other dissolved gases; this is typically estimated using other techniques. A disadvantage of this age-dating technique is that it is limited to about 60 years of measurement (4.5 half-lives). Other disadvantages include the need for a specialty laboratory (noble gas mass spectrometer with ultra-high vacuum extraction system) for measurement and the time required for the ^3He in-growth analysis.

Analysis

Chlorofluorocarbons

Analyses of CFCs are performed on a gas chromatograph fitted with an electron capture detector (table 3), which allows for the measurement of CFC-11, CFC-12 and CFC-113 to concentrations as low as 0.5 to 1.0 picogram/kilogram. The concentrations of CFC-11, CFC-12, and CFC-113 were calculated from the concentrations in the water sample, the water temperature, and the volumes of water and headspace in the ampoules. Details of the measurements, including descriptions of the equipment used to collect samples and measure CFC concentrations, measurement procedures, and detailed quality assurance and quality control methods and procedures, are provided at http://water.usgs.gov/lab/cfc/lab/analytical_procedures_cfc.html. The analytical procedures also are described in detail by Bullister (1984), and Bullister and Weiss (1988).

Ages were interpolated from the measured concentrations by curve matching to CFC concentration curves from Niwot Ridge, Colorado. Ages were corrected using an altitude of 2700 meters and the recharge temperature and excess air values from the measured dissolved gas concentrations determined using the $^3He/^3H$ dating method (Plummer and Busenberg, 2000).

Helium-3 / Tritium Dating

For analysis, the dissolved gases were separated from the waters in an ultra-low vacuum extraction system (P ~ 1 x 10^{-9} torr). Concentrations of the major gas components (Ar, N_2, O_2, CH_4) were measured using a quadrapole mass spectrometer, and helium and neon were separated from the sample gas and analyzed for their isotopic composition of helium (^{3}He and ^{4}He) and total concentration of Ne using a magnetic sector–field mass spectrometer. See table 3 for additional information regarding analytical techniques and equipment used. Recharge temperature and altitude values were determined by procedures outlined by Ballentine and Hall (1999) and Aeschbach-Hertig and others (1999) using concentrations of Ne, Ar, and N_2 from the dissolved-gas samples and an excess air model for the resolution of the components.

Tritium concentrations were determined using the ^{3}He in-growth technique (Clark and others, 1976; Bayer and others, 1989). Each sample was transferred to an extraction vessel, completely degassed under low vacuum for 30 minutes, and sealed in the extraction flask. The flask was stored at room temperature for no less than 2 months to allow for the production of ^{3}He from the decay of ^{3}H within the sample. The evolved headspace gas was then analyzed for ^{3}He and the amount of ^{3}H was calculated based on the amount of time stored.

Results

Helium-3 / Tritium Dating

Helium isotope ratios presented in this section are expressed as R/RA, ^{3}He components are expressed in tritium units (TU) for the purpose of age calculation, one TU equals one ^{3}He atom per 1018 H atoms.

The range of recharge temperatures calculated from dissolved gas data (table 7) is consistent with the average annual air temperature in the Red River of 4°C between 1915 and 2002 (LoVetere and others, 2004). Calculated recharge altitudes for most of the wells appear reasonable compared to land-surface altitudes in and around the sampling points within the Red River drainage basin (fig. 1).

Table 7. Dissolved gas concentrations, helium isotopic composition, and calculated recharge temperature and altitude

[µcc/kg, micro cubic centimeters per kilogram; cc, cubic centimeter; C°, degrees Celsius; mcc = 10^{-6} cc, micro; kg, kilograms; R, ^{3}He/^{4}He ratio in the sample; RA, ^{3}He/^{4}He ratio in air TU, tritium units; <, less than]

Well	Date Sampled	He (µcc/kg)	R/RA	^{4}He terrigenic (µcc/kg)	Ne (µcc/kg)	Ar (cc/kg)	N_2 (cc/kg)	^{3}He total (measured) (TU)	^{3}He total (modeled) (TU)	Recharge Temperature (°C)	Recharge Altitude (meters)
CC1B	8/19/2003	50.1	1.24	5.1	191	0.336	14.9	34.5	34.5	4.0	3,048
CC2A	8/19/2003	39.3	0.97	3.8	153	0.290	11.8	21.3	21.3	8.0	3,048
CC2B	8/19/2003	89.2	0.76	32.2	234	0.370	19.6	37.5	37.5	2.5	3,048
Hottentot	8/20/2003	55.9	1.14	7.0	206	0.352	15.2	35.5	35.5	2.3	2,896
La Bobita	8/20/2003	49.2	1.11	<0.5	224	0.348	14.8	30.4	33.6	3.4	2,896
Hansen	8/20/2003	35.0	1.00	<0.5	153	0.297	11.9	19.5	19.5	7.8	2,743

Samples from CC1B, CC2A, SC2B, Hottentot and Hansen have gas concentrations consistent with an excess air model for ground water/gas equilibration, while samples from SC6A, SC7A, SC8A, (Naus and others, 2005) and La Bobita have gas chemistries with a poor correlation to the excess air model used to correct for tritiogenic ^{3}He. This poor correlation is reflected in the difference between the modeled (based on modeled helium solubility) and measured total ^{3}He concentrations (table 8).

Table 8. Helium-3 (^{3}He) concentrations associated with different sources, tritiogenic ^{3}He concentrations, tritium (^{3}H) concentrations, and ground-water ages

[σ, standard deviation; TU, tritium units; ---, not analyzed; <. less than; >, greater than; ---. no data]

Well	^{3}He solubility (TU)	^{3}He excess air (TU)	^{3}He terrigenic (TU)	^{3}He tritiogenic (TU)	^{3}H (TU)	Age (years)
CC1B	18.6	6.26	0.06	9.60	3.90	22.1
CC2A	18.2	1.32	0.04	1.71	2.27	10.0
CC2B	18.7	12.8	0.36	5.62	< 0.18	> 60
Hottentot	19.1	7.90	0.08	8.43	4.17	19.7
La Bobita	19.0	11.0	---	1.99	---	---
Hansen	18.9	0.34	---	0.33	8.11	0.7

One reason for the poor correlation may be that the excess air model used is not adequate to define the observed gas chemistry. Another model, such as a partial re-equilibration model, a multi-step partial re-equilibration (Stute and others, 1995) or a closed-system equilibration with entrapped air (Aeschbach-Hertig and others, 2000) may yield a better correlation. These models each explain a specific behavior of gas concentrations associated with ground water isolation from the atmosphere after recharge to the aquifer to produce "excess air-like" concentrations by a specific mechanism of recharge. For these models to be used, krypton (Kr) and xenon (Xe) concentrations must be measured to define the behavior of the heavier (more soluble) gases and the observed fractionation between the light and heavier gases. Measurement of both these species was beyond the scope of this investigation; thus, such models cannot be readily applied to the data sets.

Another explanation for the poor correlation is that these samples may represent mixed ground waters. The sample may contain a mixture of waters from different ground-water flow systems that have differing amounts of excess air and a different solubility associated with recharge temperature. Mixing of dissolved gas components causes errors in the determination of recharge temperature and amount of excess air from a specific sample, and thus results in a poor approximation of the various components of ^{3}He concentration in the sample. In the La Bobita sample, the modeled ^{3}He is greater than the measured ^{3}He, indicating a loss of helium from the sample. These losses could be a real effect of mixing of helium within the system or an artifact of the model interpretation of the other gas components (also mixed) producing either a high or low total helium value. For interpreted results, the measured ^{3}He and modeled ^{3}He were averaged, and the deviation between the results was added to the error in the interpretation for tritiogenic ^{3}He.

Tritium results are presented in Table 8. Almost all of the samples contained ^{3}H except CC2B and La Bobita, and thus are classified as modern ground water (< 60 years in age). The tritium analysis for the La Bobita sample failed during laboratory extraction (air leak into the flask). The ^{3}H value for sample CC2B is very close to the ^{3}He detection limit for the period allowed for production of ^{3}He.

The ground-water ^{3}He/^{3}H ages are representative of a wide variety of flow conditions associated with the Red River drainage basin. Samples taken from the base of scar areas (Hottentot, La Bobita, and Hansen) give a large age range for ground water flow from the scars. Hottentot water was the oldest at 19.7 years, while Hansen had a nearly no age (0.7 yr). La Bobita appears to have a ^{3}He* value

consistent with an age of about 10 to 15 years (^{3}He* = 1.99 TU), however since the ^{3}H analysis failed no value can be determined.

Monitoring wells taken from near the base of the Red River Valley show a consistent age distribution with the exception of SC8A. Samples taken from Capulin Canyon (CC1B, CC2A, and CC2B) are from a well cluster associated with a moderate age gradient. Assuming the water table (~1.5 meters below ground surface) taken from CC1B represents a zero age boundary, the first vertical velocity would be from the water table to CC2A (~ 34 cm/yr), the second would be from CC2A to CC1B (~55 cm/yr), and the third from SC1B to SC2B (~ 62 cm/yr). It is difficult to determine recharge rates using only one cluster. With no control on horizontal flow velocities, mass flux calculations cannot be determined accurately, however it can be stated that there is a downward gradient for ground-water flow associated with the Capulin Canyon cluster.

Notable quantities of excess ^{4}He (^{4}He$_{terrigenic}$) are noted in water samples from wells CC2B and Hottentot, with lesser amounts in CC1B and CC2A. The amount of excess ^{4}He and low value for ^{3}H indicate that modern ground water in well CC2B (32.2 µcc/kg excess ^{4}He) is mixing with a sub-modern component associated with the deep ground-water flow system in the bedrock. The ground-water sample from the Hottentot well shows a similar pattern of mixing; however, a sufficient quantity of the modern component is present within the system to allow an age to be determined (19.7 years assuming binary mixing between modern and sub-modern components). The lesser amounts of excess ^{4}He in samples from wells CC1B and CC2A may be attributed to intrinsic sources of ^{4}He such as a basal He flux or accumulation by radiogenic decay of U/Th series elements contained in the aquifer (Solomon, Hunt, and Poreda, 1996).

Chlorofluorocarbon Data

Ground-water ages from CFC analysis of samples from wells CC1B and CC2B are in agreement with ages determined from ^{3}He/^{3}H. However, the CFC data for the remaining samples shows some ambiguity between ages determined from the various CFC components (table 9) and ^{3}He/^{3}H ages. The sample from La Bobita was contaminated with respect to CFCs, having CFC concentrations 2 to 10 times the amount found in modern (present day) water.

For ground-water samples from Hansen and Hottentot wells, all of the CFC ages are older than the ^{3}He/^{3}H age. The older calculated CFC ages likely result from degradation of the CFCs in anaerobic conditions (less than 1.0 mg/L dissolved O_2). In anaerobic conditions microbial degradation of CFCs can occur in the presence of sulfate-reducing bacteria, preferentially degrading CFC-11 relative to CFC-12 (Plummer and others, 1998; Plummer and Busenberg, 2000). Depending on DOC and sulfate concentrations in the water under reducing conditions, the degradation sequence for CFCs is expected to first be CFC-11, followed by CFC-113, then CFC-12. In some cases, CFC-11 and CFC-113 may be entirely removed from the system.

Samples from CC1B and CC2B have a good correlation in age dates (average 26.1 and 39.7 years, respectively) based on ages determined from the three CFCs. The dates also agree well to the ^{3}He/^{3}H data (22 and >60 years), with minor degradation occurring in CC1B and possible mixing of pre-modern water occurring in CC2B noted by the amount of excess ^{4}He.

Table 9. Chlorofluorocarbon data

[CFC, chlorofluorcarbon; pg, picogram; kg, kilogram; CFC ages calculated using recharge altitude, recharge temperatures and excess air values taken from the dissolved gas data; ---, not analyzed]

	CFC concentrations			CFC Ages		
	CFC-11	CFC-12	CFC-113	CFC-11	CFC-12	CFC-113
Sample	(pg/kg)	(pg/kg)	(pg/kg)	(years)	(years)	(years)
CC1B	354	153	28.6	28.1	27.6	23.6
CC2A	---	---	---	---	---	---
CC2B	72.6	36.1	3.9	39.6	40.6	39.0
Hottentot	145	138	17.0	37.0	30.1	30.0
La Bobita	4,889	3,176	178		Contaminated	
Hansen	509	301	80.6	18.1	Modern	11.6

SUMMARY

Seven monitoring wells were installed in small catchments in the Red River Valley outside of the Straight Creek catchment as part of a second phase of well development for characterizing ground-water chemistry. Eight monitoring wells were originally installed, monitored, and water chemistry interpreted in phase I for the Straight Creek catchment as described in Naus and others (2005). Two additional wells in Straight Creek (SC7A and SC8A) were installed later as part of phase II but the chemical data were included in Naus and others (2005). Wells were completed in the debris fans of the Hottentot and Hansen catchments, the La Bobita sediment fan, and in bedrock and alluvial deposits unaffected by waste-rock drainage or other mining activities in the upper part of Capulin Canyon. Two surface-water samples in the Hottentot catchment and two surface-water samples in the Hansen catchment also were collected and analyzed to compare surface-water and ground-water compositions within these drainages. One sample from the inactive Questa U.S. Forest Service Ranger Station well was collected and analyzed.

Water chemistry, including major ions and trace elements, was monitored over a period of about 1 year and 66 samples were analyzed. These analyses included several duplicates and filtered and unfiltered-acidified (total recoverable) sample splits. There were 32 dissolved sample analyses, of which 3 were duplicates. The duplicate sample concentrations were averaged, and subsequently, 29 samples were used for plotting and calculations. The data were interpreted using geochemical speciation calculations, especially saturation indices, and by comparison with dilution trend lines derived from linear regressions on paired solute constituents from the Straight Creek data. The results allowed an evaluation of (1) possible mineral solubility limits that might control solute concentrations, (2) dilution trends, similar to those found for Straight Creek, that might control solute concentrations, and (3) the extent to which Straight Creek data may be an analog for weathering reactions occurring elsewhere in similar mineralized rock along the north side of the Red River (along the Questa caldera boundary) between the town of Red River and the U.S. Forest Service Questa Ranger Station.

Charge imbalances for 32 filtered samples averaged +1 percent with a standard deviation of ±5.8 and the largest C.I. was 11 percent. These values are well within the acceptable range for speciation computations. The range of effective ionic strength was 0.01 to 0.055 molal, well within the acceptable range for speciation computations using the ion association method (Nordstrom and Munoz, 1994).

Ground-water samples collected from Hottentot, Hansen and La Bobita were acidic with a range in pH of 2.6 to 4.5. Samples collected from Capulin Canyon wells and the Questa Ranger Station

well were circumneutral with a range in pH between 6 and 7.3. Specific conductance values ranged from 500 (Questa Ranger Station well) to 3,000 µS/cm (upper Hottentot surface water) and correlated linearly with sulfate concentration because of the overwhelming dominance of sulfate among the anions in these samples. An evaluation of redox potential measurements and their correlation with redox potentials calculated from Fe(II) and Fe(III) concentrations and speciation calculations for activities was done in a manner equivalent to that done for the Straight Creek phase I data (Naus and others, 2005). The results indicate that the range of 0.02 to 0.2 mg/L of Fe(III) (0.46 to 4.6 micromolar) was found to be the transition concentration below which the Nernstian equilibrium potential is no longer operative after detection limits were considered.

Iron concentrations in the phase II data were similar to the trends found in the phase I data. Total dissolved iron concentrations did not correlate well with sulfate concentrations because dynamic oxidation-reduction reactions occur in the catchments. Surface waters contained predominantly oxidized iron (dissolved Fe(III)) and ground waters contained predominantly reduced iron (dissolved Fe(II)). Saturation indices demonstrated that ferrihydrite provides a solubility limit for Fe(III) concentrations and siderite provides a solubility limit for Fe(II). The driving force for reaching siderite saturation appears not to be the dissolution of siderite but rather the dissolution of calcite and possibly rhodochrosite and dolomite.

Constituents that followed the trends and solubility limits established by the Naus and other (2005) for phase I data included iron, aluminum, magnesium, strontium, silica, sodium, potassium, cobalt, nickel, barium, and dissolved organic carbon. Sodium and potassium concentrations were less variable and were within a lower concentration range of values than those from wells SC1B and SC5B, giving further confirmation that SC1B and SC5B were contaminated from man-made sources.

Constituents that followed the trends and solubility limits established by phase I data with one or two exceptions included manganese, calcium, lithium, zinc, and beryllium. The main exception was the data from well CC2A that contained high concentrations of manganese, zinc, lithium, beryllium, and fluoride. This exception suggests a local mineralized zone in the vicinity of this well. The high beryllium concentrations seem to be related to the high fluoride concentrations and are likely a result of beryllium-fluoride complexing in solution. This hypothesis is consistent with similar data from other wells in the Red River Valley. This well may have been contaminated with waste-rock leachate but it is difficult to determine how such contamination might have occurred because the location of the well with respect to the drainages should have excluded such a possibility.

The Hansen ground water contained manganese, lithium, zinc, and copper concentrations that were below the phase I concentration trends. This difference is likely caused by less intense hydrothermal alteration and reduced mineralization in the Hansen scar area compared with other areas. The Hansen area may be more distant from local centers of hydrothermal activity than Straight Creek or Hottentot, and the disparity is related to geologic control on ground-water chemistry. Calcium concentrations follow the phase I trends except for the Hottentot data. The Hottentot scar contains an exposure of rhyolite porphyry that is deficient in calcium compared with the other dominant rock types and appears to have less gypsum and calcite available for weathering.

Fluoride, copper, and cadmium concentrations do not follow the phase I data trends. These elements are strongly affected by mineralization of alteration zones; that is, they are affected by the spatial distribution of mineral assemblages resulting from successive hydrothermal events and from pressure and temperature gradients during hydrothermal alteration that control mineral formation. The Straight Creek data do not provide a reliable analog for these elements unless the location of the weathering surface, with respect to the spatial distribution of the alteration zones, is carefully taken into account.

Speciation calculations with the phase II data confirmed that mineral-solubility equilibria provided an upper limit to the dissolved concentrations of several constituents in the Red River ground waters. After careful screening of the redox measurements and their correlation with redox potentials derived from Fe(II/III) determinations and speciation computations, ferrihydrite solubility provides a

limit on Fe(III) concentrations. However, the trend can only be demonstrated up to a pH of about 4.5 because at higher pH values the Fe(III) concentrations were too low to be reliable for redox potential measurements. Siderite precipitation limits Fe(II) concentrations for anoxic ground waters with pH values at or greater than 6.0. Siderite is not a common mineral in the Red River Valley and approach to saturation appears to be driven by dissolution of other carbonates, primarily calcite, dolomite, and rhodochrosite. Manganese concentrations reflect an upper limit imposed by crystalline to disordered rhodochrosite at pH values at or greater than 6.0.

Aluminum concentrations generally followed dilution trends similar to those in the phase I data for pH values below 4. When the pH reaches 4, depletion in aluminum concentrations relative to sulfate concentrations occurred, consistent with decreases in silica concentrations and consistent with the phase I data. The low concentrations of aluminum at pH values higher than 4 are consistent with an $Al(OH)_3$-like phase that has been called microcrystalline to amorphous gibbsite. Because the silica concentrations also decreased and because these circumneutral pH samples also were at saturation with respect to kaolinite, an aluminosilicate clay such as poorly ordered kaolinite (or imogolite or allophane) should be forming.

Calcium concentrations covered a large range and reached (a) gypsum solubility equilibrium for the low-pH Hansen Creek samples and (b) calcite solubility equilibrium for the high pH samples from CC1B and CC2B. These two minerals are common in the Red River Valley. Fluorite solubility equilibrium appeared to be reached for waters from CC2B and possibly CC1B. Samples from CC2A are supersaturated with respect to fluorite by an order of magnitude and it is not clear whether this supersaturation is real or an artifact of the speciation calculations. The effect has been seen for other ground-water compositions with pH near 6.0, high fluoride concentrations, and low aluminum concentrations. All samples in this study were undersaturated with respect to dolomite, celestite, and strontianite.

Barium concentrations are limited entirely by crystalline to microcrystalline barite solubility because of its low solubility. Other trace elements do not reach equilibrium solubility. For example, all samples were well undersaturated with respect to smithsonite and thus smithsonite solubility is not limiting to zinc concentrations; all samples are well undersaturated with respect to otavite and its solubility was not limiting cadmium concentrations; and all samples are well undersaturated with respect to bronchantite and malachite and their solubilities were not limiting to copper concentrations.

For phase II wells, the DOC is in the range of 0.5 to 2.5 mg/L and is consistent with other non-contaminated wells in the area. The hydrogen and oxygen isotopic composition indicates that the ground waters are meteoric, recent in origin, and have minimal evaporation.

Based on the $^3He/^3H$ data, ground-water ages within the Red River drainage basin range from present day to older pre-modern waters. The dissolved gas chemical data indicate possible mixing of ground water associated with the basal Red River drainage basin as it receives ground-water discharge emanating from the debris-fan aquifers associated with erosional scars. Chloroflourocarbon-age data rarely correlate well with $^3He/^3H$ data and are influenced by microbial degradation. In some cases $^3He/^3H$ ages are also questionable because of possible mixing.

This interpretation of major-and trace-element concentrations for ground waters outside the Straight Creek catchment has helped to determine to what extent the Straight Creek results serve as a useful analog for estimating the pre-mining ground-water quality at the Questa molybdenum mine site.

REFERENCES CITED

Anders, E., and Ebihara, M, 1982, Solar-system abundances of the elements: Geochimical et Cosmochimica Acta, v. 46, p. 2362-2380.

Aeschbach-Hertig, W., Peeters, F., Beyerle, U., and Kipfer, R., 1999, Interpretation of dissolved atmospheric noble gases in natural waters: Water-Resources Research, v. 35, p. 2779-2792.

Aeschbach-Hertig, W., Peeters, F., Beyerle, U., and Kipfer, R., 2000, Palaeotemperature reconstruction from noble gases in ground taking into account equilibration with entrapped air: Nature, v. 405, p. 1040-1044

Aiken, G.R., 1992, Chloride interference in the analysis of dissolved organic carbon by the wet oxidation method: Environmental Science and Technology, v. 26, p. 2435-2439.

American Public Health Association (APHA), 1985, Method 428C. Methylene blue method for sulfide, in Standard methods for the examination of water and wastewater (14th ed.): American Public Health Association, p. 403-405.

Ball, J.W., and Nordstrom, D.K., 1991, User's manual for WATEQ4F, with revised thermodynamic data base and test cases for calculating speciation of major, trace, and redox elements in natural waters: U.S. Geological Survey Open-File Report 91-183, 189 p.

Ballentine, C.J., and Hall, C.M., 1999, Determining palaeotemperature and other variables by using an error-weighted, nonlinear inversion of noble gas concentrations in water: Geochimica et Cosmochimica Acta, no. 63, p. 2315-2336.

Barnard, W.R., and Nordstrom, D.K., 1980, Fluoride in precipitation – I. Methodology with the fluoride-selective electrode: Atmospheric Environment, v. 16, p. 99-103.

Barringer, J.L., and Johnsson, P.A., 1989, Theoretical considerations and a simple method for measuring alkalinity and acidity in low pH waters by gran titration: U.S. Geological Survey Water-Resources Investigations Report 89-4029, 35 p.

Bayer, R., Schlosser, P., Bonisch, G., Rupp, H., Zaucker, F., and Zimmek, G., 1989, Performance and blank components of a mass spectrometric system routine measurement of helium isotopes and tritium by ^{3}He ingrowth method: Sitzungsberichte der Heidelberger Akademie der Wissenschaften. Mathematisch-naturwissenschaftliche Klasse: Heidelberg, Springer Verlang, p. 241-279.

Brinton, T.I., Antweiler, R.C., and Taylor, H.E., 1995, Method for the determination of dissolved chloride, nitrate, and sulfate in natural water using ion chromatography: U.S. Geological Survey Open-File Report 95-426A, 16 p.

Bullister, J.L., 1984, Atmospheric chlorofluoromethanes as tracers of ocean circulation and mixing–Studies in the Greenland and Norwegian seas: La Jolla, University of California, San Diego, Ph.D. dissertation, 172 p.

Bullister, J.L., and Weiss, R.F., 1988, Determination of CFC3F and CCI2F2 in seawater and air: Deep Sea Research, 35, p. 839-854.

Caine, J.S., 2003, Questa baseline and pre-mining ground-water quality investigation. 6. Preliminary brittle structural geologic data, Questa mining district, southern Sangre de Cristo Mountains, New Mexico: U.S. Geological Survey Open-File Report 03-280, 7 p.

Clark, I., and Fritz, P., 1999, Environmental isotopes in hydrology: New York, Lewis Publishers.

Clark, W.B., Jenkins, W.J., and Top, Z., 1976, Determination of tritium by mass spectrometric measurements: International Journal of Applied Radioactive Isotopes, v. 27, p. 515-522.

Coplen, T.B., 1994, Reporting of stable hydrogen, carbon, and oxygen isotopic abundances: Pure and Applied Chemistry, v. 66, p. 273-276.

Coplen, T.B., Wildman, J.D., and Chen, J., 1991, Improvements in the gaseous hydrogen-water equilibrium technique for hydrogen isotope ratio analysis: Analytical Chemistry, v. 63, p. 910-912.

Epstein, S., and Mayeda, T., 1953, Variation of 17O content of water from natural sources: Geochimica et Cosmochimica Acta, v. 4, p. 213-224.

Fishman, M.J., and Friedman, L.C., 1989, Methods for determination of inorganic substances in water and fluvial sediments: U.S. Geological Survey Techniques of Water-Resources Investigations, book 5, chap. A1, 545 p

Gale, V.G., and Thompson, A.J.B., 2001, Reconnaissance study of waste rock mineralogy: Questa, New Mexico, Petrography, PIMA Spectral Analysis and Rietveld Analysis: PetraScience Consultants, Inc., January 31.

Garbarino, J.R., and Taylor, H.E., 1995, Inductively coupled plasma-mass spectrometric method for the determination of dissolved trace elements in natural water: U.S. Geological Survey Open-File Report 94-358, 88 p.

Gibs, J., and Wilde, F.D., 1999, Ground-water sampling: Preparations and purging methods at water-supply wells and monitoring wells, in National field manual for the collection of water-quality data: U.S. Geological Survey Techniques of Water-Resources Investigations, book 9, chap. A4.2., p. 61-90.

Giesemann, A., Jäger, H.J., Normann, A.L., Krouse, H.R. and Brand, W.A.: 1994, On-line sulfur isotope determination using an elemental analyzer coupled to a mass spectrometer: Analytical Chemistry, v. 66, p. 2816–2819.

Johnson, C.M., and Lipman, P.W., 1988, Origins of metaluminous and alkaline volcanic rocks of the Latir volcanic field, northern Rio Grande rift, New Mexico: Contributions to Mineralogy and Petrology, V. 100, p. 107-128.

Kennedy, V.C., Jenne, E.A., and Burchard, J.M., 1976, Backflushing filters for field processing of water samples prior to trace-element analyses: U.S. Geological Survey Water-Resources Investigations Report 76-126, 12 p.

Kennedy, V.C., Jones, B.F., and Zellweger, G.W., 1974, Filter pore-size effects on the analysis of Al, Fe, Mn, and Ti in water: Water Resources Research, v. 15, p. 687-702.

Knight, P.J., 1990, The flora of the Sangre de Cristo Mountains, New Mexico, in P.W. Bauer, S.G. Lucas, C.K. Mawer, and W.C. McIntosh, eds., Tectonic Development of the Southern Sangre de Cristo Mountains, New Mexico: New Mexico Geological Society Forty-First Annual Field Conference, September 12-15, p. 94-95.

Langmuir, D. Chrostowski, P., Vigneault, B., and Rufus, C., 2004, Issue paper on the environmental chemistry of metals: U.S. Environmental Protection Agency, Risk Assessment Forum.

Laxen, D.P.H., and Chandler, I.M., 1982, Comparison of filtration techniques for size distribution in freshwaters: Analytical Chemistry, v. 54, p. 1350-1355.

Lilley, T.H. and Briggs, C.C., 1976, Activity coefficients of calcium and sulfate in water at 25ºC: Proceedings of the Royal Society London, Series A, v. 349, p. 355-368.

Lipman, P.W., 1981, Volcano-tectonic setting of tertiary ore deposits, southern Rocky Mountains: Arizona Geological Society Digest, v. 14, p. 199-213.

Lipman, P.W., 1988, Evolution of silicic magma in the upper crust; the mid-Tertiary Latir volcanic field and its cogenetic granitic batholith, northern New Mexico, U.S.A.: Transactions of the Royal Society of Edinburgh, Earth Sciences, v. 79, p 265-288.

Livo, K.E., and Clark, R.N., 2002, Mapped minerals at Questa, New Mexico, using airbourne visible-infrared imaging spectrometer (AVIRIS) data–preliminary report: U.S. Geological Survey Open-File Report 02-0026, 13 p.

LoVetere, S.H., Nordstrom, D.K., Maest, A.S., and Naus, C.A., 2004, Questa baseline and pre-mining ground-water quality investigation. 3. Historical ground-water quality for the Red River Valley, New Mexico: U.S. Geological Survey Water-Resources Investigations Report 03-4186, 44 p.

Ludington, S.D., Plumlee, G.S., Caine, J.S., Bove, D., Holloway, J.M., and Livo, D.E., 2004, Questa baseline and pre-mining ground-water quality investigation. 10. Geologic influences on ground and surface waters in the Red River watershed, New Mexico: U.S. Geological Survey Scientific Investigations Report 04-5245, 45 p.

Maest, A.S., Nordstrom, D.K., and LoVetere, S.H., 2004, Questa baseline and pre-mining ground-water quality investigation. 4. Historical surface-water quality for the Red River, New Mexico, 1965-2001: Scientific Investigations Report 2004-5063, 150 p.

McCleskey, R.B. Nordstrom, D.K., and Naus, C.A., 2004, Questa baseline and pre-mining ground-water quality investigation. 16. Quality assurance and quality control of water analyses: U.S. Geological Survey Open-File Report 2004-1341, 102 p.

McCleskey, R.B., Nordstrom, D.K., and Ball, J.W., 2003, Metal interferences and their removal prior to the determination of As(T) and As(III) in acid mine waters by hydride generation atomic absorption spectrometry: U.S. Geological Survey Water-Resources Investigations Report 03-4117, 166 p.

Meyer, J.W., and Leonardson, R.W., 1990, Tectonic, hydrothermal and geomorphic controls on alteration scar formation near Questa, New Mexico: Guidebook - New Mexico Geological Society, v. 41, p. 417-422.

Meyer, J.W., and R.W. Leonardson, 1997, Geology of the Questa Mining District: Volcanic, plutonic, tectonic and hydrothermal history: New Mexico Bureau of Mines and Mineral Resources Bulletin, Open File Report 431, 187 pp.

Molycorp, Inc., [n.d.], Molybdenum-Questa, NM-History, accessed from the World Wide Web on July 22, 2004 at www.molycorp.com.

Morris, J. C., and Stumm, W., 1967. Redox equilibria and measurements of potentials in the aquatic environment, in Stumm, W., ed., Equilibrium concepts in natural water systems: American 47 Chemical Society Advances in Chemistry Series 67, American Chemical Society, Washington, D.C., p. 270-285.

Naus, C.A., McCleskey, R.B., Nordstrom, D.K., Donohoe, L.C., Hunt, A.G., Paillet, F.L., Morin, R.H., and Verplanck, P.L., 2005, Questa Baseline and Pre-Mining Ground-Water-Quality Investigation. 5. Well Installation, Water-Level Data, and Surface- and Ground-Water Geochemistry in the Straight Creek Drainage Basin, Red River Valley, New Mexico, 2001-03: U.S. Geological Survey Scientific Investigations Report 2005-5088, 220 p.

Nordstrom, D. K., 1977, Thermochemical redox equilibria of ZoBell's solution: Geochimica et Cosmochimica Acta, v. 41, p. 1835-1841.

Nordstrom, D.K., and Munoz, J.L., 1994, Geochemical thermodynamics (2nd ed): Boston, Mass., Blackwell Scientific Publications, 493 p.

Nordstrom, D.K., Wright, W.G., Mast, M.A., Bove, D., and Rye, R.O, 2005, Aqueous-sulfate stable isotopes – A study of mining-affected and unmined acidic drainage, Chapter E8 in Church, S.E., von Guerard, Paul, and Finger, S.E., eds., Integrated investigations of environmental effects of historical mining in the Animas River watershed, San Juan County, Colorado: U.S. Geological Survey Professional Paper 1651 – E81.

Ozima, M., and Podosek, F.A., 1983, Noble gas geochemistry: Cambridge University Press, 367 p.

Plummer, L.N., and Busenberg, Eurybiades, 2000, Chlorofluorocarbons, in Cook, P.G., and Herczeg, A.L., eds., Environmental tracers in subsurface hydrology: Boston/Dordrecht/London, Kluwer Academic Publishers, p. 441-478.

Plummer, L.N., Busby, J.F., Lee, R.W., and Hanshaw, B.B., 1990, Geochemical modeling of the Madison aquifer in parts of Montana, Wyoming, and South Dakota: Water Resources Research, v. 26, no. 9, p. 1981-2014.

Plummer, L.N., Busenberg, Eurybiades, Drenkard, S., Schlosser, P., Ekwurzel, B., Weppernig, R., McConnell, J.B., and Michel, R.L., 1998, Flow of rover water into a karstic limestone aquifer - 2. Dating the young fraction in groundwater mixtures in the Upper Floridan aquifer near Valdosta, Georgia: Applied Geochemistry, v. 13, no. 8, p. 1017-1043.

Rehrig, W.A., 1969, Fracturing and its effects on molybdenum mineralization at Questa, New Mexico: PhD Dissertation to the University of Arizona, 194 p.

Robertson GeoConsultants, Inc. (RGC), 2000, Interim background characterization study, Questa Mine, New Mexico: Report number 052008/6, June, 33 p.

Robertson GeoConsultants, Inc., 2001, Background study data report, Questa Mine, New Mexico: Report No. 052008/12, prepared for Molycorp Inc., 40 p.

Roth, D.A., Taylor, H.E., Domagalski, J., Dileanis, P., Peart, D.B., Antweiler, R.C., and Alpers, C.N., 2001, Distribution of inorganic mercury in Sacramento River water and sediments: Archives of Environmental Contamination and Toxicology, v. 40, p. 161-172.

Schilling, J.H., 1956, Geology of the Questa molybdenum (moly) mine area, Taos County, New Mexico: Socorro, New Mexico Bureau of Mines and Mineral Resources, Bulletin 51, 87 p.

Silva, R.I., Bidoglio, G., Rand, M.H., Robouch, P.B., Wanner, H. and Puigdomenech, I, 1995, Chemical Thermodynamics of Americium: Elsevier, Amsterdam, 374 pp.

Slifer, Dennis, 1996, Red River groundwater investigation, Final report: New Mexico Environment Department, Surface Water Quality Bureau, March, 26 p.

Smolka, L.R., and Tague, D.F., 1989, Intensive water quality survey of the Middle Red River, Taos County, New Mexico, September 12–October 25, 1988: New Mexico Environmental Improvement Division, Surveillance and Standards Section, Surface Water Quality Bureau: May 1989, 87 p.

Solomon, D.K., Hunt, A.G., and Poreda, R.J., 1996, Source of radiogenic helium 4 in shallow aquifers-Implications for dating young groundwater: Water-Resources Research, v. 32, no. 6, p. 1805-1813.

South Pass Resources, Inc., 1995, Supplemental report—Discussion of the geology, hydrology, and water quality of the mine area, Molycorp Facility, Taos County, New Mexico: Scottsdale, Ariz., February 15, 15 p.

Steffen Robertson & Kirsten, 1995, Questa molybdenum mine geochemical assessment: SRK Project no. 09206, Lakewood, Colo., April 13, 44 p.

Stookey, L.L., 1970, Ferrozine-A new spectrophotometric reagent for iron: Analytical Chemistry, v. 42, p. 779-781.

Stute, M., Forster, M., Frischkorn, H., Serejo, A., Clark, J.F., Schlosser, P., Broecker, W.S., and Bonani, G., 1995, Cooling of tropical Brazil (5 degrees C) during the last glacial maximum: Science, v. 269, no. 5222, p. 379-383.

Taylor, H.E., and Garbarino, J.R., 1991, The measurement of trace metals in water resources-Monitoring samples by inductively coupled plasma-mass spectrometry: Spectrochemica Acta Reviews, v. 14, no. 1-2, p. 33-43.

Taylor, H.E., Berghoff, K., Andrews, E.D., Antweiler, R.C., Brinton, T.I., Miller, C., Peart, D.B., and Roth, D.A., 1997, Water quality of springs and seeps in Glen Canyon National Recreation Area: National Park Service Technical Report NPS/NRWRD/NRTR-97/128, 26 p.

To, T.B., Nordstrom, D.K., Cunningham, K.M., Ball, J.W., and McCleskey, R.B., 1999, New method for the direct determination of dissolved Fe(III) concentration in acid mine waters: Environmental Science and Technology, v. 33, p. 807-813.

URS, 2001, Final report, Molycorp Questa Mine site-wide comprehensive hydrologic characterization report: Denver, Colo., March, 95 p.

URS, 2002, Molycorp Remedial Investigation/Feasibility Study (RI/FS) work plan, sections one through three, v.1 draft final: Denver, Colo., July.

U.S. Department of Agriculture Forest Service, 2001, Wildland Urban Interface Areas in USDA FS Southwestern Region: Southwestern Region GIS Datasets, accessed July 22, 2004 from the World Wide Web at URL http://www.fs.fed.us/r3/gis/datasets.shtml#regional.

U.S. Environmental Protection Agency, 2000, NPL Site Narrative for Molycorp, Inc., accessed July 22, 2004 from the World Wide Web at URL http://www.epa.gov/superfund/sites/npl/nar1599.htm.

U.S. Geological Survey, 1997-99, National field manual for the collection of water-quality data: U.S. Geological Survey Techniques of Water-Resources Investigations, book 9, chaps. A1-A9, 2 v., variously paged. [Also available online at http://pubs.water.usgs.gov/twri9A; updates and revisions are summarized at http://water.usgs.gov/owq/FieldManual/mastererrata.html]

U.S. Geological Survey, 2004a, Daily streamflow for the Nation, USGS 08265000 Red River near Questa, NM, accessed July 22, 2004 from the World Wide Web at URL http://nwis.waterdata.usgs.gov/nwis/discharge/.

U.S. Geological Survey, 2004b, Isotope fractionation project: U.S. Geological Survey, Reston Stable Isotope Laboratory, accessed March 23, 2004 from the World Wide Web at URL http://isotopes.usgs.gov/.

Vail Engineering, Inc., 1989, A geochemical investigation of the origin of aluminum hydroxide precipitate in the Red River, Taos County, New Mexico: June, 43 p.

Verplanck, P.L., Antweiler, R.C., Nordstrom, D.K., and Taylor, H.E., 2001, Standard reference water samples for rare earth element determination: Applied Geochemistry, v. 16, p. 231-244.

Western Regional Climate Center, 2003, Historical climate information: New Mexico climate summaries, Red River, New Mexico (297323), accessed July 17, 2003, from the World Wide Web at URL http://www.wrcc.dri.edu/.

Wilde, F.D., and Radtke, D.B., 1998, Field Measurements, in National field manual for the collection of water-quality data: U.S. Geological Survey Techniques of Water-Resources Investigations, book 9, chap. A6.

ZoBell, C.E., 1946, Studies on redox potential of marine sediments: 8. Other methods: Bulletin of the American Association of Petroleum Geologists, v. 30, p. 477-509.